Dissertation ETH No 13769

Functional diversity of contractile isoproteins: Expression of actin and myomesin isoforms in striated muscle

A dissertation submitted to the
SWISS FEDERAL INSTITUTE OF TECHNOLOGY, ZURICH

for the degree of
Doctor of Natural Science

presented by
Irina Agarkova
Dipl. Biophys., Moscow Institute of Physics and Technology
citizen of Russia

accepted on the recommendation of
Prof. Dr. J.-C. Perriard, examiner
Prof. Dr. H. M. Eppenberger, co-examiner
Prof. Dr. M. C. Schaub, co-examiner

Zurich, 2000

The structure of the dissertation

This Dissertation consists of two distinct but related parts. The first part describes my research of actin isoform expression during the cytoarchitecture remodelling in cultured cardiomyocytes. The second part reports the study of myomesin isoform expression in striated muscles of vertebrates. Although distinct, these two projects are closely related to each other: both address the question how the isoform diversity of sarcomeric proteins leads to the functional diversity of sarcomeres in different muscle types. The obtained results underline the functional significance of sarcomeric isoproteins during development and by myofibril adaptation to varying physiological conditions. Thus, this work contributes to the complete understanding of fundamental principles and the function of striated muscle.

Table of contents

Summary

The sarcomere, the structural unit of striated muscle, is a highly organized natural machine that produces mechanical force. Despite the striking similarity at the level of the electron microscope, the different types of striated muscle fibers are characterized by distinct contractile properties. These adaptations to specific physiological requirements are associated with the isoform diversity of contractile proteins. This study concerns the expression of two sarcomeric proteins: actin, which is associated with force generation, and myomesin, which is involved in force transmission.

Actin is one of the most conserved and ubiquitous proteins in nature. The characteristic property of actin is its ability to dynamically assemble into various structures in eucariotic cell. At least 6 actin isoforms different in their isoelectric point was found in mammalian tissue. The differential expression of the isoactins as well as the high conservation of the specific isoforms between the species indicates the functional importance of actin isoforms. Here, the study of actin isoforms expression during the remodeling of cytoarchitecture in cultivated cardiomyocytes is reported. The coexistence of the functional myofibrils with non-sarcomeric cytoskeleton in the same cell makes cultivated cardiomyocytes a well-suited system for the study of differential sorting of isoactins. The expression pattern and localization of actin isoforms in cultivated adult (ARCs) and newborn rat cardiomyocytes (NRCs) were studied by actin isoform specific antibodies using immunofluorescence and western blot analysis. It was found that expression of the sarcomeric (cardiac and skeletal) α-actins that are the dominating actin isoforms in cardiomyocytes does not change significantly during the cultivation. These isoactins seems to participate equally well in both sarcomeric and non-sarcomeric cytoskeleton. This suggests that although the evolutionary more advanced sarcomeric actins are designed to optimize the actomyosin interaction, they retain the ability to build the non-sarcomeric structures. The embryonic isoform of smooth muscle α-actin was detected in NRCs and in ARCs after some period of cultivation. It is expressed heterogeneously in both cell types, and its colocalization with the other α-actins in sarcomeric structures does not interfere with developing of functional contractile apparatus. The results of cytoplasmic β-actin expression were contradictory. Whereas the monoclonal antibody against cytoplasmic β-actin did not detect the significant expression of this isoactin in cultivated cardiomyocytes, the polyclonal antibody against the cytoplasmic β-actin demonstrated the weak but stable expression of this isoform there. The RT-PCR analysis with the β-actin specific primers confirms the presence of β-actin message in the cultivated cardiomyocytes. While the antibodies recognizing the muscle actins stain uniformly the whole length of the thin filaments, the staining with anti-cytoplasmic β-actin antibody is concentrated in narrow stripes around the Z-disks. These findings rise the possibility that some modified form of β-cytoplasmic actin is expressed in cardiac tissue and has the specific destiny in the sarcomeric structure.

The second part of this study addresses the myomesin isoform diversity in vertebrates. Myomesin is structural component of the M-band, which is expressed in all types of striated muscle. Its primary function seems to be the maintenance of the thick filament lattice and its anchoring to titin. This study provided the comprehensive analysis of

myomesin isoform expression in high vertebrates. By means of RT-PCR, immunofluorescent and immunoblotting analysis it was proved that two alternative splicing events give rise to four isoforms in birds, contrary to only one splicing event that produces two isoforms in mammals and reptiles. It is shown that the myomesin isoform expression is regulated in both developmental- and tissue-specific fashion. The splicing event at the C-terminus is a unique peculiarity of avian myomesin. It results in two splice variants, termed H-myomesin and S-myomesin, representing the major myomesin species in heart and skeletal muscle of birds, respectively. In embryonic heart of birds, mammals and reptiles, another alternative splicing event gives rise to the isoform, which is termed EH-myomesin. This isoform dominates in the early embryonic heart, but is rapidly downregulated around the birth. This strict regulation of the EH-myomesin makes it an ideally suited marker for embryonic heart. The analysis of the circular dichroism spectra of recombinant EH-segment revealed the absence of defined secondary structure. The ectopic expression of the EH-segment in the cultivated cardiomyocytes leaded to its diffuse distribution in the cytoplasm, indicating for the lack of interaction with sarcomeric proteins. It is suggested that inclusion of EH-segment provide additional elasticity and flexibility to the myomesin molecule; these features might have important functional implications in embryonic heart. Further, the study of myofibrillogenesis in the embryonic heart using the generated myomesin isoform-specific antibodies provided a strong argument that myomesin is essential part of the basic cytoskeletal lattice of the sarcomere.

Zusammenfassung

Das Sarkomer, der Grundbaustein der Myofibrillen, ist eine hochorganisierte Maschine, die mechanische Kraft produziert. Trotz ihrer grossen Ähnlichkeit im Elektronenmikroskop zeichnen sich die verschiedenen Typen der quergestreiften Muskulatur durch unterschiedliche Kontraktionseigenschaften aus. Diese Anpassungen an spezifische physiologische Anforderungen werden durch die Expression unterschiedlicher Isoformen der kontraktilen Proteine ermöglicht. Die vorliegende Arbeit befasst sich mit dem Expressionsmuster von zwei verschiedenen Proteinen des Sarkomers: Aktin, das zur Kraftentwicklung benötigt wird, und Myomesin, das bei der Übermittlung von Kraft eine Rolle spielt.

Aktin ist eines der am höchsten konservierten und am weitesten verbreiteten Proteine. Eine typische Eigenschaft von Aktin ist die Fähigkeit, sich dynamisch in verschiedene Strukturen in der Eukaryontenzelle umzuwandeln. In Säugern wurden sechs verschiedene Aktinisoformen gefunden, die sich in ihrem isoelektrischen Punkt unterscheiden. Das unterschiedliche Expressionsmuster der Isoaktine und der hohe Grad an Konservierung der einzelnen Isoformen verschiedener Spezies weisen auf die Bedeutung der Aktinisoformen hin.
In dieser Arbeit wurde die Expression verschiedener Aktinisoformen während der Umbauphase der Zellarchitektur in kultivierten Herzzellen untersucht. Da in Herzzellen in Kultur funktionelle Myofibrillen und nicht-sarkomerische Elemente des Zytoskeletts nebeneinander existieren, bieten sie sich als ideales System an, um das unterschiedliche Verteilungsmuster verschiedener Aktinisoformen zu analysieren. Das Expressionsmuster und die Lokalisation verschiedener Aktinisoformen in kultivierten adulten (ARCs) und neonatalen Rattenherzzellen (NRCs) wurden mit isoformspezifischen Antikörpern mittels Immunfluoreszenz und Immunoblotting untersucht. Es wurde festgestellt, dass sich die Expression der sarkomerischen α-Aktine (cardiac und skeletal muscle) während der Kultur nicht signifikant verändert. Diese Aktinisoformen wurden sowohl in den Sarkomeren als auch im nicht-sarkomerischen Zytoskelett gefunden. Die embryonale Isoform, α-smooth muscle Aktin, konnte in NRCs und ARCs erst nach einigen Tagen in Kultur nachgewiesen werden. In beiden Zelltypen zeichnet sich diese Isoform durch eine sehr heterogene Expression aus und ihre Kolokalisation mit den anderen α- Aktinen in den Myofibrillen scheint keinen Effekt auf die Bildung eines funktionstüchtigen kontraktilen Apparates zu haben.
Die Ergebnisse zur Expression von β-cytoplasmic Aktin waren widersprüchlich. Mit einem monoklonalen Antikörper gegen diese Isoform konnte keine signifikante Expression dieses Isoaktins in kultivierten Herzzellen nachgewiesen werden, ein polyklonaler Antikoerper gegen diese Isoform zeigte hingegen eine zwar schwache aber stabile Expression. RT-PCR Analyse mit isoform-spezifischen Primern bestätigte die Existenz der mRNA für β-cytoplasmic Aktin in Herzzellprimärkulturen. Während Antikörper gegen die Muskelaktine die dünnen Filamente in ihrer gesamten Länge anfärben, ist das Signal mit dem polyklonalen β-Aktinantikörper nur in schmalen Streifen in der Region der Z-Scheibe konzentriert. Diese Ergebnisse legen den Schluss nahe, dass im Herzgewebe eine

modifizierte Form von β-cytoplasmic Aktin exprimiert ist, die eine besondere Funktion in der Myofibrille ausüben könnte.

Im zweiten Teil dieser Arbeit wurde die Bedeutung verschiedener Isoformen von Myomesin in Vertebraten untersucht. Myomesin ist ein struktureller Bestandteil der M-Bande und wird in allen Typen von quergestreifter Muskulatur exprimiert. Hauptfunktion von Myomesin scheint die Erhaltung der Struktur des dicken Filamentes und seine Verankerung mit dem Titin-Filamentsystem zu sein. Mittels RT-PCR, umd Immunfluoreszenz bzw. Immunoblotanalyse mit isoformspezifischen Antikörpern konnte gezeigt werden, dass in Vögeln zwei alternative Splicings zu vier Isoformen führen können, wohingegen in Säugern und Reptilien nur ein alternatives Splicing möglich ist, das zu zwei verschiedenen Isoformen führt. Die Expression der Myomesinisoformen ist entwicklungsstadien- und gewebsspezifisch reguliert. Das alternative Splicing am C-Terminus scheint eine Besonderheit von Myomesin der Vögel zu sein. Es führt zu zwei Splice-Varianten, die H-Myomesin und S-Myomesin genannt wurden und die hauptsächlich in Herz bzw. in Skelettmuskulatur exprimiert werden. Im embryonalen Herz von Vögeln, Säugern und Reptilien führt ein weiteres alternatives Splicing zu einer Isoform, die EH-Myomesin genannt wurde. Im embryonalen Herz früher Stadien ist diese Isoform vorherrschend; ihre Expression wird jedoch zum Zeitpunkt der Geburt rasch runterreguliert. Dank diesem spezifischen Expressionsmuster ist EH-Myomesin ein idealer Marker für embryonales Herz. Eine Analyse des CD-(circular dichroism) Spektrums von rekombinantem EH-Segment ergab, dass dieses Peptid keine klar definierte Sekundärstruktur aufweist. Eine ektopische Expression des EH-Segments in kultivierten Herzzellen ergab ein diffuses Verteilungsmuster, was darauf hindeutet, dass keine Interaktion zwischen diesem Segment und anderen Proteinen des Sarkomers stattfindet. Daher scheint dieses EH-Segment dem Myomesinmolekül eher zusätzliche Elastizität und Flexibilität zu verleihen; Eigenschaften, die im embryonalen Herz besonders wichtig sein könnten. Zusätzlich wurde mit den isoformspezifischen Myomesinantikörpern die Myofibrillogenese im embryonalen Hühnerherz untersucht und es konnte festgestellt werden, dass Myomesin ein essentieller Teil eines Grundgerüstes aus Zytoskelettproteinen ist, das zum Zusammenbau des Sarkomers benötigt wird.

Chapter 1:

ACTIN ISOFORMS EXPRESSION DURING THE REMODELLING OF CYTOARCHITECTURE IN CULTURED CARDIOMYOCYTES

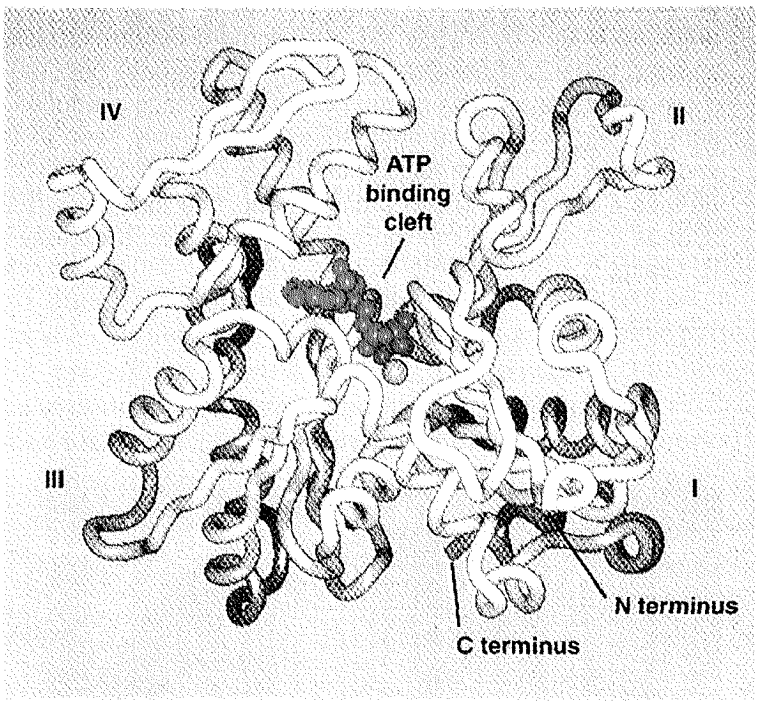

Figure 1.1.1: Atomic structure of actin monomer. Actin is a globular protein with molecular weight close to 42 kD. Actin monomers (also known as globular or G-actin) have four approximately equal size subdomains separated by a cleft. Each mole of actin also carries one mole of ADP or ATP (shown in red) and one divalent cation (the yellow ball). The N- end C-termini lies in the subdomain I. Adapted from Schutt *et al.*, (1993).

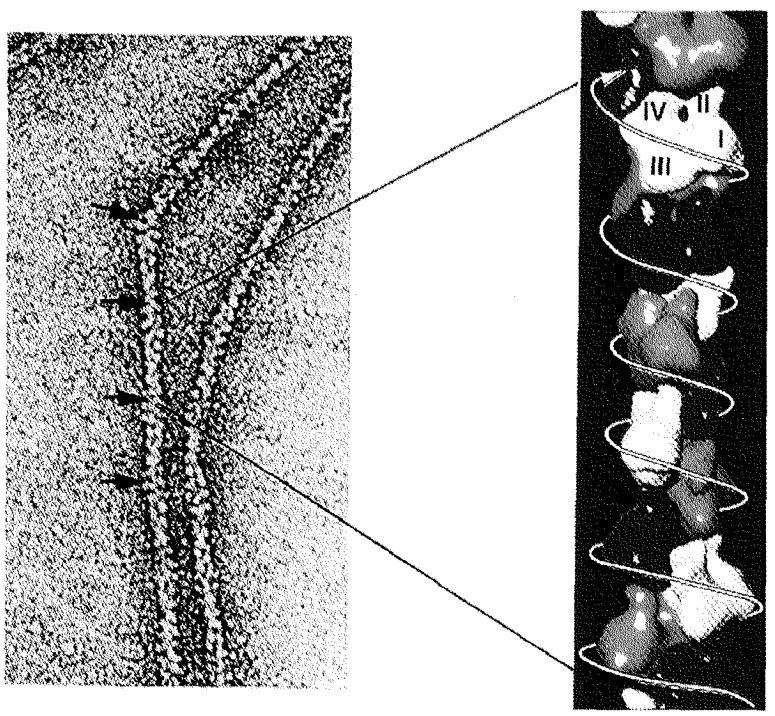

Figure 1.1.2: Packing of actin molecules in a filament. Under physiological conditions G-actin polymerizes into double helical filament structure (F-actin). The F-actin helix has a diameter of about 9 nm, with 13 actin molecules per 6 turns and repeats axially after about 36 nm. Each monomer in helix contacts with the neighbors above and below it and with whose from opposite strand. Adapted from Schmid *et al.*, (1994).

1.1 Introduction

1.1.1 The structure of actin

Actin is one of the most conserved and ubiquitous proteins in nature. Its presence in all eukaryotic species suggests that it was the development of the supporting actin cytoskeleton that allowed the first eukaryots to dispense with the prokaryotic cell wall and become motile predators. Actin can assemble into many structures and participates in a wide range of processes in eucariotic cells. It plays an essential role in maintaining the cell shape, cell motility, phagocytosis, cytokinesis and muscle contraction.
Actin is a globular protein with a single polypeptide chain of about 375 amino acids and molecular weight close to 42 kD. The actin molecule consist of two halves, each of these is further subdivided into two subdomains (see Figure 1.1.1). There is a deep cleft between the halves, which is responsible for harboring the nucleotide (ATP or ADP) and the divalent ion (Mg^{2+} or Ca^{2+}) (Kabsch et al., 1990).
In low salt buffer, actin is a monomeric globular protein (G-actin), but under physiological conditions it associates into a double helical filament structure (F-actin) (Pollard, 1990). The polymerization is a dynamic process that is regulated by the hydrolysis of a tightly bound nucleotide. The F-actin helix has a diameter of 90 Å with 13 actin molecules per 6 turns and repeats axially after about 360 Å (see Figure 1.1.2). The rotation per molecule is about 166° giving the overall appearance of two right-handed steep helices which wind gradually around each other (Holmes et al., 1990). Each monomer in F-actin contacts its neighbors above and below it and those from the opposite strand. Actin filament has a polarity because the actin monomer is asymmetric. The association kinetics of monomers is different at actin polymer ends (Pollard, 1990). The so called barbed (fast growing) and pointed (slow growing) ends of actin filaments can be determined by decoration with myosin S1 fragments which form arrow heads pointing towards the pointed end.

1.1.2 The thin filament

The ability of actin to polymerize-depolymerize reversibly is the major reason for the many forms of activity. Actin is involved in a wide range of cellular structures, from the stiff core of microvilly to the dynamic microspikes and lamellipodia at the leading edge of a migrating cell. A comparatively new evolutionary achievement is its participation in muscle contraction, the basis of which is the sliding of myosin along the actin filament. The length of actin (e.g. thin) filament in striated muscles is precisely regulated by its interaction with a group of associated actin-binding proteins. According to current opinion the main element of the controlling mechanism for thin filament length in skeletal muscles is nebulin (Trinick, 1994). Immunoelectron microscopy studies indicate that a single nebulin molecule extends from the Z-disk to the thin filament pointed end (Wang and Wright, 1988). Tropomyosin and troponin tightly associated with thin filament are responsible for the regulation of the Ca2+ mediated muscle contraction (Farah and Reinach, 1995). The working model of the thin filament structure in skeletal muscle (adapted from (Kreis and Vale, 1999)) is shown in the Figure 1.1.3. In this hypothetical model, each of the seven-

module nebulin super-repeats binds one tropomyosin and one troponin complex, consisting of troponin T, troponin I and troponin C subunits. Two strands of this regulatory chain wind around the outer actin domains along the double-helical filament. Tropomodulin is supposed to cap the actin filament pointed end and also plays an important role in the regulating of the thin filament length (Gregorio and Fowler, 1995). It remains unclear however, how the length of the thin filament is controlled in cardiac muscle which does not contain nebulin (Trinick, 1994). A similar protein found in cardiac muscles, nebulette, is much shorter than nebulin and extends only a short distance along the actin filament (Moncman and Wang, 1995). The comparison of primary sequence of this two proteins suggested that nebulette is the functional homolog of up to 100 kDa of nebulin's C-terminal segment (Moncman and Wang, 1999). Therefore, nebulette is predicted to substitute the Z-disk integrative function of nebulin in the heart muscle (Millevoi et al., 1998). However, some other proteins, one of them might be cardiac isoform of tropomodulin (E-Tmod), are responsible for the regulation of the filament length in cardiac muscle (Almenar-Queralt et al., 1999).

1.1.3 The Z-disk structure

The barbed ends of actin filaments are anchored to the Z-disk. Each actin filament overlaps with four filaments from the opposite sarcomer, forming a square lattice which is cross-connected in a ziz-zag pattern by Z-filaments, the latter are assumed to consist of α-actinin (Luther, 1991). The number of α-actinin crosslinks and therefore, the thickness of Z-disks vary in different muscle types, but is tightly regulated within a given myofibril (Squire, 1981). The nebulin mentioned above and the giant protein titin (Wang et al., 1979) are candidates for the organizing elements of the Z-disc assembly (for review see (Trinick, 1994). Recently the analysis of protein interaction between the main Z-disc components produced the model of molecular structure of the Z-disc (Young et al., 1998). According to this model (see Figure 1.1.4), two types of titin interactions are involved in the assembly of α-actinin into Z-disks. The first interaction (denoted by a big red circle on Figure 1.1.4) takes place between the single binding site on the titin and the two central spectrin-like repeats of the outermost pair of the α-actinin molecules. The second one takes place in the central part of the Z-disk, where titin interacts with multiple a-actinin molecules via their C-terminal domains. The titin N-terminus is presumably located in the vicinity of the barbed end of the actin filament, so that the regulatory phosphorylation site that was found previously (Gautel and Goulding, 1996) is involved in the control of the thin filament capping. Therefore, titin is responsible for constructing the central region of the Z-disks, including the number and positions of the α-actinin cross-links, while nebulin /nebulette could determine the ending of Z-disk structure and the transition to the I-band (Millevoi et al., 1998).

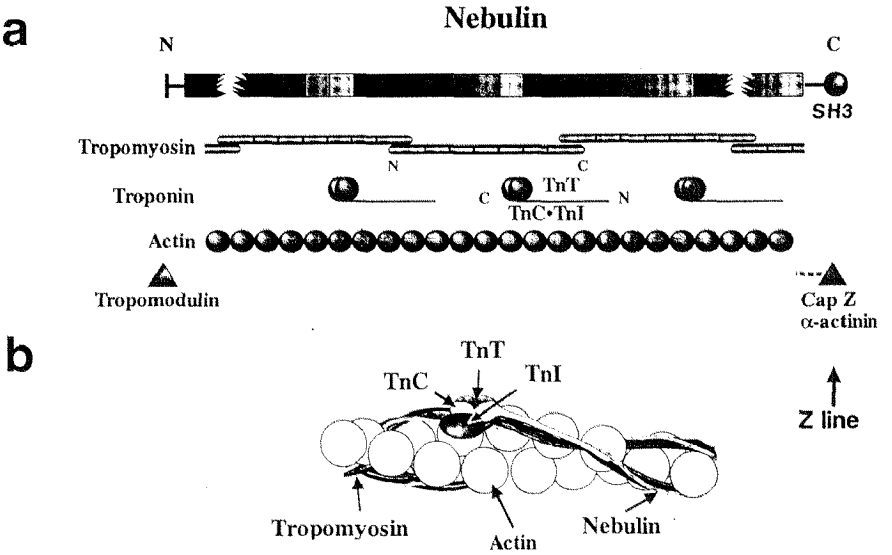

Figure 1.1.3: Thin filament structure.
a: Main structural components of the thin filament.
b: Hypothetical model of the regulatory complex associated with the thin filament of the skeletal muscle sarcomere. In this working model, each seven-module nebulin super-repeat binds one tropomyosin, possibly through the seven charged clusters along the length of tropomyosin, and one troponin complex, consisting of the TnT, TnI and TnC. Each nebulin super-repeat binds to seven actin monomers. Two strands of this regulatory complex are depicted as winding around the outer actin domains along the double-helical polymer. Tropomodulin is supposed to bind the pointed end of the actin filament. Adapted from Kreis and Vale, (1999).

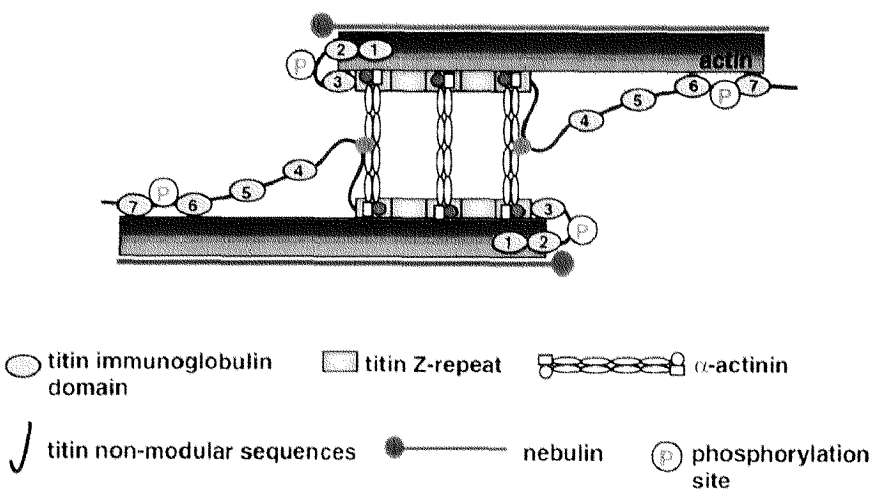

Figure 1.1.4: Molecular structure of the sarcomeric Z-disk. The most likely arrangment of titin is parallel to the thin filament for most of its lengh. Titin interacts via a single binding site with the central spectrin-like repeats of the outermost pair of α-actinin molecules (highlighted in big red circles). In the central Z-disks, titin interacts with multiple α-actinin molecules via their C-terminal domains (small red circle). The nebulin SH3 domain (green circle) and the proline-rich N-terminus of titin are in close proximity and could interact. The position of the SP-rich phosphorylation sites is shown. Only every second α-actinin molecule isn shown in the central Z-disk for reasons of simplicity. Adapted from Young *et al.*, (1998).

1.1.4 Actin isoforms

1.1.4.1 Classification of actin isoforms

Many organisms synthesize multiple isoforms of actin that are very similar in amino acid sequence. In mammals, there are at least six different actin isoforms, each encoded by a separate gene (for review see (Herman, 1993). The expression of each isoactin gene is regulated in developmental and tissue specific manner. All actins fall into three classes: α, β and γ-actins, depending on their isoelectric point (Garrels and Gibson, 1976). According to their tissue distribution and amino acid sequence these isoforms have been additionally sub-divided into muscle and cytoplasmic actins (Vandekerckhove and Weber, 1981). The muscle group consists of skeletal α, cardiac α, and smooth muscle α–actin isoforms which are found in skeletal, cardiac and smooth muscle tissue respectively (McHugh and Lessard, 1988; Otey et al., 1988). Enteric γ (also called smooth muscle γ–actin) isoform, which is accumulated in stomach, intestine and blood vessels also belongs to the muscle actins (McHugh and Lessard, 1988; Otey et al., 1986). The cytoplasmatic group consists of β-and γ-actins, which are major cytoskeletal proteins in non-muscle cells (Otey et al., 1986). The distinction between the muscle and non-muscle actins may be a characteristic of higher animals since it is also observed in insects but not in the nematode *Caenorhabditis elegans* (Mounier et al., 1992). Muscle actin genes are thought to derive from non-muscle actin genes by gene duplication and subsequent divergence events. Interestingly, skeletal and cardiac α-actins genes are single copy, whereas the cytoskeletal actin genes are present in multiple copies in human genome (Ponte et al., 1983).

1.1.4.2 The most differences between actin isoforms are concentrated on the N-terminus

Vertebrate actin isoforms are composed of 374 or 375 amino acids and display more than 93% identity at the amino acid level. The most striking is the strong conservation of actin throughout the evolution. There is, for instance, 93-97% similarity between actins from the human to Drosophila (Mounier and Sparrow, 1997). Most of the heterogeneity between the actin isoforms is in the N-terminus (Vandekerckhove and Weber, 1978). This isoform specific region of the actin molecule is directly involved in binding to myosin and is also very important for regulation of polymerization (Chaponnier et al., 1995). A recent study based on the comparison of the atomic models for G- and F-actins proposed that a N-terminal protruding region is responsible for most of structural and functional difference between isoactins: it is more compact and less flexible in muscle than in nonmuscle actins (Mounier and Sparrow, 1997). This adaptive change may have permitted new or better interactions of muscle actins with some muscle-specific ligands; for instance, it may have optimized the interaction with myosin by muscle contraction.

1.1.4.3 Biochemical differences between actin isoforms

The differential expression of the isoactins as well as the high conservation of the specific isoforms between the species indicates the functional importance of actin isoforms. Considerable efforts have been made to understand how the different isoforms fulfil their various functions despite their extremely high sequence identity. Many studies reported isoactin-specific behavior in vitro. The main observations are the following:

- Polymerization characteristics of the muscle and non-muscle actin, although similar, are not exactly identical (Gordon et al., 1977; Kabsch and Vandekerckhove, 1992).
- In cell-free system muscle α-actin incorporates 3 times more efficiently than β-cytoplasmic actin into isolated myofibrils (Peng and Fischman, 1991).
-The actin gels, formed from different isoforms have different viscoelastic properties (Allen et al., 1996).

These observations allow one to speculate that different behavior in vitro reflects the isoactin functional diversity in vivo but do not explain how the minimal sequence differences lead to diverse biochemical properties or how these differences help actin isoforms to fulfil the specific functions in vivo.

1.1.5 Subcellular sorting of isoactins

1.1.5.1 Investigation strategies

One approach to the problem of isoform function has been to study whether actins are separated in specialized locations within the cell. The evidence for subcellular sorting of isoactins comes from the numerous studies including isoform-specific antibody, mRNA localization studies, cDNA transfection and gene replacement studies [for review see (Gunning et al., 1998; Herman, 1993). One of the biggest problems of the first immunochemical studies was that the specificity and reactivity of antibodies was insufficient to allow definitive conclusion concerning actin isoform localization. Because the isoforms of this highly conserved protein are very similar in sequence, it has been difficult to obtain useful actin antibodies that bind specifically to only one actin isoform. The problem was solved by using the variability at the N-termini of the actin molecule as a key for producing isoform-specific antibodies (Gimona et al., 1994; Otey et al., 1986; Skalli et al., 1988; Skalli et al., 1986; Yao et al., 1995). In order to distinguish reliably between different α-actins the corresponding isoform specific antibody has to be sensitive to the exchange of only two adjacent amino acids in the N-terminal peptides (Chaponnier et al., 1995; Clement et al., 1999; Otey et al., 1988).

1.1.5.2 mRNA determines the actin localization

Although the amino-acid sequence is nearly identical between the actin isoforms, the actin mRNA 3' UTR are isoform unique and evolutionarily conserved (Ponte et al., 1983; Vandekerckhove and Weber, 1984). Thus, the sorting might easily occur at the level of mRNA that can be translated many times, making it an efficient mechanism for producing high local protein concentration. The concept that mRNA can be localized at special sites was pioneered by the work of Singer and co-workers, who demonstrated the association of the β-actin mRNA with the motile regions in fibroblasts (Lawrence and Singer, 1986). Two studies have shown that β-actin message accumulates at the periphery of cultured myoblasts, whereas the messages for α- and γ-actin are restricted to the perinuclear region (Hill and Gunning, 1993; Kislauskis et al., 1993). The convincing evidence for the direct relationship between the sorting of mRNA and the corresponding protein is given by the observation that inhibition of the peripheral localization of β-actin mRNA results in a dramatic change in lamellipodial structure (Kislauskis et al., 1994) and reduces cell motility

(Kislauskis et al., 1997). The same group of investigators identified a 54-nucleotide stretch of the 3' UTR that is responsible for cortical β-actin message localization (Kislauskis et al., 1994). The ability of this "zipcode" to control mRNA sorting is both sequence and position-dependent. Surprisingly, recent studies in our laboratory reveal that exogeneous β-actin is recruited to cellular protrusions even in the absence of the β-actin 3' UTR within the expression constract (von Arx et al., 1995). These results indicate that in addition to mRNA sorting some different mechanisms are needed to selectively direct the β-actin protein into the membrane cytoskeleton.

1.1.5.3 Actin-bindings protein can facilitate the actin sorting

The association of actin-binding proteins with actin is necessary for modulating the behavior and organization of the actin cytoskeleton (for review see (Ayscough, 1998)). In this way isoform-specific actin binding proteins can contribute to the specific tasks of isoactins in the cell and participate in the actin sorting (Sheterline et al., 1995). It was shown that the actin monomer sequestering proteins profillin and thymosin β4 have significantly greater affinities for the non-muscle than for muscle isoactins (Weber et al, 1992). It is plausible then, that isoform-specific monomer sequestering or filament binding proteins determine whether a particular isoform of actin is incorporated e.g. into contractile structures or into spreading cytoplasmic structures.

Recent reports demonstrate that the membrane-cytoskeleton linking proteins can participate in the actin sorting. It was shown that ezrin preferentially associates with β-actin filaments and some unknown actin-binding protein participates in this interaction (Shuster and Herman, 1995). It is consistent with the striking colocalization of the β-actin and ezrin, which was demonstrated in gastric parietal cells (Yao et al., 1995). A success of the Herman group was the characterization of this mysterious intermediary between β-actin and ezrin, that they named βcap73, because of its isoform-specific interactions with the barbed end of actin filaments (Shuster et al., 1996). Together, ezrin and βcap73 may represent a novel isoactin-specific filament capping complex, coordinatly acting to direct β-actin filaments to the cortical cytoplasm.

1.1.5.4 β-actin is sorted to the structures having high capacity of remodelling

Practically every paper dealing with isoactin sorting mentions β-actin and this demonstrates its special status among other isoforms. The accumulation of β-actin at the cell periphery was reported in myoblasts (Hill and Gunning, 1993; Kislauskis et al., 1993), fibroblasts (Hill et al., 1994) and neurons (Hannan et al., 1998; Kaech et al., 1997). According to these observations the location of the β-actin mRNA and protein to the regions associated with cell motility is unique to this isoform. The recent study demonstrated that during development, β-actin accumulation is observed in actively growing structures in neurons and in adult cerebellar cortex β-actin is preferentially found in the structures which are known to retain their capacity for morphological modifications (Micheva et al., 1998). Such a plentitude of papers demonstrating the specific sorting of β-actin not only reflects of the abundance of this isoform in different cell types but also indicate its strongest sorting capacity among all actin isoforms.

1.1.5.5 Actin sorting in muscle cells

The convincing evidence for the efficient actin sorting came from the study of smooth muscle cells, there β-actin isoform is clearly located in the cytoskeletal compartments, whereas the smooth muscle isoforms was found in the myosin-containing contractile regions (DeNofrio et al., 1989; North et al., 1994). The situation in striated muscle seems to be more controversial. According to prevalent opinion, the sarcomeric actin isoforms form the thin filaments of contractile apparatus, whereas the non-muscle isoforms participate in a non-sarcomeric cytoskeleton (Gunning et al., 1998). This conclusion is based on the observations that β-actin in skeletal myocytes is associated with plasma membrane and is highly enriched in neuromuscular junctions (Lubit, 1984) while γ-actin was found in costameres (filaments, linking Z-disks with the plasma membrane) and also in filaments, surrounding mitochondria (Pardo et al., 1983). Note however, that these studies are related to the adult muscles, where the cytoplasmic β– and γ-actin isoforms make up only a negligible fraction of total skeletal muscle actin. In contrast, considerable mixing of isoforms makes up the actin pool in the developing muscle (Gunning et al., 1998). Several independent studies demonstrate that non-muscle actins participate in the contractile apparatus of differentiating skeletal muscle (Gunning et al., 1998; Handel et al., 1989; Otey et al., 1988). Moreover, it was shown recently that microinjected β-and γ-actin can be incorporated into myofibrils in developing skeletal muscle cells, although less efficiently as the α-actins (Hayakawa et al., 1996). This suggests that during the early stage of myofibrillogenesis the sarcomeric and non-sarcomeric actin isoforms do not only coexist in the same cell but to some extent, are co-assembled in the contractile apparatus. It is likely that it is the gene regulation and not sorting that is responsible for the dominance of sarcomeric actins in adult sarcomeres.
The issue of β-actin presence in adult muscle cells remains so far unclear; according to some studies, β-actin is completely absent from striated muscles (Gimona et al., 1994; Glyn and Ward, 1998), whereas the other reports the expression of this isoform in the skeletal muscle cells (Otey et al., 1988) and myocardium (Carlyle et al., 1996).

1.1.6 Exchangeability of actin isoforms

The question if actin isoforms can replace each other remains mostly unresolved despite many attempts to address it using new methods. The difficulty of discriminating between the introduced and the endogenous actin have always hampered a study of the specific role of the particular actin isoform. Epitope tagging allows to overcome this problem by tracking the proteins with the antibodies directed against the tag (Soldati and Perriard, 1991). Insertion of the 11-amino acid peptide, derived from the vesicular stomatitis virus (VSV-tag) at the C-terminus of different actin isoforms has been used to study their distribution relative to the endogenous actin in fibroblasts and cardiomyocytes (von Arx et al., 1995). The four muscle actin constructs integrate preferentially into sarcomeric sites and did not noticeably disturb the cellular structure and function. In sharp contrast, the ectopic expression of the two cytoplasmic actin isoforms results in the rapid cessation of beating and induced severe morphological alterations characterized by an exceptional outgrowth of filopodia and cell flattening. These results emphasize the functional heterogeneity between different actin isoforms. This conclusion is further confirmed by the

observation that cytoplasmic actins are not able to complement muscle actins in the formation of contractile structures of indirect fly muscle of *Drosophila* (Schoenenberger et al., 1995).
Cardiac actin is the predominant isoform of actin in the adult vertebrate heart (Alonso et al., 1990) so it is not surprising that the majority of the cardiac α-actin deficient mice do not survive to birth and the rest generally die during the first two weeks (Kumar et al., 1997). It is amazing that these mice can be rescued by ectopic expression of the smooth muscle γ-actin in their hearts. However, this actin isoform can not restore all functions of the α-cardiac actin because the contractility rate is reduced in such rescued mice, obviously due to the small differences between cardiac α- and smooth muscle γ-actin.
From these observations one can conclude that the four muscle actins are to some extent interchangeable in their functions albeit the evolutionary new sarcomeric α-actins (cardiac and skeletal isoforms) are optimal for the effective interaction with myosin in striated muscle. Cytoplasmic actins belong to a separate category, they are not able to replace muscle actins in their contractile functions and are used to preserve cell shape and cell motility that is not related to myosin.

1.1.7 Actin isoforms expression in developed heart

As already mentioned above, the expression of actin is strictly developmentally regulated (Caplan et al., 1983). The cytoplasmic actins are ubiquitously expressed during development in striated muscle as well as in other cell types whereas at the adult stage the sarcomeric isoforms predominate (McHugh et al., 1991). The sarcomeric actins (skeletal and cardiac α-actins) accumulate rapidly with the onset of muscle fiber formation and at the same time the expression of non-muscle actins rapidly falls (Caravatti et al., 1982). Both sarcomeric actins are coexpressed in skeletal and cardiac muscle until birth, after which the α-actin isoform characteristic of the adult tissue rapidly becomes predominant (Gunning et al., 1998). The proportion in which the α-skeletal actin is expressed in myocardium drops from 40% by newborn rat myocardium up to less than 5% by adult animal (Carrier et al., 1992). It is interesting that adult mouse heart contains about the same amount of skeletal α-actin transcript (Garner et al., 1989), while myocardium of larger animals has much more. In adult pig, bovine and human heart the skeletal α-actin comprises about 20% of total actin (Vandekerckhove et al., 1986). Some works report that skeletal actin may even comprise more than 50% of the total actin in adult human heart (Boheler et al., 1991; Gunning et al., 1983). It is possible that this is due to pathological differences of the individuals examined, because increase in skeletal actin mRNA and protein expression has been demonstrated in some cases of myocardial hypertrophy (Clement et al., 1999; Schiaffino et al., 1989). The large variability in the expression of the sarcomeric actins in the adult myocardium of different species leads to the conjecture that these two isoforms are redundant and functionally indistinguishable (Bandman, 1992). However, it has not been excluded that after all there are some subtle differences in physiological properties between these two actins, although we cannot detect them, and that these differences represent functional "fine-tuning" of the system. Some insight is provided by the study of mutant BALB/c mice in which the increased level of α-skeletal actin transcript is correlated with increased heart contractility (Hewett et al., 1994).

In addition to two sarcomeric actins, the transient expression of the smooth muscle α-actin was detected in embryonic rat striated muscle (Woodcock et al., 1988). This actin is present in both cardiac and skeletal myocytes in significant amounts during most of the gestational development and is incorporated into sarcomeres (Sawtell and Lessard, 1989). Also, smooth muscle α-actin was proposed as an "embryonic sarcomeric actin" during chicken heart development (Ruzicka and Schwartz, 1988). Consequently, the expression of this isoform might change during development, it might also happen in certain physiological, experimental and pathological situations (Skalli et al., 1988). Work from our laboratory has shown that adult rat cardiomyocytes, after some period of cultivation, can re-express the fetal isoform of α-smoth muscle actin, which was considered as a sign of hypertrophic response (Eppenberger-Eberhardt et al., 1990).

1.1.8 Cardiomyocytes in culture

1.1.8.1 Cultivated cells as useful experimental model

Cells for culturing are isolated from the original tissue by mechanical or enzymatic disaggregation. The extraction of cells from the three-dimensional surrounding, destroying the cell-cell contact sites and subsequent cultivation on two-dimensional substrate leads to a loss of specific interactions and to the appearance of new cytoskeletal characteristics. The culture environment also lacks many components involved in homeostatic regulation. Most of the cell cultures require a supplement of serum that contains many undefined elements such as hormones, growth factors and other regulatory components. Thus, the conclusions obtained in cell culture should be carefully applied to the behavior of these cells in vivo. One major advantage of a cell culture is the possibility to control the physiochemical environment (pH, temperature, O_2 or CO_2 content) and physiological conditions which can be kept relatively constant. Another advantage is a good accessibility of single cells compared to the observation of cells in situ that is rather difficult.

1.1.8.2 Cultivated adult rat cardiomyocytes

In order to isolate single cells from adult rat heart, the tissue is exposed to proteolitic enzymes that cleave the connection of individual cells with the extracellular matrix. After the isolation two types of cells are observed: the typical rod-shaped and round cells that seem hypercontracted. In serum-containing media the cardiomyocytes gradually attach to the substrate and begin to spread (Eppenberger et al., 1988; Eppenberger-Eberhardt et al., 1990). At the same time, the myofibrillar apparatus degenerates, at least partially, and spontaneous beating stops. Both initially distinct cell species develop pseudopodia, flatten and become indistinguishable. Some time later, new myofibrils appear in the central perinuclear region near the substratum (Messerli et al., 1993). Simultaneously, the ARCs actively synthesize the proteins while the volume of cells, cultured for 12 days in vitro is more than twice as big as the volume of freshly isolated cells (Rothen-Rutishauser et al., 1998). The significant increase in mass per cells reflects the hypertrophic reaction which may be comparable to certain aspects of cardiac hypertrophy occuring in vivo (Messerli et al., 1993; Rothen-Rutishauser et al., 1998; Schaub et al., 1997). In the course of growth and

spreading the cardiomyocytes gradually reestablish the intercalated discs like structures at sites of intercellular contacts (Eppenberger et al., 1995; Eppenberger and Zuppinger, 1999). After the re-assembly of their sarcomeric structures, cardiomyocytes restore the functional beating phenotype, which is closely related to the one in vivo, but is different with respect to the orientation towards the substrate. The primarily bipolar and rod-shaped cells acquire a flat and polygonal cell shape. In the native cardiac cell all myofibrils run in parallel to the long axis whereas the myofibrils of the cultured cells do not have a preferred orientation (Eppenberger et al., 1988; Messerli et al., 1993).
In addition to the sarcomeric apparatus the new cytoskeletal structures are developed in the cell periphery. These structures were defined as premyofibrils in cultured embryonic chicken cardiomyocytes (Rhee et al., 1994) and stress-fiber-like structures (SFLS) in cultivated rat cardiomyocytes (Dlugosz et al., 1984; Harder et al., 1998; Messerli et al., 1993). The typical myofibrillar proteins such as C-protein, myomesin and titin are absent in these structures while the others, such as actin, myosin and α-actinin lose their regular periodic distribution. The continuity between the myofibrils and the SFLS leads one to the assumption that these structures serve as molecular scaffold during myofibrillogenesis (Eppenberger et al., 1988; Messerli et al., 1993; Rhee et al., 1994).
The reorganization of cytoarchitecture in cultivated ARCs is accompanied by the re-expression of the fetal genes, like ANF, α-smooth muscle actin and β-MHC (Eppenberger-Eberhardt et al., 1990; Eppenberger-Eberhardt et al., 1993; Schaub et al., 1997). Reexpression of these genes also occurs during cardiac hypertrophy in vivo and is considered to be a marker for the hypertrophic reaction.

1.1.8.3 Cultivated newborn rat cardiomyocytes

In contrast to ARCs, the NRCs (newborn rat cardiomyocytes) isolated by spinner-flask method are round with intact sarcomeric structures near membranes (Rothen-Rutishauser et al., 1998). Similarly to ARCs, they reorganize their cytoskeleton but develop more quickly and start to beat after one day in culture (Goncharova et al., 1992). After 2-3 days in culture they are nicely filled with myofibrils and acquire the characteristic in vitro morphology. During 12 days of cultivation the NRCs increase their volume by a factor of 5 but never reach a volume comparable to cultured ARCs (Rothen-Rutishauser et al., 1998). A fast restoration of contractile properties of NRCs is favored by the preservation of intact sarcomeric structures during the isolation. Neonatal cardiomyocytes are less differentiated than adult cells and have a larger adaptational potential. It is possible that the NRCs have a more elastic cytoskeleton that is able to endure strong mechanical stress during the division of cardiomyocytes happening in embryonic heart.
The recent experiments in our lab have demonstrated that the intrinsic differences between NRCs and ARCs during adaptation to cell culture conditions are also reflected in a distinct response to agents, which affect cytoskeleton. In contrast to ARCs, NRCs were able to spread and generate the new myofibrils even after the destruction of their microtubules (Rothen-Rutishauser et al., 1998).

1.1.9 Aim of this study

Cultivated cardiomyocytes have been used recently in numerous studies of cytoskeleton remodeling, myofibrillogenesis and hypertrophic responce (Claycomb and Palazzo, 1980; Eppenberger et al., 1988; Harder et al., 1998; Messerli et al., 1993; Rhee et al., 1994; Schaub et al., 1998). The rearrangement of cytoskeleton clearly divides the cell into two different regions: the central sarcomeric field and peripheral region where actin is organized in SFLS (stress fiber-like structures). The differences between these regions were demonstrated by the myosin light chain sorting experiments (Soldati and Perriard, 1991). Thus, the presence of the functional myofibrils coexisting with well-developed cytoskeleton in the same cell makes cultivated adult and newborn rat cardiomyocytes a well-suited system for the study of differential sorting of isoactins. It remains unclear what kinds of isoactins participate in new non-sarcomeric structures that appear during the cytoskeletal rearrangement. Moreover, it seems very likely that the fast re-building of cytoarchitecture in cultivated cardiomyocytes are followed by changes in the actin isoforms expression. This was supported by the discovery that cardiomyocytes re-express the fetal isoform of α-smooth muscle actin after some period of cultivation (Eppenberger-Eberhardt et al., 1990). Interestingly, in the cardiomyocytes, which begin to produce this actin isoform, it was found predominantly in the stress fiber-like structures. The reason and the mechanism of this sorting in ARCs remain unexplained because in NRCs the anti-smooth muscle α-actin antibody uniformly stains both stress fiber-like structures and sarcomeres. It has not been checked yet whether cardiomyocytes also reexpress some cytoplasmic actin isoform that can participate in the formation of non-sarcomeric structures. This assumption looks very attractive because β–actin was reported to accumulate in the regions that have the high capacity for remodelling.

To summarize, the goal of my work was to analyze the expression and localization of actin isoforms during the remodelling of cytoskeleton in cultivated adult and neonatal rat cardiomyocytes.

1.2 Results

1.2.1 Reorganization of actin cytoskeleton during cultivation of cardiomyocytes

Initially, after isolation from the tissue, the adult rat cardiomyocytes have a rod-shape form the same that they had in vivo. However, when put into culture in the presence of serum they first round up, their myofibrils contract and lose practically all noticeable features of sarcomeric organization. During the first days in vitro they attach to the substratum and begin to flatten. After some time the newly formed myofibrils assemble in the central part of the cell around the nuclei and the cells start to beat. After about one week in culture the adult rat cardiomyocytes acquire their characteristic morphology in vitro with the central perinuclear region filled with myofibrils and the peripheral region with SFLS (stress fibers like structures) fanning out in radial direction. It is not at all clear what happens with the preexisting sarcomeric elements during this process. To visualize the rearrangement of the actin cytoskeleton that takes place during the cultivation we performed the immunofluorescent staining of the ARCs, incubated for 4 days in vitro (Figure 1.2.1). In order to emphasize the morphological changes in the spreading cardiomyocytes the 3D images were reconstructed from the multilayered confocal data set (Figure 1.2.1, a and b). The corresponding superimposed images of one layer near the substratum that was doubly stained for F-actin (in green) and sarcomeric marker myomesin (in red) are shown in a' and b'. The regeneration process typically is asynchronous in different cells and thus one observes different stages in the same culture. Three different types of cells (denoted as 1, 2 and 3 in Figure 1.2.1) can be clearly distinguished in this culture. Type 1 represents rod-shaped cells that still preserve sarcomeric organization of actin and myomesin. Type 2 denotes cells that lost the sarcomeric organization of actin but preserved some periodic organization of myomesin. Finally, type 3 covers the cells that has already spread on the bottom of the culture dish and began to rebuild their sarcomeric apparatus. In the latter the periodic organization of actin and myomesin can be clearly seen in the perinuclear region whereas in the peripheral flattened regions actin forms the SFLS that participates in attachment to the substrate. If cultivated further, the cardiomyocytes continue to develop new sarcomeric apparatus; depending on the culturing conditions the myofibrils either fill almost all cell volume or remain restricted to the central perinuclear region (Harder et al., 1996). This experiment shows that during the first days in vitro the cardiomyocytes lose all preexisting sarcomeric actin organization and begin to build new myofibrils and actin containing structures that are not observed in situ. Further, in our work we investigate which isoactins participate in the formation of new cytoskeletal structures during the cardiomyocytes remodelling.

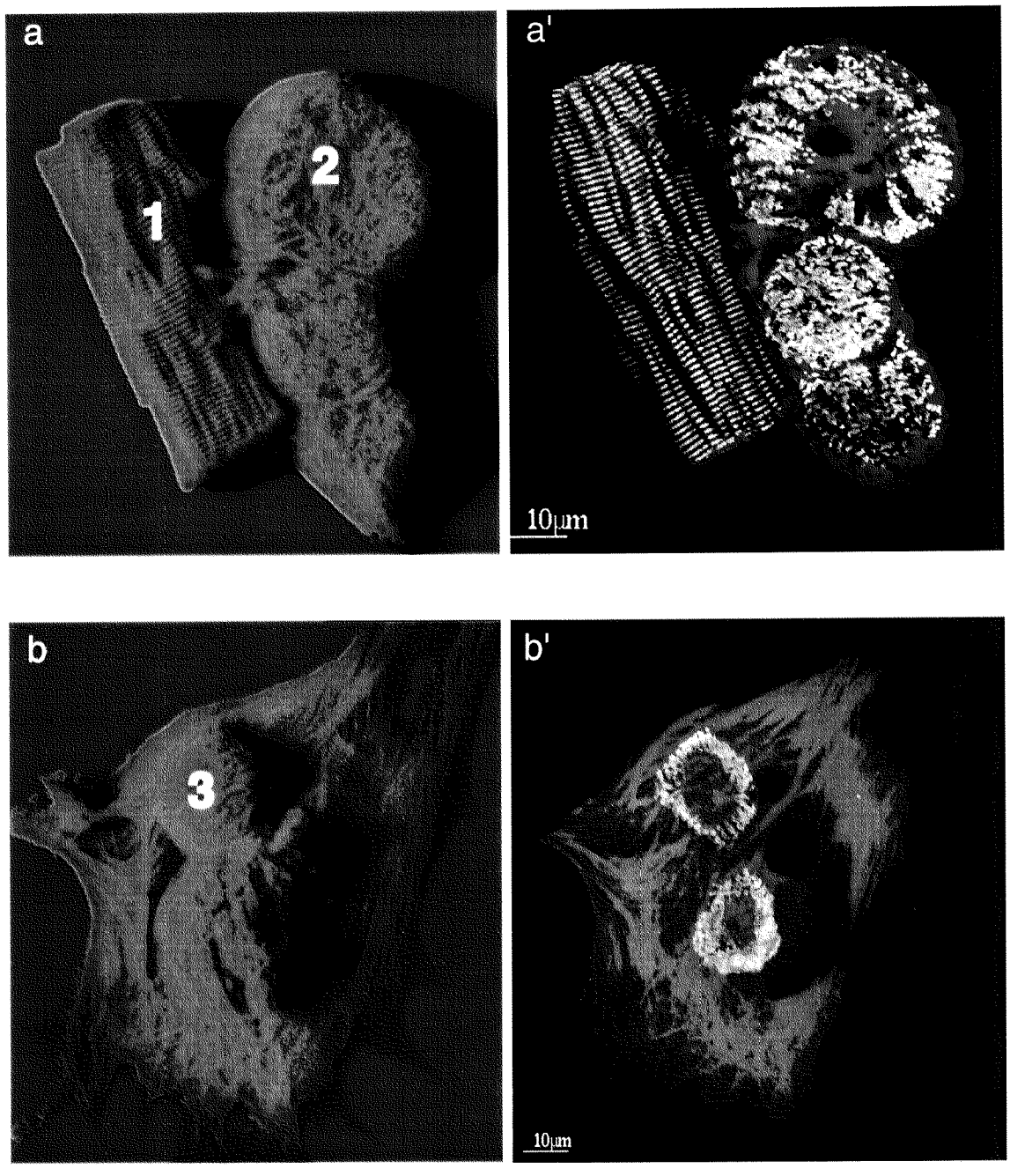

Figure 1.2.1: ARCs, placed for 4 days in culture begin to reorganize their actin cytoskeleton. 3D reconstructions of F-actin stainings are shown in a and b, the superimposed images of one layer, stained for F-actin with phalloidin (green) and the sarcomeric marker myomesin (red) are shown in a' and b'. Three different types of cells (marked 1, 2 and 3) can be clearly defined in culture: type 1 represents rod-shaped cells with preserved sarcomeric organisation of the actin, type 2 represents rounded (contracted) cells where the cross-striation of actin is lost, and type 3 represents cells, which begin to spread and to rebuild the sarcomeric apparatus. Scale bars 10 µm.

1.2.2 Expression of isoactins in cardiomyocytes

1.2.2.1 Experimental set up

To investigate the expression of actin isoforms we keep the ARCs and NRCs for different periods in culture and study them via isoform-specific antibodies using immunofluorescence and western blot analysis. We began by making a few preliminary experiments in order to estimate the suitability of each of the available antibody for these methods of investigation. The results are shown in Table 1.1.

N	Name	Source	Isoform Specificity	Immunoblot	IFS
1	monoclonal anti-sarcomeric α-actin (5C5)	Sigma	skeletal α cardiac α	+	+/-
2	monoclonal anti-cardiac α-actin (Ac-1)	Progen	skeletal α cardiac α	+	+
3	monoclonal anti-smooth muscle α-actin (1A4)	Sigma	sm α	+	+
4	polyclonal anti-cytoplasmic α-actin (G2)	gift from J.C.Bulinski	cyt. γ sm γ sm α	+	+/-
6	monoclonal anti-cytoplasmic β–actin (A5441)	Sigma	cyt. β	+	+
5	polyclonal anti-cytoplasmic β-actin poRaβcyto	gift from C. Chaponnier	cyt. β	+	+

Table 1.1: The summary of the antibodies against different actin isoforms, which are used in the study. sm denote smooth muscle, cyt denote cytoplasmic; IFS denote immunofluorescent staining; + means "react well", - means "no reaction", +/- means "variable and unspecific staining".

This table demonstrates that several antibodies do not identify actin isoforms unambiguously; namely, the 5C5 antibody reacts with both skeletal and cardiac α-actin isoforms (Skalli et al., 1988) while anti cytoplasmic γ-actin antibody reacts with even three isoforms: cytoplasmic γ-, smooth muscle γ- and smooth muscle α-actin isoforms (Otey et al., 1987). Recently, another actin isoform specific antibody, Ac-1, was produced; it was claimed that it reacts only with cardiac α-actin isoform (Franke et al., 1996). In order to establish its suitability for our task we have performed a number of tests. We found that their reactivity in western blot does not differ from the antibody against sarcomeric actin 5C5. The Ac-1 antibody reacts with neither erythrocyte nor with fibroblast extracts but reacts identically strong with the blotted extracts of cultivated NRCs and ARCs (data not shown). Since it is established that the relative amount of cardiac α-actin in adult rat myocardium is significantly different from the one of newborn animals (Carrier et al., 1992) a distinct reaction was expected if the Ac-1 antibody really recognizes only the cardiac isoform. The absence of such difference lead to the conclusion that this antibody reacts equally well with both sarcomeric isoforms, analogously to 5C5 antibody. This is not unexpected because Ac-1 antibody was generated against the cardiac α-actin N-terminal decapeptide that differs from the corresponding fragment of skeletal α-actin only by the

Glu-Asp transposition in positions 2 and 3 (Vandekerckhove and Weber, 1978). However, Ac-1 antibody has significant advantages compared to 5C5 antibody for immunofluorescent staining because it provides better signal resolution and less background. This is why we have chosen this antibody for this analysis (see Figure 1.2.5).

We also found that reactivity of some available actin antibodies varies in different assays . For instance, although 5C5 and G2 antibodies specifically recognize corresponding proteins in western blot analysis, they demonstrate a lot of unspecific staining by immunofluorescent detection. This result is not surprising because it is well known that the state of denaturation and accessibility of epitopes are different for western blot extraction and for immunofluorescence fixation.

1.2.2.2 The expression of the sarcomeric actin isoforms does not change significantly during the cultivation

To study whether the expression of actin isoforms changes during the cultivation we performed western blot analysis of extracts of NRCs and ARCs at different cultivation stages (Figure 1.2.2). Using the anti-sarcomeric actin antibody 5C5, we showed that the amount of corresponding protein varies in neither in NRCs cultured from zero to four days (Figure 1.2.2, a, lines 2 and 3), nor in ARCs cultured from zero up to 11 days (Figure 1.2.2, a, lines 4-8). However, small changes in the expression of these isoforms can not be detected in such assays because sarcomeric actins strongly dominate all other isoforms in the adult rat myocardium (Vandekerckhove et al., 1986).

1.2.2.3 Expression of smooth muscle α-actin is upregulated in ARCs

In the next experiment we probed the same extracts with the monoclonal antibody against the smooth muscle α-actin 1A4 (Figure 1.2.2, b) and with polyclonal antibody against smooth muscle γ-actin G2 (Figure 1.2.2, c). Both antibodies did not show much difference of expression of these isoactins between the freshly isolated NRCs and NRCs after four days of incubation (lines 2 and 3), whereas the strong difference is evident in ARCs (lines 4-8). The freshly isolated ARCs do not express smooth muscle α-actin isoform (line 4), but re-express it after about one week in culture (lines 7 and 8). This is consistent with classical results from our laboratory (Eppenberger-Eberhardt et al., 1990). In the case of smooth muscle γ-actin the same tendency was observed with only one exception: a small amount of the protein is available also in the freshly isolated ARCs and ARCs after a few days of incubation (Figure 1.2.2, c, lines 4-6). But it has to keep in mind that this antibody crossreacts with all three isoactin: cytoplasmic γ-, smooth muscle γ- and smooth muscle α-actin isoforms (see Table 1.1). It is very likely that in this blot the superimposition of the expression pattern of the smooth muscle α-actin and the weak steady expression of the cytoplasmic γ-actin is observed, as far as the absence of the smooth muscle γ-actin from myocardium was established on the both mRNA (McHugh et al., 1991) and protein level (Sawtell and Lessard, 1989).

1.2.2.4 The monoclonal and polyclonal anti-cytoplasmic β-actin antibody produce contradictory results in cardiomyocytes

The most puzzling results were observed in the blots incubated with different antibodies against cytoplasmic β-actin (Figure 1.2.2, d and e). To clarify the situation equal amounts

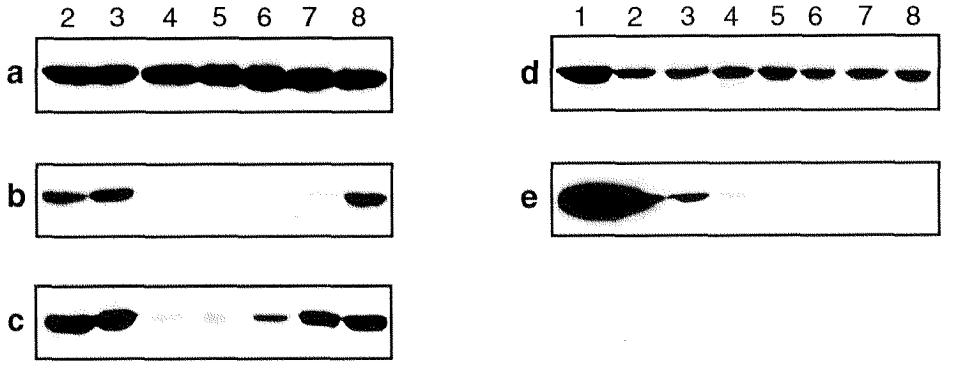

Figure 1.2.2: Expression of different actin isoforms in cultured rat cardiomyocytes. Extracts of fibroblasts from newborn rat (1), freshly isolated NRCs (2), NRCs cultured for 4 days (3), freshly isolated ARCs (4), ARCs, cultured for 2 days (5), 4 days (6), 7 days (7) and 11 days (8) were probed with an antibody against sarcomeric α-actin 5C5 (a), anti-smooth muscle α-actin antibody 1A4 (b), anti-cytoplasmic γ-actin antibody G2(c), a polyclonal anti-cytoplasmic β-actin antibody pRabcyto (d) and a monoclonal antibody against cytoplasmic β-actin antibody A5441(e).

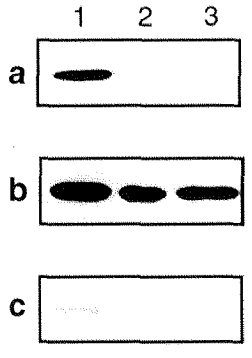

Figure 1.2.3: The reaction of the polyclonal antibody against cytoplasmic b-actin can be blocked with the specific peptide. Extracts of fibroblasts from newborn rat (1), NRCs cultured for 4 days (2) and ARCs cultured for 11 days (3) were probed with a monoclonal antibody against cytoplasmic β-actin A5441(a), a polyclonal antibody against cytoplasmic β-actin pRaβcyto (b) and the polyclonal antibody against cytoplasmic β-actin pRaβcyto, after preincubation with the peptide that was used for immunization (c).

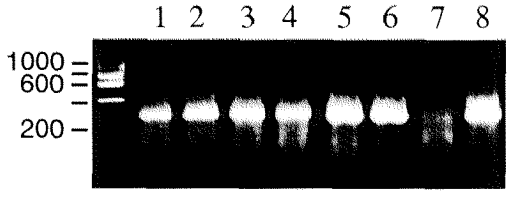

Figure 1.2.4: β-actin message is present in striated muscle extracts and in cardiomyocytes. RT-PCR analysis with β-actin specific primers of total RNA extracted from ARCs after 14 days in culture (1), NRCs after 4 days in culture (2), HH38 chicken heart (3), HH 38 chicken skeletal muscle (4), heart of newborn mouse (5), skeletal muscle of newborn mouse (6) and mouse kidney cells (8). Line (7) corresponds to the negative control (i.e. RT-PCR mix without template). Fragment sizes are indicated on the left in bp. A single product of 285 bp is amplified not only from striated muscle extracts of chicken and mouse (lines 3-6), but also from extracts of cardiomyocytes cultured many days in vitro, where the contamination of fibroblasts is negligible (lanes 1-2).

of extracts of myofibroblast isolated from the newborn rat were loaded to the gel together with the cardiomyocyte extracts (line 1). We see that both antibodies react strongly with the fibroblast extracts (line 1), this is not surprising because β-actin is one of the main components of cytoskeleton in this type of cells (Otey et al., 1986). However, these antibodies demonstrate the contradictory results by reacting with the cardiomyocyte extracts. Clearly, polyclonal anti-cytoplasmic β-actin antibody poRaβcyto shows the stable expression at all stages of cultivation in both NRCs and ARCs (Figure 1.2.2, d, lines 2-8), whereas the monoclonal antibody A5441 shows that the specific protein is practically absent in cardiomyocytes (Figure 1.2.2, e, lines 2-8). A weak response observed in NRCs and ARCs at the early stages of the cultivation might be explained by weak fibroblast contamination (Figure 1.2.2, e, lines 2, 3 and 4). The very strong reaction of the monoclonal anti-β actin antibody A5441 with the fibroblast extract (Figure 1.2.2, e, line 1) is due to the fact that this blot was overexposed in order to visualize the extremely weak reaction with the extracts of NRCs and freshly isolated ARCs. Since the absence of cytoplasmic actin expression from adult striated muscle was postulated, a plausible explanation of this contradictory result is unspecific crossreaction of the polyclonal anti-β actin antibody with some different protein. Therefore, before reaching any conclusions, we decided to verify the specificity of the anti-β-actin antibodies by immunological assays.

1.2.2.5 The staining of the polyclonal anti-β actin antibody can be blocked by synthetic peptide used for immunization

In order to characterize the specificity of polyclonal antibody against β-cytoplasmic actin we checked whether the staining with this antibody can be blocked by addition of β–actin N-terminal synthetic peptide which was used as immunogen for the generation of this antibody (Yao et al., 1995). The results are shown on the Figure 1.2.3. Contrary to the monoclonal antibody against β–cytoplasmic actin (Figure 1.2.3, a, lines 2 and 3), the polyclonal antibody recognizes specific protein in the cultivated NRCs and ARCs (Figure 1.2.3, b, lines 2 and 3), but does not react with the same extracts after preincubation with the blocking peptide (Figure 1.2.3, c). This experiment demonstrates that the polyclonal anti-β-actin antibody specifically recognizes some epitope in the β-actin N-terminal sequence.

Thus the difference in the results obtained with these antibodies might be explained by the presence of some, previously uncharacterized, form of β-actin in cardiomyocytes. Further, it could be assumed that this form is different by modification or substitution of a few amino acids on the N-terminus so that it is no longer recognized by monoclonal antibody, while polyclonal antibody react specifically with it. To check this hypothesis we checked whether β-actin message is present in cardiomyocytes and skeletal muscles.

1.2.2.6 RT-PCR analysis confirm the presence of β-actin in cardiomyocytes

To study whether the β-actin mRNA is present in striated muscle the RT-PCR analysis of total RNA isolated from cultivated rat cardiomyocytes, as well as from heart and skeletal muscles of different species was performed (Figure 1.2.4). Using the cytoplasmic β–actin specific primers a single product of 285 bp was amplified from NRCs and ARCs extracts (lines 1 and 2), from heart and skeletal extracts of chicken (lines 3 and 4) and mouse (lines 5 and 6). Although the signal from the striated muscle extracts might be explained by the

presence of myofibroblasts that get into the extract with myocytes, this explanation fails for cardiomyocytes after many days of cultivation where the fibroblast contamination is negligible due to the presence of ara C in the medium. The same product of 285 bp was amplified from mouse kidney cells extract which was used as a positive control (line 8) and no signal appeared in the same RT-PCR mixture without template which was used as negative control (lane 7). Thus, the RT-PCR assay confirms that the β-actin specific message is expressed in cultivated cardiomyocytes.

1.2.3 Localization of different actin isoforms in cultured ARCs

1.2.3.1 Sarcomeric actins participates in both the sarcomeric and the non-sarcomeric parts of cytoskeleton in cardiomyocytes

To find out whether there is some sorting of the sarcomeric actin in the cultivated cardiomyocytes we compared the immunostainings with Ac-1 antibody (which crossreacts with both cardiac and skeletal α-actins) of freshly isolated ARCs with ARCs after 11 days of cultivation (Figure 1.2.5). These isoactins localize in a typical myofibrillar pattern in the sarcomeres of both freshly isolated ARCs (Figure 9, a) and ARCs after 11 days in culture (Figure 9, b). However, in the latter ARCs, with already remodeled cytoskeleton, cardiac isoactin localizes equally well in SFLS (Figure 9, b). Thus, also the endogenous sarcomeric actins are not only able to form the thin filaments in the sarcomeres of the cultivated cardiomyocytes but also associate with SFLS in the non-sarcomeric part of the remodeled cytoskeleton.

1.2.3.2 Expression of smooth muscle α-actin does not influence the sarcomeric organization in ARCs

To study the localization of different actin isoforms we stained the ARCs after 11 days of incubation with actin isoform specific antibodies (Figure 1.2.6). The cells were stained for F-actin with phalloidin (a, red), cytoplasmic β-actin poRaβcyto (b, green) and smooth muscle α-actin 1A4 (c, white): the superimposed image is shown in (d). After 11 days in vitro the cells flattened and acquired the characteristic morphology of cultured cardiomyocytes with clearly distinguishable sarcomeric and non-sarcomeric compartments. Both cells shown in this figure have a well-developed sarcomeric apparatus despite the fact that one of them expresses smooth muscle α-actin whereas the other does not. In the positive cell this isoform is utilized in both SFLS and sarcomeric structures. This indicates that colocalization of α-smooth muscle actin with the other α-actins in the sarcomeric structure don't interfere with the formation of well-developed contractile apparatus in remodeling ARCs.

The anti-cytoplasmic β-actin antibody also stains the sarcomeric and non-sarcomeric regions of both cells (Figure 1.2.6, b). In the SFLS it colocalizes with the anti-smooth muscle α–actin and F-actin staining, but in the sarcomeres it stains somewhat narrower bands in the Z-discs (inserts). The superimposed image (Figure 1.2.6, d) clearly demonstrates that similar to many other polyclonal antibodies, the anti-cytoplasmic β-actin antibody poRaβcyto stains nuclei. We believe that this is more likely to be due to a weak

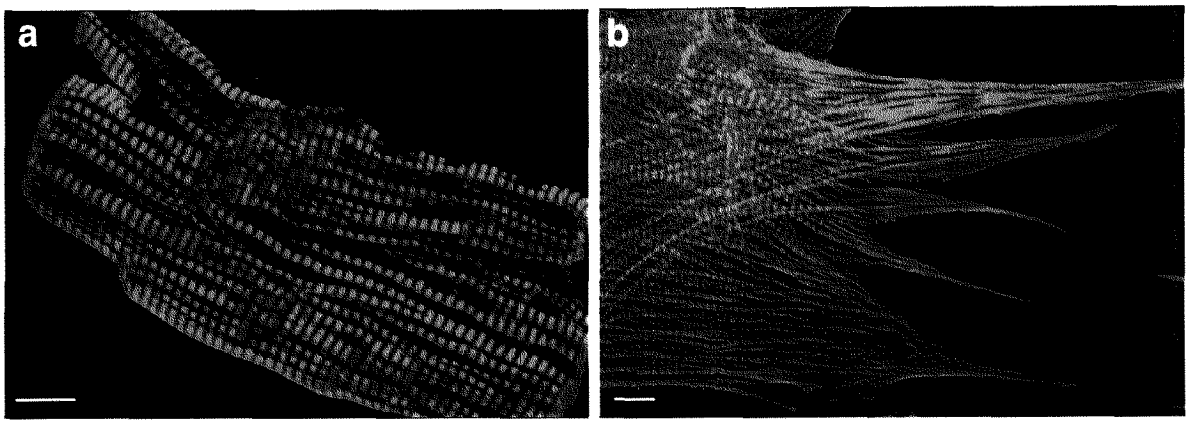

Figure 1.2.5: Sarcomeric actin participates in sarcomeric and non-sarcomeric cytoskeleton in ARCs equally well. Confocal images of freshly isolated, rod-shaped ARC (a) and ARC after 14 days in culture (b). The cells are stained with anti-cardiac α-actin antibody Ac-1. Scale bars 10 μm.

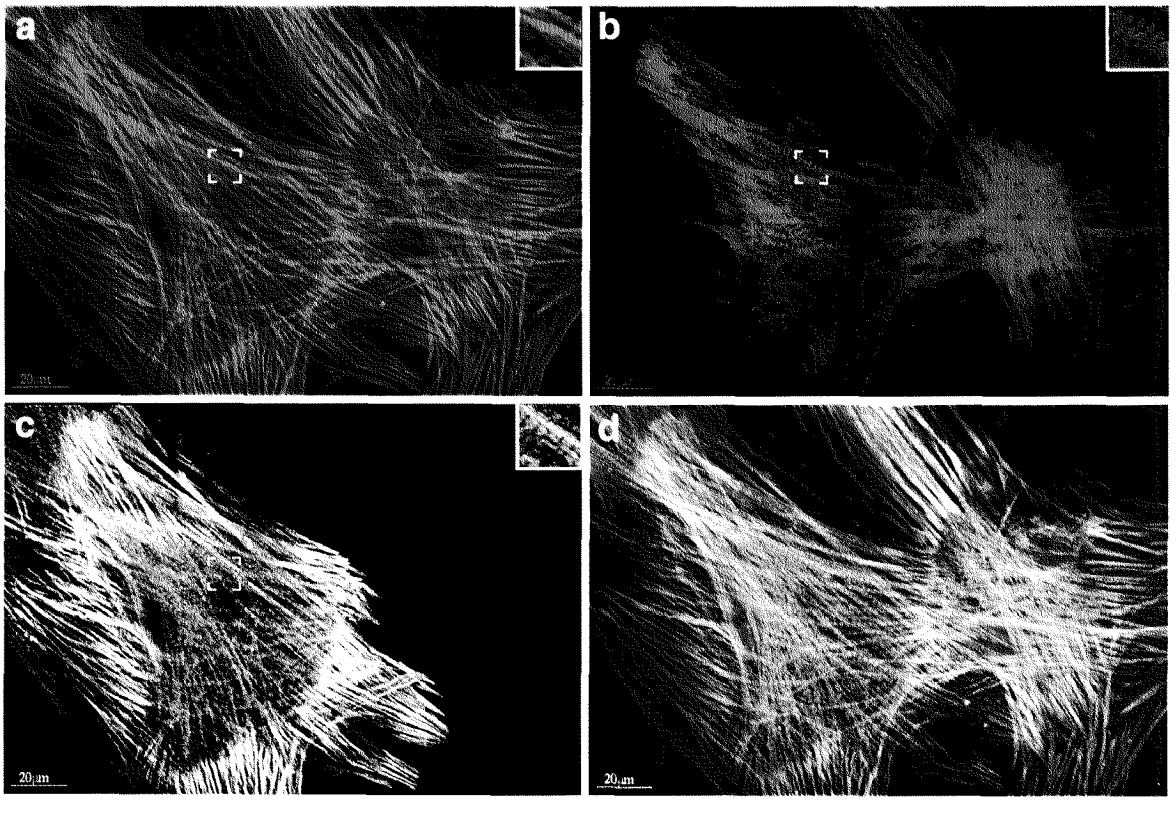

Figure 1.2.6: The expression of different actin isoforms in ARCs. Confocal images of ARCs after 11 days in culture. The cells are stained with phalloidin (a, red), anti-cytoplasmic β-actin antibody poRaβcyto (b, green) and anti-smooth muscle α-actin antibody 1A4 (c, white). (d) represents the superimposed image (the staining with 1A4 antibody is shown in blue). The inset pictures are two times magnified. Scale bars 20 μm.

crossreation of this antibody with some nuclear protein than to a presence of β-actin in the nucleus because neither phalloidin nor other anti-actin antibodies stain nuclei.
This experiment shows that, first, polyclonal antibody against β-actin specifically react with actin because the staining with this antibody overlaps F-actin staining in the SFLS. Second that the localization of the protein that is recognized by this antibody is slightly different from that of other actin isoforms in the sarcomere.

1.2.3.3 Cytoplasmic β-actin is localized in narrower bands as the muscle actins

Having found the expression and specific sorting of the β-actin isoform in the sarcomeres of ARCs, which already reorganize their actin cytoskeleton, we checked whether the same phenomena could be observed in the freshly isolated rod-shaped cardiomyocytes (Figure 1.2.7). The ARCs after one day of incubation are stained for phalloidin to visualize F-actin (a, red) and anti-cytoplasmic β-actin antibody poRaβcyto (b, green), the superimposed image is shown in (c). The cells are filed with myofibrils, while the both phalloidin and β-actin staining can be detected in all sarcomeres. The comparison of the bands, dyed with F-actin and anti-β-actin antibody reveals however that the latter are noticeably narrower.
Thus, this phenomenon is observed also in the cardiomyocytes that were freshly isolated from the heart and preserve their in situ organization and wherefore is not related to the process of cytoskeleton remodeling that begins later.

1.2.4 Localization of different actin isoforms in cultured NRCs

1.2.4.1 Smooth muscle α-actin participates in NRCs in both sarcomeric and non-sarcomeric cytoskeleton and colocalizes with sarcomeric α-actin

In order to verify our conclusions obtained for ARCs, we studied the localization of different actin isoforms in the cultivated neonatal rat cardiomyocytes. In contrast to ARCs in culture, NRCs rapidly assemble new sarcomeres and start to beat after less than one day in vitro. Figure 1.2.8 shows the NRCs after four days in culture that were stained with the antibody against sarcomeric α-actin 5C5 (a), anti-cytoplasmic β-actin antibody poRaβcyto (b) and anti-smooth muscle α-actin antibody 1A4 (c). Superimposed image is shown in (d). Here the cells are flattened and have formed new myofibrils, which take up almost all of the cell volume. Only one out of the two neighboring cells is positive in smooth muscle α-actin. This indicates that NRCs express this embryonic isoform heterogeneously similar to ARCs in culture. The stainings with the sarcomeric and smooth muscle α-actins specific antibodies coincide in the non-sarcomeric region of cytoskeleton, suggesting that isoactins can copolymerize in the stress-fibers like structures. Moreover, the sarcomeric and smooth muscle α-actin stainings overlap also in the sarcomeric region (inserts, a and c). Thus, both sarcomeric α-actins and smooth muscle α-actin are equally able to get incorporated in the sarcomeric and non-sarcomeric cytoskeleton of cultivated NRCs if both species are coexpressed

1.2.4.2 β-cytoplasmic actin localizes also in narrow bands in the Z-disks in NRCs

The staining with the anti-β-actin antibody poRaβcyto reveal that although β-actin colocalizes with the muscle actins in the SFLS in the cell periphery, its distribution in the sarcomeric region is noticeably different (Figure 1.2.8). Whereas the antibodies recognizing

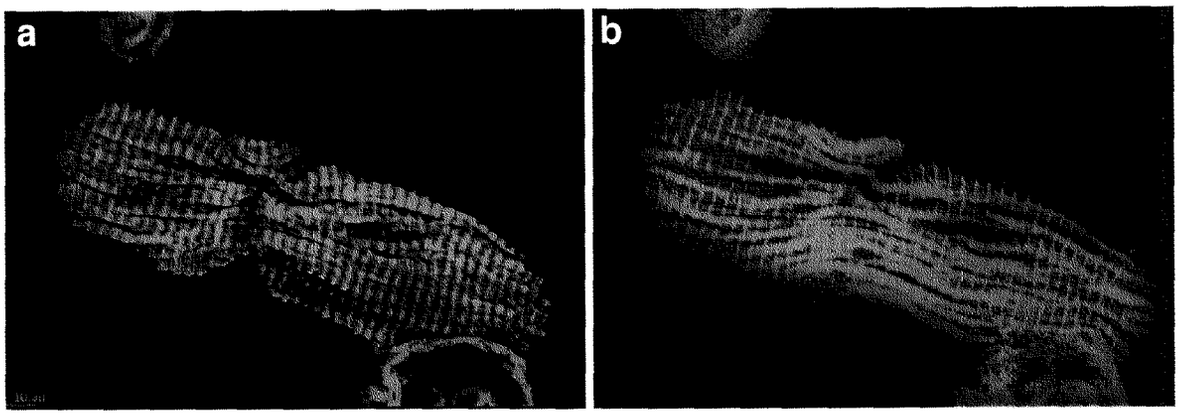

Figure 1.2.7: The polyclonal anti β-actin antibody recognizes the protein in rod-shaped ARCs as well. Confocal images of rod-shaped ARCs after 1 day in culture. The cells are stained for sarcomeric α-actin with 5C5 antibody (a) and cytoplasmic β-actin with antibody poRaβcyto(b). Scale bars 10 μm.

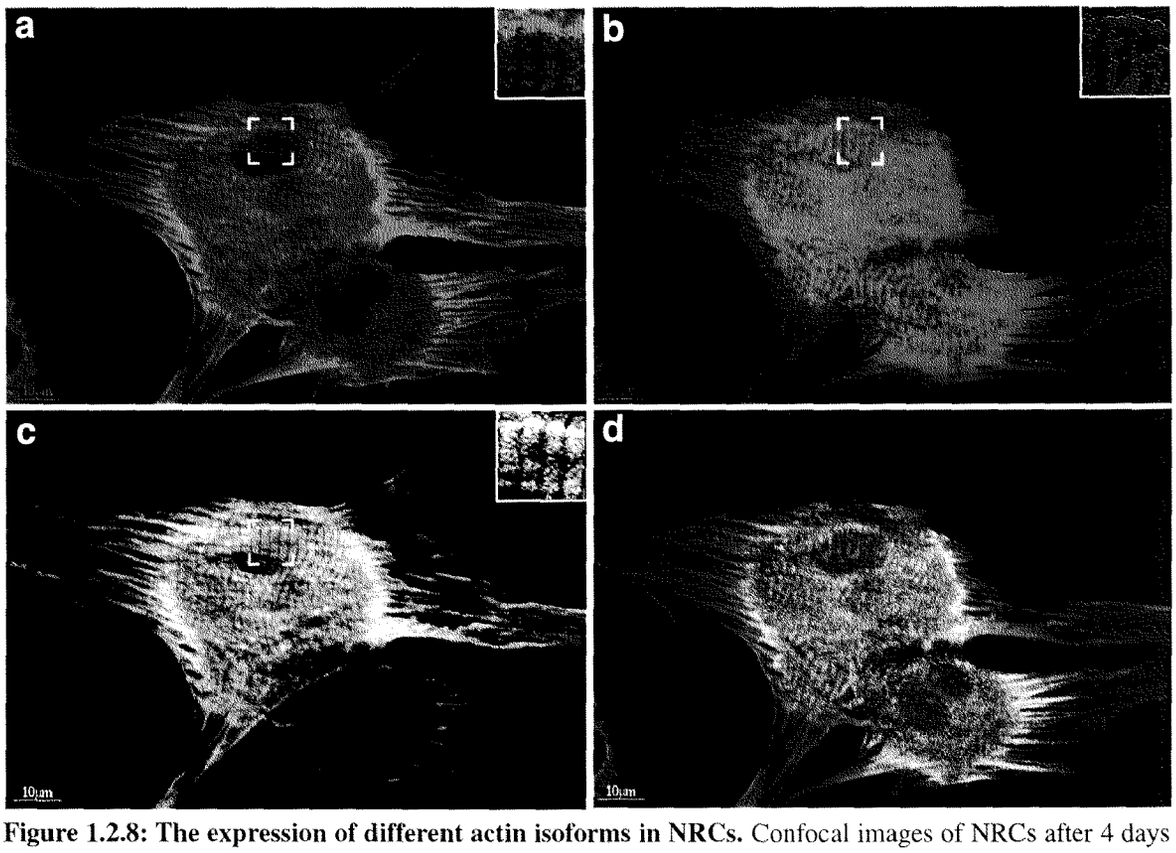

Figure 1.2.8: The expression of different actin isoforms in NRCs. Confocal images of NRCs after 4 days in culture. The cells are stained for sarcomeric α-actin with 5C5 antibody (a), cytoplasmic β-actin with antibody poRaβcyto((b) and smooth muscle α-actin with antibody 1A4 (c). (d) represents the superimposed image. Scale bars 10 μm.

the muscle actins stain uniformly the whole length of the thin filaments, the staining with anti-cytoplasmic β-actin antibody is concentrated in the region near the Z-disks (Figure 1.2.8, inserts). This also confirms the results obtained by ARCs that in the sarcomeric cytoskeleton the cytoplasmic β-actin is specifically sorted to the narrow stripes near the Z-disks.

1.3 Discussion

1.3.1 The expression of sarcomeric actin doesn't change during the cultivation of cardiomyocytes

The cytoskeleton of the cultivated cardiomyocytes significantly differs from the one in the heart tissue. When isolated from their native environment and cultured on the artificial two-dimensional substrate, they reorganize the cytoskeleton and assembly non-sarcomeric structures that do not occur in situ. We studied the expression pattern and localization of actin isoforms in cultivated adult (ARCs) and neonatal rat cardiomyocytes (NRCs) during the remodeling of the cytoarchitecture. We found that the expression of the sarcomeric α-actin isoforms (cardiac and skeletal actin) which dominate all other actin isoforms in cardiomyocytes is not significantly changed during the cultivation in either NRCs or in ARCs (Figure 1.2.2 a). This implies that the amount of the sarcomeric actin produced by cells is proportional to the total amount of protein, which is increased with the cell volume during the cultivation process. One might have expected that the relative amount of sarcomeric actin decreases in ARCs during the cultivation because they begin to synthesize the embryonic isoform of smooth muscle α-actin (Eppenberger-Eberhardt et al., 1990). However, we could not observe any significant change in the amount of sarcomeric actin that was determined by western blot analysis and by immunofluorescence. Most likely, this is due to the fact that the ratio of smooth muscle α-actin to the total actin amount remains low even after 11 days of ARC cultivation in the culture and sarcomeric α-actin remains the dominant form of actin. Thus, the changes in this actin isoform amount are too small to be detected by western blot analysis. This is also confirmed by the observation that in NRCs, where the expression level of smooth muscle α-actin is initially comparable with its expression level in ARCs after 11 days (Figure 1.2.2, b), signal from α-sarcomeric actin is also similar in intensity to that of ARCs (Figure 1.2.2, a).

1.3.2 The relation between cardiac and skeletal α-actin isoforms in cultivated cardiomyocytes

Two α-actin isoforms comprise the group of sarcomeric α-actins that dominates in quantity the other actin isoforms in striated muscles: cardiac α-actin and skeletal α-actin. These isoforms are almost identical, differing only by four amino acids out of the total of 375 residues (Vandekerckhove and Weber, 1978). Both isoactins are co-expressed during development in both types of striated muscles, while after birth the a-actin isoform (the one corresponding to a given adult tissue) usually dominates (Gunning et al., 1983). As was already mentioned in the introduction, the amount of skeletal α-actin in adult myocardium varies strongly with species, age and pathological situation. Thus, it is interesting to establish whether there is any change in the relative amount of cardiac and skeletal actins during the cultivation of cardiomyocytes. Unfortunately, the specificity of available monoclonal antibody Ac-1, directed against cardiac α-actin, was not sufficient to discriminate between the sarcomeric actins.

Quite recently, after our work was completed, there appeared a paper reporting the production of new polyclonal antibody anti-α-SKA1 that specifically recognizes the

skeletal isoform of α-actin (Clement et al., 1999). This paper shows that this isoform is non-uniformly distributed in adult rat myocardium and confirms that the expression of this isoactin is increased during the development of cardiac hypertrophy. It is reasonable to assume that a similar upregulation occurs in cultivated ARCs, which are considered to represent a model for hypertrophy in vitro (Eppenberger et al., 1988; Eppenberger-Eberhardt et al., 1990; Eppenberger-Eberhardt et al., 1993; Schaub et al., 1997). Thus, this new antibody might be a powerful tool for the survey of the relation between the two sarcomeric actins in cultivated cardiomyocytes.

1.3.3 Sarcomeric actins can universally build the both sarcomeric and non-sarcomeric structures in cardiomyocytes

The fact that the relative amounts of sarcomeric actins do not change during the cultivation of cardiomyocytes suggests that these actins participate in building of both sarcomeric and non-sarcomeric parts of the cytoskeleton. Indeed, our experiments demonstrate that sarcomeric α-actin localizes not only in the myofibrils of the cultivated cardiomyocytes but equally well in the SFLS of remodeled ARCs (Figure 1.2.5). This is also in agreement with the results of Pierre von Arx who found that the exogenous sarcomeric α-actin is utilized not only by sarcomeric structures but also by SFLS of the cardiomyocytes and even by the stress-fibers in fibroblasts (von Arx et al., 1995). Analogously, the microinjected muscle actin is incorporated equally well into striated and non-striated myofibrils of embryonic chicken cardiomyocytes (Suzuki et al., 1998). This implies that besides performing evolutionary new functions (such as muscle contraction) sarcomeric actin is also able to support "classical" functions of cytoplasmic actin, for instance, anchoring to substrate and maintenance of the cell shape. In other words, actin isoforms have distinct but overlapping functions in the cell.

The strong conservation of actin sequences indicates a great restriction in the rate and nature of amino acid changes in this protein during the evolution. Only substitutions compatible with the folded structure and protein function (including the ability to polymerize) have been retained. The detailed comparison the sequential differences between actin isoforms shows that a few internal substitutions observed between muscle and nonmuscle actins are often compensatory changes of pairs of residues, indicating that actins are even more conserved than it is apparent from primary sequence (Mounier and Sparrow, 1997). Another conclusion of this study is that muscle actin may differ from non-muscle actins by a more compact and stiffer N-terminus. This region is important for the muscle actomyosin complex formation (Chaponnier et al., 1995) and might allow new or better interaction of actin with other muscle-specific ligands. Taken together these and our results indicate that evolutionary the more advanced sarcomeric actins play more universal role in the cytoskeleton than cytoplasmic actins and may interact with broader range of different proteins.

1.3.3 Differential localization of α-smooth muscle actin in NRCs and ARCs

Earlier it was found in our laboratory that after about one week in vitro ARCs begin to re-express the embryonic isoform of smooth muscle α-actin, which was considered as a sign of dedifferentiation and return to embryonic phenotype (Eppenb.1990). Immunofluorescent staining with anti-smooth muscle α-actin antibody revealed that this isoform is localized mostly in SFLS of remodeled cardiomyocytes leaving the central myofibrilar field free in the typical crown-like pattern (Eppenberger-Eberhardt et al., 1990; Harder et al., 1996) Harder, 1998 #396]. These and other data led to the picture of smooth muscle α-actin expression that can be summarized as follows (Harder et al., 1998; Harder et al., 1996). First, the smooth muscle α-actin is incorporated reluctantly into striated myofibrils. Second, its expression is the evidence of the cell return to its embryonic phenotype. Third, it restricts the sarcomere assembly and grows. Below we discuss these conclusions in the light of our results.

We begin with the slow rate of smooth muscle α-actin incorporation into striated myofibrils. This conclusion is mostly based on the observation of the sorting mentioned above. Although this sorting is not ubiquitous (in all cultures we found a few cells where smooth muscle α-actin was present in sarcomeric structures) in most of the cells that are positive for this isoform it concentrates in the non-sarcomeric region. The reason for this prominent sorting remains unclear because in NRCs and adult atrial cardiomyocytes it is uniformly distributed in both sarcomeric and non-sarcomeric parts of cytoskeleton (see Figure 1.2.8, (Eppenberger-Eberhardt et al., 1997; Rothen-Rutishauser et al., 1998). This phenomenon becomes even more puzzling when we recollect that ARCs usually integrate ectopic smooth muscle α-actin into sarcomeres as well as into SFLS (von Arx et al., 1995).

The sequence of the smooth muscle α-actin is almost indistinguishable from the α-cardiac actin, differing by only six residues from 375, of which only the change from Val to Cys at position 17 is nonconservative (Sheterline and Sparrow, 1994). These actins differ in neither polymerization dynamics (Kabsch and Vandekerckhove, 1992) nor in the interaction with myosin in *in vitro* motility assay ((Harris and Warshaw, 1993)).

It is likely that the intriguing difference in the localization of α-smooth muscle actin in neonatal and adult cardiomyocytes is due to the fact that this isoform is already present in NRCs at the time of isolation while in ARCs it re-appears later when cytoskeletal structures are already formed. Experiments with microinjection of labeled actin monomers into cultivated chicken cardiomyocytes demonstrated that different structures within the same cell are not equivalent in the rate of actin incorporation. One of these experiments has shown, that in the striated part of the myofibrils the exchange of the actin was much slower than in the SFLS, indicating that actin molecules can not be readily incorporated into mature myofibrilar portions (Suzuki et al., 1998). Another study demonstrated that the introduced actin monomers were attached only to the external surface of mature myofibrils without really getting inside (Kouchi et al., 1993). This phenomenon might be explained by the fact that in sarcomeres the actin filaments are associated with a multitude of accessory proteins that stabilize filament structure and slow down the actin monomer exchange. In the light of these observations we believe that NRCs expressing smooth muscle α-actin at the moment of isolation either preserve some sarcomeric structures which still contain this isoform or assemble the new sarcomeres which incorporate already available smooth

muscle α-actin monomers. In contrast to NRCs, in ARCs smooth muscle α-actin starts to get produced only when new sarcomeres are already formed and thus the new isoform is incorporated first into the non-sarcomeric structures. Also, it can not be excluded that myofibrils in finally differentiated ARCs are more stable than in NRCs; this would make it even more difficult for the newly produced actin to get into the sarcomeres. Our assumption that the observed localization is due to a different exchange rate of actin monomers gets further support from the data obtained by von Arx. He found that the crown-like pattern of incorporation, which was previously supposed to be unique for smooth muscle α-actin, can be also observed by microinjection of the other muscle actin isoforms, even by microinjection of the chimeric γ-cyto/α-cardiac actin (von Arx et al., 1995).

In our experimental system the immunolocalization of smooth muscle α-actin was checked in ARCs cultured for 11 days (Figure 1.2.5), at the time when these cells begin to express a significant amount of this actin isoform (Figure 1.2.2, b). We have observed, however, that even at this stage (11 days in vitro) in some cells smooth muscle α-actin is localized in sarcomeres, although the most dense staining was observed elsewhere, in the non-sarcomeric fibers radiating into cytoplasm (Figure 1.2.6). Thus it would be interesting to check whether the number of cells that incorporates this actin isoform into myofibrils increases if they are cultured for a longer time. If true, this would confirm our conjecture that the process responsible for the observed localization is indeed slow exchange of the actin monomers with the mature myofibrils.

We now turn to the discussion of the biological significance of the re-expression of smooth muscle α-actin in cultured adult cardiac myocytes. In previous works it was concluded that this expression is the evidence of cell return to the embryonic phenotype. It has been demonstrated that the sarcomeric structures of embryonic cardiac muscle cells expressing smooth muscle isoform of actin is significantly less organized than in mature muscle (Goldstein and Traeger, 1984). However, no study has shown a direct influence of the smooth muscle α-actin expression on the degree of sarcomere organization and contractility.

Interestingly, the ectopic expression of this actin isoform is observed not only in embryonic striated muscle, but also in other tissues in some pathological situations. The expression of smooth muscle α-actin was detected in alveolar myofibroblasts during pulmonary hypertension. The authors propose that mechanical stretch due to capillary congestion may be responsible for induction of this actin isoform (Kapanci et al., 1990). Analogously, the increased level of this isoactin was detected in myofibroblasts from human breast carcinomas (Ronnov-Jessen et al., 1992). Many studies report the reappearance of smooth muscle α-actin in stress fibers of fibroblastic cells during pathological situations involving contractile phenomena such as wound healing and fibrocontractive decease's (reviewed in (Janmey and Chaponnier, 1995). Another study reported the re-expression of this isoform in atrial cardiomyocytes as a result of chronic fibrillation, which was induced in goats by electrical pacing (Ausma et al., 1997). In the light of these observations it seems likely that ex novo expression of smooth muscle α-actin in adult cardiomyocytes in culture should be regarded as a constituent part of the stress response due to the isolation and cultivation procedure rather than a signature of a return to the embryonic phenotype.

Finally, we discuss the influence of the expression of smooth muscle actin on sarcomeric assembly. The conclusion of the previous studies was that it restricts the sarcomere assembly. In our study we have observed that the expression of this isoactin in the ARCs is

very heterogeneous and that some cells accumulate the significant amount of the protein. One such cell (adjacent to the cell that does not expressed smooth muscle α-actin) can be seen in Figure 1.2.6. Despite the difference in the isoactin expression, both cells have well-developed sarcomeric structures, as can be estimated from phalloidin staining; this indicates that the expression of the smooth muscle α-actin does not disturb the formation of functional contractile apparatus in ARCs. This is in agreement with the results of von Arx who has shown that the expression of heterologous muscle actin isoforms (including smooth muscle α-actin) does not interfere with the sarcomeric organization of ARCs (von Arx et al., 1995). Additional studies are needed however, to compare e.g. the rate of contractility between cells containing different amount of this actin isoform.

1.3.4 A modified form of cytoplasmic β-actin may be expressed in cardiomyocytes

When studying the expression of the cytoplasmic β-actin in cultivated cardiomyocytes we were puzzled by the fact that two available anti-β-actin antibodies gave contradictory results. While monoclonal anti-β-actin antibody A5441 does not react with cardiomyocyte extracts (Figure 1.2.2, e), the polyclonal anti-β-actin antibody pRaβcyto detects the stable expression of this isoform in the same extracts (Figure 6, d). The absence of the reaction of monoclonal antibody against β-actin with skeletal and cardiac muscle has been reported previously in the characterization study of this antibody (Gimona et al., 1994). Thus, the simplest explanation of this disagreement is that the polyclonal anti-β-actin antibody is not specific and crossreacts with another protein in cardiomyocytes. However, several independent lines of evidence convinced us that this is not true and that this antibody indeed recognizes a novel actin isoform that is most likely a modification of β-actin.

First, the polyclonal anti-β-actin antibodies detect only actins (not another protein) in cardiomyocytes because they react only with the 42 kDa band in western blot (Figure 1.2.2, d) and its staining of SFLS in cardiomyocytes overlaps with the staining of antibodies agains different actin isoforms (Figures 1.2.6 and 1.2.8). Second, the staining of this antibody can be blocked by synthetic peptide used for immunization (Figure 1.2.3). This indicates that the antibody specifically recognizes some epitope in the ten N-terminal amino acids of cytoplasmic β-actin sequence.

However, the possibility exists that this antibody crossreacts with some another actin isoform, that is present in cardiomyocytes. What actin isoform can it be? This can not be one of α-actins because sarcomere-staining pattern with the anti-sarcomeric and anti-smooth muscle α-actin isoforms is slightly different from the one of anti-β-actin antibody (Figure 1.2.6 and 1.2.8). This can not be γ-actin either because characterization of anti-β-actin antibody demonstrates that it does not react with the γ-actins in 2D blot (Yao et al., 1995).

Thus, we have to assume that cardiac cells express some modified form of β-cytoplasmic actin which is either slightly different in the N-terminal sequence from the conventional β-actin, or this sequence of β-actin is modified in cardiomyocytes and is thus not recognized by monoclonal antibody. Both cases are in agreement with the fact that RT-PCR analysis with the β-cytoplasmic actin specific primers confirmed the presence of β-actin mRNA message in cultivated cardiomyocytes (Figure 1.2.4).

It is known that each of the actins is coded by separate gene (Vandekerckhove and Weber, 1978). Interestingly, while the α-actin genes exist in singles copies, the cytoskeletal actins, β and γ, are present in multiple copies in the genome of high vertebrates ((Ponte et al., 1983). Later studies have established that the majority of the β-actin genes are in fact pseudogenes of the reverse transcript type (Moos and Gallwitz, 1983; Ng et al., 1985). However, it is difficult to exclude the possibility that more than one functional β-actin gene exists. Since one would expect minor sequence differences in such duplicated genes, it is conceivable that different cell types express slightly different cytoplasmic actins.
Note that we are not the first group believing to have found the novel isoactin species in higher vertebrates. A new cytoplasmic actin isoform, differing from the conventional β- and γ-actins by four amino acid replacement has been reported in chicken (Bergsma et al., 1985). Two putative brush border isoactins which appear to be hybrid cytoplasmic/striated muscle isoforms have been identified in rat (Sawtell et al., 1988). In addition, the mutated β-actin that differs from the conventional β-actin by the replacement of one amino acid in the N-terminal sequence was detected in mouse B16-melanoma cells (Sadano et al., 1988; Taniguchi et al., 1986). These results confirm our belief that some not identified so far, isoform of cytoplasmic β-actin may exist in vertebrate tissue, in particular, in myocardium. For brevity in the following discussion we shall refer to it as β_{mod} (modified β-actin isoform).

1.3.5 The functional aspect of β-actin localization in cardiomyocytes

The immunofluorescent stainings with the polyclonal anti-β-actin antibody reveals that β_{mod}-actin resides in both sarcomeric and non-sarcomeric parts of cytoskeleton. Localization of this isoactin in the SFLS of cultivated cardiomyocytes does not differ from α-actin isoforms. However, in the sarcomeric region the staining pattern is slightly different. The width of the I-bands, stained with polyclonal anti-β-actin antibody is noticeably narrower than that of α-actins (Figures 1.2.6 and 1.2.8). We have verified that a similar phenomenon is present in freshly isolated rod-shaped ARCs, so it is unlikely to be a culturing artifact (Figure 1.2.7).
Interestingly, a similar observation was made in the case of another cytoplasmic actin. Immunofluorescent staining with the isoform specific antibody has shown that γ-actin is localized in a more narrow band than α-actin in the sarcomeres of cultivated chicken cardiomyocytes (Handel et al., 1991). Occasionally the different width of bands was recorded in the experiments using microinjections of fluorescently labeled cytoplasmic and muscle actins in cultivated chicken cardiomyocytes (McKenna et al., 1985).
We speculate that the reason for this sorting might be a different affinity of the various parts of the thin filament to β_{mod}-actin. Further, isoform specific actin-binding proteins participating in thin filament assembly might regulate this difference. These interactions would result in free incorporation of β_{mod}-actin into the Z-disk structure and its repulsion from the region of the filaments contacting with myosin. Consequently, this cytoplasmic actin leaves a room for muscle actin that is functionally optimized for the participation in muscle contraction.
This assumption introduces a new understanding of the results obtained by von Arx who has shown that ectopic expression of two cytoplasmic actin isoforms results in the cessation of beating and to the partial destruction of the sarcomeric structure (von Arx et al., 1995).

We assume that the overexpression of these proteins in the cultivated cardiomyocytes leads to a significant misbalance between cytoplasmic actins and isoform-specific actin binding proteins; the latter has catastrophic consequences for the thin filament stability.

1.3.6 How the problem can be solved

Thus, in our study we have shown that it is likely that some modification of β-actin is expressed in cardiomyocytes and that it is specifically involved in sarcomeric structure. However, we could not publish these findings because these conclusions are based on the data obtained with only one polyclonal antibody and, despite all our efforts, we could not prove convincingly that it reacts specifically. In this case, we could not rely on the results of the RT-PCR that demonstrate the presence of β-actin transcript in myocardium either because the sensibility of this assay is such that even a small amount of myofibroblasts in the extract might lead to the appearance of the specific response.

Thus, it seems that the following strategy would be more successful. One needs to construct a number of β-actin specific primers, and use them to amplify the coding sequence of β_{mod}–actin from the cardiomyocyte mRNA. Then, the comparison of this sequence with a conventional β-actin sequence would allow one to trace the putative replacements on the N-termini. When the existence of this β-actin genetic variant is proved one might check its mRNA expression in different tissues with specific primers.

However, if the β-actin in cardiomyocytes is produced from the same gene as in fibroblasts while different reactivity is due to a posttranslational modification of the β-actin N-terminal sequence the analysis will be more complicated because we do not know what is this modification. One may try to remove the putative modification by treating the cardiomyocytes extract with different agents. Hopefully, this treatment will allow the reaction of monoclonal antibody with cardiomyocytes extract.

It is clear, that many additional studies are necessary to clarify these questions and determine the possible functional role of the β_{mod}–actin isoform in cardiomyocytes.

Seite Leer /
Blank leaf

Chapter 2:

MYOMESIN ISOFORM DIVERSITY IN VERTEBRATES

2.1 Introduction

2.1.1 The contractile apparatus

2.1.1.1 The sarcomere is the basic structural unit of cross-striated muscle

Striated muscle is a well-ordered and efficient machine for converting chemical energy into physical work. These muscles are called "striated" because of their transversely banded structure: alternating I-bands (appearing as light bands) and A-bands (appearing as dark bands) are seen in the light and electron microscope (Figure 2.1.1, a). The A-band of the sarcomere is the region of interdigitation between thick (mostly myosin) and thin (mostly actin) filaments, whereas the I-band contains only thin filaments. The basic unit of the contractile apparatus of striated muscles is the sarcomere. It is schematically shown in Figure 2.1.1 b. The Z-disks are usually considered as the sarcomere borders, they divide the I-band and anchor the thin filaments. Analogously, the M-band, lying in the center of the sarcomere, marcs the middle of the A-band and holds the thick filaments together in their center. The typical vertebrate sarcomere is about 2 μm long. The sarcomeres, in turn, are linked together in series, forming the myofibrills. Many parallel myofibrils are comprised within a muscle fiber.

2.1.1.2 General principle of muscle contraction: the sliding filament model

The model of muscle contraction represents one of the most fascinating biological achievements (Huxley and Hanson, 1954). According to this model, the relative sliding of the actin and myosin filaments in a sarcomere results in the overall shortening of the whole muscle. The updated view of this process is discussed in detail in many publications and was summarized by (Squire, 1981) thus only a short sketch is presented here.
The contraction mechanism involves a cyclic binding/unbinding of myosin heads, also called S1, to the thin actin filaments. This process is controlled by calcium [Ca^{2+}] and ATP. The process of contraction starts with a relaxed state characterized by a low cytosolic [Ca^{2+}] concentration. In this state myosin binds either ADP or ATP with high affinity. ATP is hydrolyzed by the S1 portion of myosin, but the products ADP and Pi remain at the active site. In this state myosin binds weakly to actin and myosin heads are oriented nearly perpendicular to the thin filaments. After activation of the contractile mashinery, triggered by increase of cytosolic calcium concentration, the myosin heads bind to the adjacent actin filament. The initially bound Pi is released from the myosin heads and is followed by the dissociation of ADP. While the myosin head is still bound to actin, it undergoes a conformational change that is facilitated by flexible regions in the myosin molecules, so-called hinges. The S1 moves to an angle of about 45°, pulling the thin filament towards the center of the sarcomere. Subsequent binding of ATP decreases the interaction of the myosin heads with the actin filament and they return to perpendicular orientation, preparing for the next contraction cycle.
After calcium activation all sarcomeres within the myofibrils contract synchronously. At the ends of the myscle fibers the contractile force is applied to the extracellular connective tissue of the tendons. In this way the synchronous microscopic process of sarcomeric contraction results in macroscopic muscle shortening.

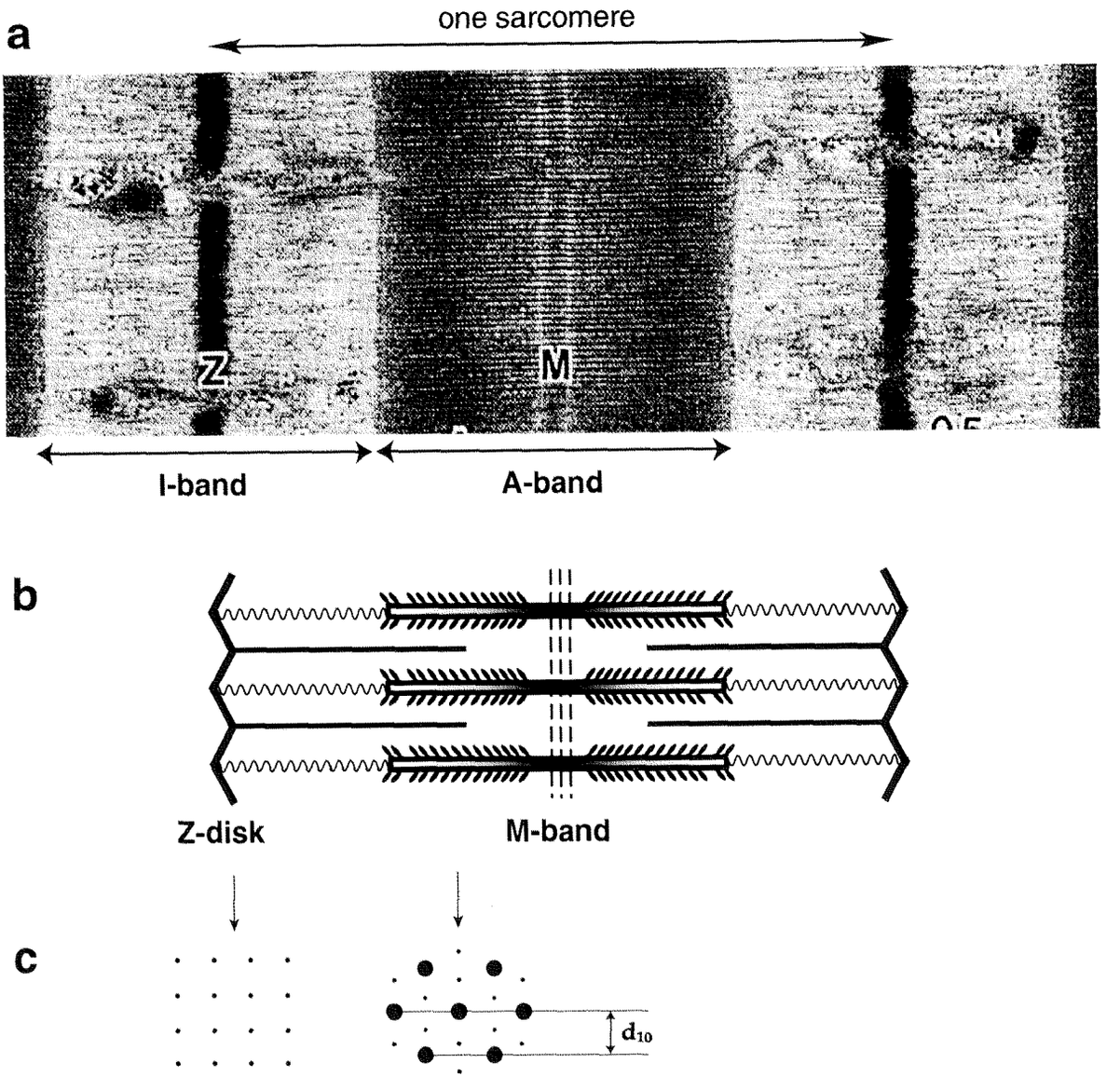

Figure 2.1.1 Basic structure of the vertebrate muscle sarcomere.
a: electron micrograph of a longitudinal section through a skeletal muscle sarcomere. Z-disc (Z), at either end of the sarcomere are attachment sites for the thin filaments composed of actin and associated proteins; the M-band (M) link adjacent thick filaments composed of myosin and associated proteins to each other.
b: schematic diagram of a single sarcomere, showing the origin of the dark and light bands seen in the electron micrographs.
c: diagramm of filament lattice near the Z-disk and in the A-band. Thick filaments are represented by a big circles, whereas the thin filaments by small circles. The d_{10} lattice plane coresponds to the first order of equatorial X-ray difraction pattern. Adapted from Squire, (1997).

2.1.1.3 Muscle types

While the basic mechanism of force generation is the same for the different types of muscle, they are not identical in structure. Two main types of muscles are commonly distinguished in vertebrates: striated and smooth; these names are due to their appearance in the light microscope. The cross-striated muscles act directly on the bones and therefore cause movement of the skeleton, typically they are subject to voluntary control. All vertebrate skeletal muscles are synchronous muscles, namely, they respond to electrical stimulus by a single twitch.
The smooth muscles in vertebrate intestines, veins and arteries do not show a striated appearance. They are involuntary muscles, in the sense that their contractile behavior is not regulated primarily by the nervous output from the brain. Heart muscle is a special case because, like smooth muscle, it is not under voluntary control, but in the light microscope it appears cross striated like the skeletal muscle and has sarcomeres as building units.

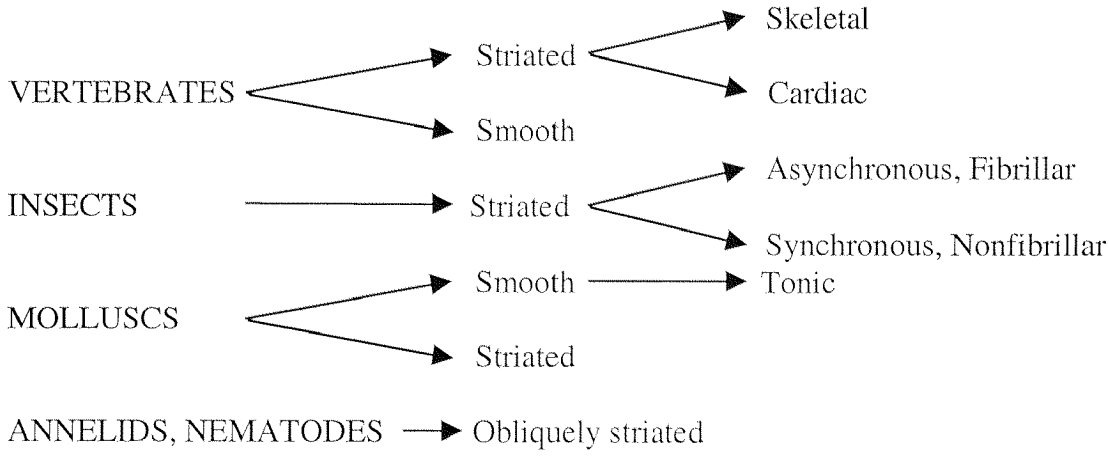

Figure 2.1.2: Classification of the major muscle types. Adapted from Squire, (1981).

Although all insect muscles are striated, some of them do not show the synchronous kind of response to stimulation found in vertebrate skeletal muscle. The asynchronous insect muscles, when stimulated electrically, display continious oscillation of the cross-bridges as long as cytosolic calcium concentration is elevated. This effect permits the insect's wings to beat extremely rapidly, sometimes up to 1000 times per second giving them a clear advantage in flight.
The mollusk muscles are also of two main types. Only a few mollusk muscles are striated, while most of them are smooth muscles, rather different from vertebrate smooth muscles in their structure and properties. The unique property of mollusk muscle is the ability to generate and maintain tension over a considerable period of time with comparatively little expenditure of energy. This property enables these animals to hold their shells closed for long periods.
The obliquely striated muscles of annelids and nematodes show a different organisation of sarcomeric proteins. The striations in these muscles are not perpendicular to the length of the muscle (as in the other striated muscle) but are at some angle.

2.1.2 The sarcomeric lattice

2.1.2.1 Vertebrate muscle

Electron micrographs of vertebrate skeletal muscle in transverse section (Squire, 1981) showed that the myosin filaments are arranged in a hexagonal lattice (Figure 2.1.1, c). Further, in the region of overlap between the thin and thick filaments the thin filaments are located at the trigonal points of the thick filament array, so that there are two thin filaments and one thick filament in each unit cell in cross sections. This particular arrangement is in fact characteristic for all vertebrate striated muscles. The thin filaments lattice gradually changes from being hexagonal in the overlap region to being tetragonal in the Z-band (Figure 2.1.1, b). The X-ray diffraction studies confirmed the hexagonal arrangement of thick and thin filaments and allowed the researchers to determine the sarcomere parameters from different muscle types (Table 2.1). Note that the value of d_{10} shown here corresponds to the first equatorial reflection which is characteristic to the diffraction pattern of relaxed muscle; for determination of the real spacing between thick filaments it has to be multiplied by 1.16 (see Figure 2.1.1, c).
Sarcomeric dimensions were found to be very similar in all vertebrate striated muscle (Table 2.1). The center-to center distance between thick filaments is normally about 43 nm, whereas the thick filament has a diameter of about 10-15 nm.

	thin–to-thick filament ratio	Sarcomere length (μm)	d10 (nm)
Mouse ELD/soleus	2:1	2.3	39.3
Frog sartorius	2:1	2.0	38.4
Killifish	2:1	2.1	44.0
Insect flight	3:1	2.6	45.9
Scallop striated adductor	6:1	2.2-3.7	57.5
Barnacle depressor	6:1	10-13	44.0

Table 2.1: Lattice dimensions for different relaxed vertebrate and invertebrate striated muscles.

The spacings were determined from fixed samples of relaxed muscle by equatorial X-ray diffraction. Note that the lattice dimensions measured from transverse electron micrographs are always smaller (by 10-20%) than those measured by X-ray diffraction because of shrinkage that occurs during the preparations of the specimens. In order to determine the 'center to center' distances for the thick filaments, it necessary to multiply d_{10} by 1.16. Adapted from Millman *et al.*, (1998).

2.1.2.2 Thick filaments in vertebrate muscle

Myosin is the major constituent of the thick filament and is one of the most abundant proteins in the muscle cell. Sarcomeric myosin can be roughly subdivided into two

fragments: a globular head, which is soluble, and α-helical tail, which is insoluble (Houmeida et al., 1995). The schematic structure of myosin is shown in Figure 2.1.2.

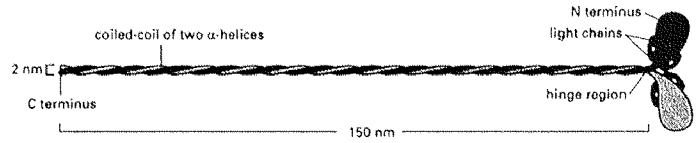

Figure 2.1.2: Schematic representation of the myosin molecule. Myosin is a hexamer composed of two heavy chains and regulatory light chains that are associated with the head region of each heavy chain. The N-terminal region of the heavy chain together with the light chains forms the globular head of myosin, the remainder of the molecule forms an extended α-helical road. Adapted from Alberts *et al.*, (1994).

Myosin has three important intrinsic properties: it is an enzyme with ATPase activity, it has the ability to bind actin and it aggregates to form filaments. The first two properties are associated with the globular head and are essential for muscle contraction, whereas the aggregating activity is due to its tail and is responsible for the formation the characteristic thick filaments. SDS-PAGE analysis revealed that myosin is a hexameric protein (Lowey and Steiner, 1972). It consists of two heavy chains with a molecular weight of 220 kD interacting along part of their length to form a two-chain, α-helical coiled-coil structure and two different types of light chains of 17- 21 kD (that are called essential and regulatory light chains) interacting with the non-helical portion of each heavy chain to form the globular head of myosin.

In the vertebrate muscles the myosin molecules are assembled into bipolar thick filaments about 1.6 μm long (Huxley, 1963). The myosin heads in the thick filament form an approximately three-stranded helix with a pitch of 3x43 nm and a repeat of 43 nm. The packing of the myosin rods is antiparallel in the middle of the filament, resulting in the so-called 'bare-zone' (devoid of myosin heads) in isolated filaments in the so-called M-region of the sarcomere and is parallel outside this area in the so-called 'bridge region'. The estimates for the diameter of the thick filament backbone (as measured in the bare zone) varies from 13 to 22 nm in different studies (Knight and Trinick, 1984; Squire et al., 1998). Transverse sections through the bare zone region show that thick filaments are predominantly of a triangular shape and always display a three-fold rotational symmetry (Luther et al., 1981).

Apart from myosin, thick filaments contain the M-band proteins and titin (see below), together with accessory proteins C-protein, X-protein and H-protein (Bennett et al., 1986), and possibly many others waiting to be detected.

2.1.2.3 Invertebrate muscles

Invertebrate striated muscles tend to show more variation in structure and function than vertebrate striated muscles (Squire, 1981). Most thick filaments from invertebrate muscle are thicker because they contain the myosin rod homologue paramyosin in varying amounts in addition to myosin (Royuela et al., 1997). According to the recent studies, the*Caenorhabditis elegans* thick filament is a rigid tubule, cross-linked at regular intervals by additional proteins (Schmid and Epstein, 1998). The analysis of the core components allows to identify at least three unique proteins, α-, β-, and γ-filagenins that are present in the hollow tubular core of the thick filaments (Liu et al., 1998).

The length of the myosin filaments and, therefore, the sarcomere length in invertebrates are usually larger than corresponding sizes of vertebrate muscles. Sarcomere lengths in invertebrates range from ~2 μm in scallop striated adductor muscle to ~10 μm in barnacle depressor muscle (Table 2.1). Interestingly, the striated scallop adductor, which has filament and sarcomere length similar to those of vertebrate striated muscle also has physiological behavior closest to that of frog sartorius muscle (Rall, 1981).
All invertebrate striated muscles have thick filaments arranged in a hexagonal lattice with the thin filaments positioned between the thick ones, but the number and positions of the thin filaments vary (Squire, 1981). In insect flight muscle there are 3 thin filaments for every thick one, whereas in scallop adductor and barnacle muscle there are 12 thin filaments around each thick filament (ratio 6:1).
In general the lattice spacings in invertebrate muscle are larger as in the vertebrate muscle (see Table 2.1). Further, the architecture of invertebrate muscles might be significantly different from those of vertebrates. For instance, the nematode muscles show oblique striations, and each sarcomere is attached to the plasmalemma via dense bodies (Z-disk analog) (Francis and Waterston, 1991). It was suggested that due to the oblique arrangement of sarcomeres the force is distributed on the application sites more evenly over the basal lamina and this allows a smooth bending of the nematode body (Burr and Gans, 1998). However, despite the variations in lattice structure in different invertebrate striated muscle and their difference from vertebrate striated muscle, the nature of lattice changes and their effect on contraction are remarkably similar in all vertebrate and invertebrate striated muscle.

2.1.3 The third filament system

2.1.3.1 The sarcomeric structure is maintained by the third filament system

In order to stabilize thin and thick filaments in the positions that are optimized for their interaction, the sarcomeres must possess an elastic lattice that is built from accessory proteins. This idea dates back to the time when the sliding model of muscle contraction was established but the nature of these proteins was unclear. Microscopic data collected in following decades provide evidence for the presence of third filament system (in addition to thick and thin filaments) in the sarcomere (for review, see (Trinick, 1994). It was also observed that muscle fibers exhibit a restoring force when they are stretched and that they return to their original length upon release (Wang et al., 1993). To distinguish it from active tension generated by actomyosin interaction, it was called passive tension. It was suggested that the restoring force is produced by the system of elastic filaments working like braces and allowing non-ATP dependent structural rearrangements (Maruyama, 1994).
Titin (Wang et al., 1979), also called connectin, (Maruyama et al., 1977) was originally identified as a high molecular weight component of striated muscle; since then it has been suggested that it is a main player responsible for passive elasticity of striated muscle (for review, see (Gregorio et al., 1999; Maruyama et al., 1994; Trinick, 1994; Trinick, 1996). Monoclonal antibodies generated against purified titin fragments labeled several epitopes stretching from the Z-disk to the M-band, proving that titin spans the entire half of the sarcomere (Furst et al., 1988; Nave et al., 1989; Wang et al., 1993). The unique position and the size of titin suggests that titin functions as the organizer of the sarcomere providing

specific, spatially defined binding sites for other myofibrillar proteins (Maruyama, 1994; Trinick, 1994; Trinick, 1996). Titin molecules with opposite polarity overlap in both the Z-disks (Gregorio et al., 1998) and M-bands (Obermann et al., 1996), forming a continuous filament system within myofibrils.
Sequencing of human cardiac titin revealed a 81 kb open reading frame encoding a 26 926 residue protein with a molecular mass about 3 000 kDa (Labeit and Kolmerer, 1995). Only a single copy of the titin gene has been identified in vertebrate genome, but many distinct isoforms are generated by alternative splicing (Labeit and Kolmerer, 1995). The titin molecule is string-like: it is about 1 μm long and consists mainly of the immunoglobulin-like (Ig) and fibronectin type III (Fn3) domains. Each of these contains about 100 amino acid residues folded in a β-sheet sandwich (Pfuhl and Pastore, 1995; Politou et al., 1995). About 10% of the titin mass is organized in nonrepetitive sequences that are situated between Ig and Fn3 repeats (Labeit and Kolmerer, 1995). A total of 17 such insertions were found, 16 of which have no significant homology to each other, or to other protein sequences known to man. One insertion located near the titin C-terminus in the M-band was identified as serine/threonin kinase domain.
Generally, the functions of titin fall into two broad categories (not counting, of course, its main function of maintenance of sarcomere integrity), involving sarcomeric assembly and elasticity, each of these categories will be discussed in detail below.

2.1.4 Titin is a sarcomeric ruler

2.1.4.1 Titin A-band sequence correlate with the thick filament structure

There is a striking similarity between the observed details of sarcomeric structure and the prediction for the domain pattern based on the titin sequence, so it is tempting to conclude that titin determines much of sarcomere structure (Trinick, 1994; Trinick, 1996). This correspondence is most evident in the A-band. The heads of myosin molecules are found at 14.3 nm intervals on helical array that repeats at every 43 nm (Squire et al., 1998). In addition so called 'accessory proteins' are found in the thick filament. The best characterized is the C-protein also called MyBP-C (myosin binding protein C) (Bennett et al., 1986). It was found in 11 positions spaced at 43 nm intervals in both halves of the A-band, giving rise to transverse stripes in electron micrographs. In its turn, the titin sequence in the A band contains 11 continuous copies of a 'super-repeat' composed of 11 Ig and Fn3 domains (see Figure 2.1.3). Each of these repeats spans about 43 nm and matches the 11 stripes in the A-band (Furst et al., 1989; Labeit and Kolmerer, 1995). The 11-domain super-repeats contain multiple domains that bind to the tail portion of myosin ((Houmeida et al., 1995). Further, the first Ig-like domain of each titin super-repeat contains the binding site for C-protein (Freiburg and Gautel, 1996). Analogously, the C-terminus of C-protein binds to the myosin tail in "*in vitro*" binding assays (Okagaki et al., 1993). Therefore, within the C-zone of the A-band, titin might specify the number and location of myosin and C-protein molecules that are incorporated into thick filament.

2.1.4.2 Titin sequence define the Z-disk structure

The sarcomeric Z-disk links titin and actin filaments from opposite sarcomere halves in a lattice connected by α-actinin (Squire, 1981). Only a small portion of titin, about 200 kDa

is localized within the Z-disk (Labeit and Kolmerer, 1995). The central Z-disk titin region (see Figure 2.1.3) contains four Ig-like domains, several phosphorylation sites and a variable number of copies of a specific protein motif, the 45-residue Z-repeat (Gautel and Goulding, 1996). The number of Z-repeats is regulated by alternative splicing. Namely, seven Z-repeats are expressed in rabbit heart muscle, a mixture of either six or four Z-repeats in rabbit soleus muscle, and four Z-repeats in rabbit psoas muscle (Sorimachi et al., 1997). It was shown, that the titin Z-repeats interact with the C-terminus of α-actinin (Ohtsuka et al., 1997). Thus, it was suggested that number of titin Z-repeats may specify the number of α-actinin cross-links resulting in different mechanical properties of the Z-disks ((Gautel et al., 1996). The thorough analysis of the titin-α-actinin interactions led researchers to the model of Z-disk structure (Young et al., 1998). According to this model the Z-repeats of titin provide the binding sites for the α-actinin doublets forming lateral Z-filaments, thus, specifying the number of these filaments (see Figure 2.1.4). Additional binding sites outside the Z-repeats interact with central domains of the outermost α-actinin pair, at the Z-disk edge, possibly serving a terminal motif for α-actinin incorporation (Young et al., 1998).

2.1.4.3 Titin serves as a molecular template during myofibril assembly

The assembly of dozens of muscular proteins into a working sarcomere occurs in the course of only few hours during early cardiac development (Ehler et al., 1999). Among all known candidates only titin is long enough to play the role of 'molecular ruler' that determines the assembly order. This idea is supported by the identification of ordered binding sites on the titin molecule, interacting with the numerous sarcomeric proteins, such as α-actinin (Young et al., 1998), teletonin (Gregorio et al., 1998), C-protein (Freiburg and Gautel, 1996; Furst et al., 1992), myomesin ((Nave et al., 1989; Obermann et al., 1997) and M-protein (Nave et al., 1989).

All current models of myofibrillogenesis imply a dominant role of titin in this process. During early stage of assembly titin colocalizes with actin and α-actinin in the so-called 'dense body-like structures' (Rhee et al., 1994; Schultheiss et al., 1990). These nascent complexes align and associate laterally to form future Z-disks, and titin was suggested to play a key role in this process (Dabiri et al., 1997). The distances between dense bodies are at first unregular and about 1 μm. Again, only titin with its colossal length may perform the function of keeping these nascent structures at distances corresponding to mature sarcomeres (Ehler et al., 1999). During this process the titin unfolds, providing the binding sites for other myofibrillar proteins and finally the C-termini of the neighboring molecules should be joined as proposed by recent M-band model (Obermann et al., 1996). This scenario is confirmed by numerous studies reporting that the organization of N-terminal titin epitopes precedes the C-terminal one (Ehler et al., 1999; Furst et al., 1989; van der Loop et al., 1996). Recently, it was demonstrated that the appearance of titin M-band epitopes coincides with the assembly of myomesin in M-bands (van der Ven et al., 1999). Therefore, it was suggested that titin together with Z-disks and M-bands forms a sarcomeric scaffold that is necessary to integrate thick filaments into developing sarcomeres (Ehler et al., 1999; van der Ven et al., 1999). The idea that titin regulates the thick filament assembly appeared long ago because no in vitro method allows myosin to assemble into filaments of the exactly tailored length of 1.6 μm (Trinick, 1994). This suggestion was borne out by the recent study which demonstrated that the mutant BC_3H-cells, synthesizing only short C-

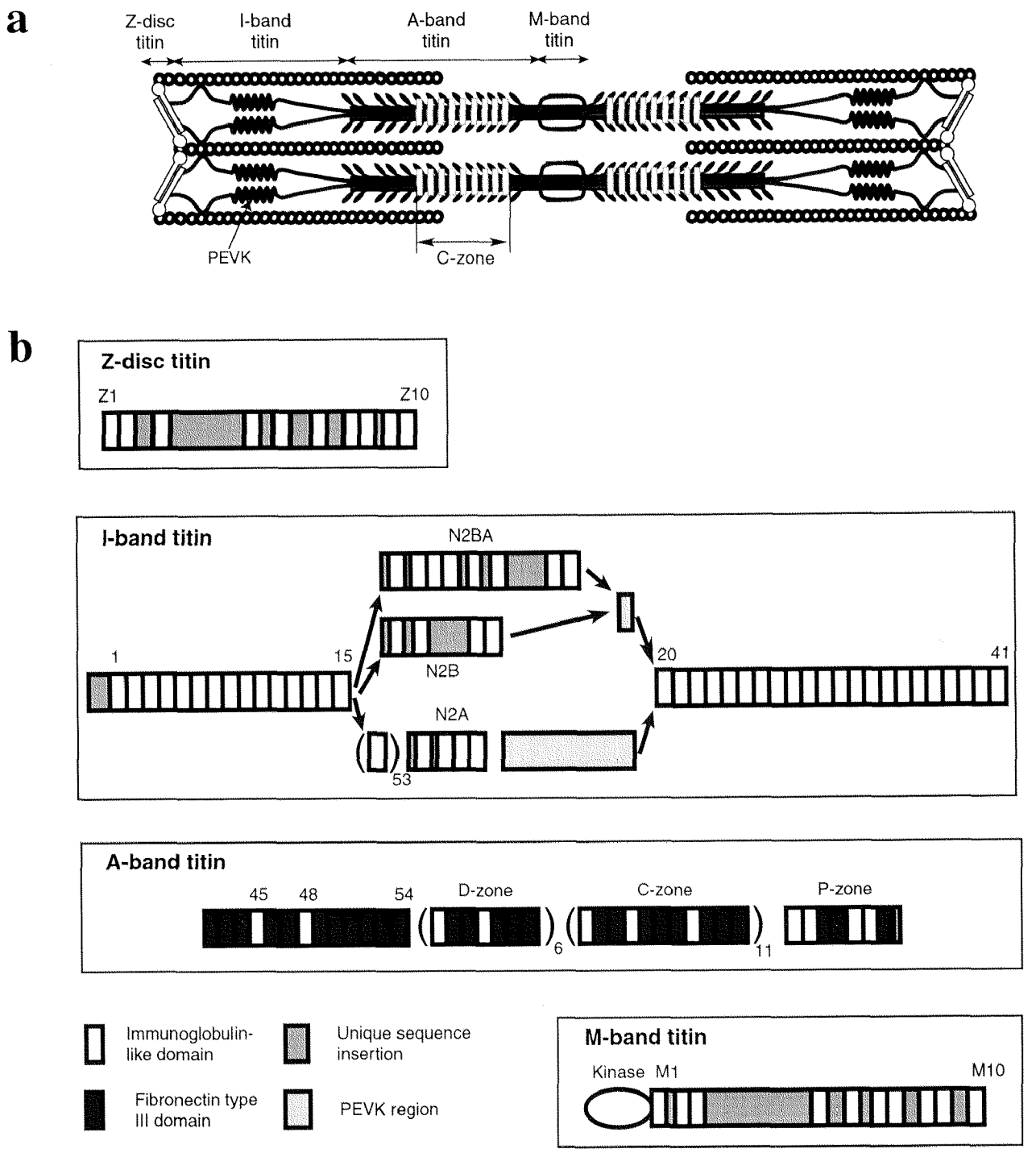

Figure 2.1.3 Modular structure of titin.
a: Giant titin molecule (shown in blau) span the entire half sarcomere. Titin filaments with opposite polarity overlap in both Z-disks and M-bands, forming a continuos elastic connection over the entire length of myofibril.
b: Titin is primarily composed of immunoglobulin-like (Ig) and fibronectin type III (Fn3) domains. In the Z-disc and in the M-band, a complicated pattern of Ig-like domains and unique sequence insertions offers several binding sites for other structural proteins such as α-actinin or myomesin. In the I-band, titin is composed of large stretches of Ig-like domains interspersed by unique sequence insertions that are defined by multiple alternative splicing events. Together with the cardiac-specific N2B region and the PEVK segment, the poly-Ig regions are responsible for sarcomeric elasticity. The A-band region of titin is assembled from two repeats of fibronectin type III and immunoglobulin-like domains that present repetitive binding sites for the myosin and myosin associated proteins such as MyBP-C. Adapted from Labait and Kolmerer, (1995).

terminal fragment of titin are not able to assemble thick filaments (van Der Ven et al., 2000).
Thus, many lines of evidence demonstrated that titin controls many aspects of sarcomere assembly. It is understood reasonably well how titin defines Z-disk, I- and A-band ultrastructures, as well as elastic properties of the sarcomeres in different muscle types (see below). But it is completely unclear how it provides the transition from the tetragonal symmetry in the Z-disk to the hexagonal symmetry in the A-band of the sarcomere. The idea of the presence of a sarcomeric scaffold might explain this puzzle, assuming that the tetragonal symmetry in the Z-disk is determined by the binding specificity of the α-actinin molecules, whereas the hexagonal structure in the A-band is determined by one of M-band proteins.
The remaining puzzle is how the highly elastic titin molecule might remain spread out in a linear fashion as a blueprint of binding sites for sarcomeric components. In particular, how it is possible, that the very long titin molecules are positioned parallel to each other in the process of sarcomeric assembly and how they interact exactly with a symmetric titin molecule coming from an apposite Z-disk. One can conjecture that the giant titin mRNA molecule assists for coordinating growth of titin filaments bundle, which provide the basic scaffold for sarcomeric assembly immediately after translation (See section 2.3.5).

2.1.5 Titin is the main source of muscle elasticity

2.1.5.1 Structures participating in muscle elasticity

The striated muscle is elastic: it develops stress if it is stretched or compressed and it snaps back to its resting length when released. When muscle is activated it shortens due to actomyosin interaction but it regains its original length when activation ceases. The elasticity of an entire muscle can be represented as sum of elastic forces arising from many intracellular and extracellurar elements working either in series or in parallel to sarcomeric apparatus. Unfortunately, most studies focus on elastic elements inside the cell, only a few papers consider the effect that is due to the extramuscular structures in skeletal muscles (Goulding et al., 1997) or to extracellular matrix in cardiac tissue (Granzier and Irving, 1995).

2.1.5.2 Elasticity of skeletal muscle

The force transmitting apparatus of skeletal muscle consists of skeletal muscles joined with non-muscular elements, such as ligaments, tendons, fasciae, and bones. Evidently, these structures do not participate in the development of passive tension. Instead, the role of these structures is to provide the physiological constraints for the muscle stretch thereby preventing the sarcomere from reaching the yelding point (Goulding et al., 1997).
The next elastic elements in muscle are sarcolemma and extracellular matrix, but their elasticity can be disregarded in muscle working range length, because they contribute significantly only in a unphysiologically stretched skeletal muscle (Magid and Law, 1985).
At the intracellular level a potential force-bearing structure is the network of intermediate filaments that envelop and interconnect the sarcomeres with the membrane-associated cytoskeleton (costameres and intercaleted disks) (Small et al., 1992; Thornell et al., 1985; Tokuyasu, 1983). This network connects the sarcomeres both in the radial direction to

parallel myofibrils and longitudinally to the adjacent sarcomeres at the Z- and M-lines; and has been assumed for a long time to be a force-transmitting device (Wang and Ramirez-Mitchell, 1983). Extraction of the sarcomeric components from the isolated muscle fiber allows to evaluate the contribution of intermediate filament to the elastic force and conclude that it is negligible within physiological range of muscle extension (Wang and Ramirez-Mitchell, 1983). However, it is conceivable, that in cases where sarcomeres are damaged and are incapable of tension generation, the associated intermediate filaments provide mechanical linkage to the remaining sarcomeres and take the function of force transmission. It seems that this function of intermediate filaments is especially important in active muscles because the knock-out of desmin, which is the most important component of intermediate filaments in muscle, leads to the destructive consequences in heart (Milner et al., 1996).

2.1.5.3 Elasticity of cardiac muscle

Passive tension is an important factor in cardiac muscle because it contributes to the diastolic wall tension that determines the extent of filling of the heart and subsequent stroke volume. The heart sarcomeres do not have constraints, imposed on skeletal muscle by bones or ligaments, but they are surrounded by a dense collagen network that is likely to function as an extracellular source of passive tension (Weber et al., 1994). A comprehensive study (Granzier and Irving, 1995) estimates the contribution of extracellular matrix and non-sarcomeric intracellular components (microtubules and intermediate filaments) to passive tension generation in the heart muscle relative to that of titin. They performed the 'functional dissection' of different structures by studying the effect of selective removing the elastic elements. These results indicate that the extracellular matrix to some degree limits the stretch of the heart tissue and does not allow sarcomeres to approach the yield point. The mechanism for this function is the following: the matrix contribution to the elasticity is small in the working range (1.9-2.1 μm) but increases a few times when the length exceeds 2.2 μm.

This study also estimates that intermediate filaments contribute about 10% of the passive force in cardiac tissue. This value is somewhat different from the results obtained for skeletal tissue there the contribution of this structure was found to be negligible (see previous Section). Note that the myofibrills in both cases were treated differently and thus these results are difficult to compare. Finally, the force, originating from microtubules was found to be not significant in all 'working range' of the sarcomere.

2.1.5.4 Titin filaments provide the main source of muscle elasticity

Thus, the results sketched in the previous two Sections show that the main contribution to the muscle elasticity comes from the system of filaments located *inside* the sarcomeres. Since the discovery of titin, its sarcomeric localization and elastic nature makes it the ideal candidate for providing the molecular basis for muscle elasticity (for review see Maruyama, 1994; Trinick, 1994). The hypothesis that titin plays a role in passive tension generation was supported by studies in which the degradation of titin either by ionizing radiation (Horowits et al., 1986) or by enzymatic digestion (Yoshioka et al., 1986) significantly decreased the passive tension exerted by skeletal muscle cells.

Titin filaments with opposite polarity overlap in both the Z-lines (Gregorio et al., 1998) and M-lines (Obermann et al., 1997), forming a continuos elastic connection over entire length

of myofibrils. Within the A-band titin is bound along thick filament (Furst et al., 1988), analogously, the N-terminal part of titin is associated with thin filament and the Z-disks (Linke et al., 1997). Thus, these parts have to be stiff under physiological extensions and only I-band region of titin is extensible under physiological stretch (Furst et al., 1988) and provides the main source of muscle elasticity.

2.1.5.5 I-band titin isoforms determine the elastic properties of muscle fibers

The I-band portion of titin exists in many variants, produced by extensive splicing events (Granzier and Irving, 1995; Labeit and Kolmerer, 1995). As a result, this region of titin from different muscle types ranges from 0.7 MDa in the cardiac isoform to 1.5 MDa in human soleus muscle. Therefore, it is reasonable to assume that expression of different titin isoforms is needed to adjust the elastic properties of the third filament system to the physiological demands on the sarcomere (Granzier and Irving, 1995; Labeit and Kolmerer, 1995). The main portion of I-band titin is made up of two structurally distinct regions (see Figure 2.2.4, b), stretches of Ig domains arranged in tandems, separated by a unique sequence of elusive secondary structure, the PEVK region (Granzier and Irving, 1995; Labeit and Kolmerer, 1995). The latter region received its name from its property of being rich in proline, glutamate, valine and lysine residues: these four amino acids together account for 70% of its amino acid content. Both regions exist in tissue-specific length variants, which are characteristic for each titin isoform. In addition to the differentially expressed Ig-repeats and PEVK domains, skeletal muscle titin contains a linker segment termed N2A region, whereas two different linker regions, N2A and N2B (see Figure 2.2.4, b) were found in cardiac titin (Linke et al., 1996). The study of titin expression on the protein level revealed recently that actually, the myocardium coexpesses two isoforms: a smaller one, containing N2B element only (N2B titin) and a larger isoform with both N2B and N2A elements (N2BA titin) (Cazorla et al., 2000). These isoforms are coexpressed on the single cell level, with the expression ratio varying greatly between different species, and even between different locations within the heart (Cazorla et al., 2000).
It was suggested that the expression of different length versions of tandem Ig domain stretches in various muscle types (Labeit and Kolmerer, 1995) may be important for the determination of the physiological sarcomeric slack length, whereas differential splicing of PEVK and N2B unique insertion sequences controls tissue-specificity of passive stiffness (Linke et al., 1996).

2.1.5.6 Current understanding of titin elasticity

The elastic properties of titin were studied extensively in last decade and have changed completely the understanding of its molecular basis (For review see (Gregorio et al., 1999; Linke and Granzier, 1998; Trinick and Tskhovrebova, 1999).
Initial concepts assumed that the reversible unfolding of Ig or Fn3 domains, which make up the 90% of titin mass represent the main source for titin elasticity (Erickson, 1994). Furthermore, since the A-band section of titin also consists of these modules, it was suggested that at high forces, unfolding of A-band titin domains might take place and contributes to elasticity (Wang et al., 1993). These ideas were soon abandoned because it was shown that the Ig-fold is thermodynamically a very stable structure (Politou et al., 1995) and that reversible unfolding of Ig-domain is associated with a large energy loss due to hysteresis (Tskhovrebova et al., 1997). Furthermore, it was found that the I-band portion

of titin contains the putatively unfolded PEVK segment, which was immediately proposed for the role of compliant spring that is stretched even during minor sarcomere elongation (Labeit and Kolmerer, 1995).

After the full titin sequence became available there appeared a possibility to investigate the titin extensibility by monitoring the location of sequence-assigned antibodies. The results of these studies implied just the opposite of what had been proposed earlier (Labeit and Kolmerer, 1995). It turned out that in slack length sarcomeres (i.e., at zero passive tension) the elastic portion of titin is not straight; instead, it is in a folded conformation (Granzier et al., 1996). Clearly, in this case the passive force appearing during minor stretch is dominated by the entropic contribution, arising from the straightening of the Ig-domain chain (Trombitas et al., 1998). Only at excessive sarcomere stretch the PEVK segment becomes important and its straightening leads to a dramatic increase in the passive tension of the sarcomere (Gautel and Goulding, 1996; Linke et al., 1996; Linke et al., 1998). This behavior can be reproduced by models that assume that the tandem-Ig segments and the PEVK segment are in fact serially linked worm-like chains (WLC) with different bending rigidities and that the Ig segment is the most compliant spring, while a PEVK is the relatively stiff one (Trombitas et al., 1998). This model allows to explain reasonably well the elastic behavior of titin throughout the working range of skeletal muscle, eliminating the need for unfolding the Ig domains under physiological conditions (Trombitas et al., 1998).

Most knowledge about titin elasticity was obtained from skeletal muscle studies. However, the passive tension is fundamentally more important in the heart where it contributes to the diastolic wall tension, a factor that determines the heart's extent of filling and subsequent stroke volume. For a long time it remained unclear how the passive tension is regulated in cardiac muscle which contains a significantly shorter I-band titin than skeletal muscle (Labeit and Kolmerer, 1995). Moreover, it was shown that the titin from cardiac muscle extends beyond the length that can be explained by the contour length of the tandem Ig and PEVK segments (Helmes et al., 1999). The detailed investigation of the cardiac titin extension revealed that the unique N2B insertion also contributes to the elongation and has a stiffness that is intermediate between Ig-segment and PEVK-region (Linke et al., 1999; Trombitas et al., 1999). Thus, the cardiac titin is a three-element molecular spring and stretches reversibly even to long physiological sarcomere lengths without unfolding of Ig-domains.

Interestingly, a recent study reports that cardiomyocytes from different species have variable stiffness that correlates with the variations in the expression of long and short titin isoforms there (Cazorla et al., 2000). Furthermore, the isoforms expression ratio varies also in different layers of ventricular wall. This implies that the resulting stiffness gradient allows stress balancing in different regions of the ventricular wall.

2.1.5.7 Titin develops restoring force in cardiomyocytes

When the heart contracts, a restoring force is employed to restore heart to its original shape during diastole. This property can be also observed in isolated cardiac myocytes; when relaxed after contraction, myocytes increase their length back to their relaxed length. Thus, any deviation from the slack length leads to the appearance of the force in the sarcomere, which brings it back to the original length. However, while the molecular basis of the passive tension development was studied in detail (see previous sections), the molecular mechanism of the restoring force development is mostly unknown.

It is resonable to assume that the same system of filaments (titin filaments) is responsible for the development of force in both directions. The titin may harness part of the actomyosin-based active force during the systole, allowing for elastic diastolic recoil and aiding the ventricular filling. Indeed, one group of researchers found that the titin is responsible for a large part of the restoring force exerted by isolated cardiomyocytes (Helmes et al., 1996). The same group proposed that the mechanism of this force is similar to the one of passive tension. Namely, the C-terminal part of I-band titin is somehow fixed and when the thick filament end passes this point in the process of sarcomere contraction, the elastic segment of titin is stretched in the opposite direction. This assumption is based on the observation that the T12 epitope remains in its place whereas the more N-terminally located titin epitopes reverse their order around the slack length (Granzier and Irving, 1995); Trombitas and Granzier, unpublished data, 1996). Indeed, a later study has shown that the I-band titin segment from Z-disk boundary to T12 epitope is rigidly attached to the actin filament and does not enlarged when the sarcomere is stretched (Linke et al., 1997). At the same time, there is no confirmation in the literature that the titin epitopes change their direction when the sarcomere is compressed; until proven correct this hypothesis will remain only a plausible speculation.
It is very likely that the restoring force that develops in the contracted sarcomere is due to the compression of the elastic segment of titin. This assumption is borne out by a small-angle scattering data demonstrating that deformation of the four Ig-domains fragment either by extension or by compression results in the appearance of the driving force that restores the relaxed state (Improta et al., 1998). Unfortunately, the elastic response of the unique sequences, in particular PEVK and N2B insertions, to the sarcomere shortening remains unknown. Therefore, the future studies will be needed to clarify the molecular mechanism of the restoring force provided by titin strands.

2.1.5.8 Sarcomere length is constant over the entire muscle fiber

The access to the yielding point, that would result in the irreversible distruction of the sarcomeric structure is prevented in skeletal muscle by extramuscular apparatus (tendinous or bony structures) (Goulding et al., 1997). However, isolated fiber can clearly be stretched far beyond this limit (Wang et al., 1991; Wang et al., 1993), and it is conceivable that under isometric contraction or sudden passive extension, local regions within the muscle might be overstretched. A recent study investigated this question by analyzing the length of the sarcomere in different parts of stretched muscle (Goulding et al., 1997); the presence of local overstretched regions would show up as differences in sarcomeres length. Interestingly these dimentions were indistinguishable near the tendinous junction and in the middle of the muscle. This suggest that the serially arranged springs of titin molecules distribute the passive tension evenly across long distances preventing destruction of sarcomeres during tetanic contractions or under rapid passive stretch.
Thus, there are three major functions of titin, that are associated with its elastic nature: development of the bi-directional forces restoring the sarcomere to its slack length from both stretched and contracted state, centering of the A-band in the sarcomere and even distribution the passive strain across the entire length of the muscle fiber.

2.1.6 M-band is involved in the maintenance of the thick filament lattice

2.1.6.1 Forces stabilizing the A-band lattice

Thick filaments in the sarcomere are positioned in an almost crystalline order, forming hexagonal lattice (see Figure 2.1.1). The stability and size of the A-band filament lattice are the result of a balance between several types of forces, acting either between filaments or on the outside of the muscle fibers (for review see (Millman, 1998). These forces tend to keep surface-to-surface separation of the thick and thin filaments at the distance of 10-12 nm (corresponding to d_{10} between 37 and 39 nm) that is optimal for the actomyosin interaction. The M-band connecting the thick filaments in the middle seems to participate in the maintenance of A-band lattice (Luther, 1981). In order to estimate the effect of M-band structure we consider in detail the factors affecting the thick filament distances.

Because a membrane enclosing the muscle fibers limits the passage of ions through it, one expects that muscle fibers behave as osmometers. Indeed, the experiments showed that within a considerable range of osmolarities muscle fibers behave as good osmometers, swelling when the external osmolarity is reduced and shrinking when it is increased (Blinks, 1965). Under most physiological conditions, that is in a fixed osmolarity, the lattice volume (cross-sectional area times sarcomere length) is constant (Elliott et al., 1965). For instance, if the length of the sarcomere is decreased by a factor of two, the distance between filaments has to increase by the factor of the square root of two. This means that structural elements, participating in the maintenance of A-band lattice, should have sufficient elasticity to allow significant changes in the lattice spacing during the muscle contraction.

When the membrane constrains are removed in skinned muscles, however, there is no mechanism left to keep lattice at constant volume and forces between filaments provide the main mechanism of the control of the lattice size. In a relaxed sarcomere, electrostatic forces between the negatively charged thick and thin filaments (electrostatic forces) provide one mechanism for the spacings control (Millman and Nickel, 1980). Another factor determining the lattice size (which becomes important at very small and very large lattice spacings) is the steric interference of the filaments themselves and the limitations in the extensions of structural elements such M-bridges (passive structural forces) (Millman and Nickel, 1980). In contracting or in rigor conditions the radial component of myosin cross-bridge force adds to the electrostatic and structural forces (Xu et al., 1993). This force appears because cross bridges linking the thick and thin filaments are normally at some angle to the filament axis, leading to the appearance of a force component in the radial direction, which can reach about one tenth of the axial force (Schoenberg, 1980). This component expand a compressed lattice and compress a swollen one, thus tending to bring the spacing to the equilibrium value, which is usually close to that found in vivo (Matsubara et al., 1984). It is possible that due to the presence of this force the lattice dimensions in the contracted sarcomeres are practically the same as in the relaxed state (Huxley and Brown, 1967), instead of being increased according to the law of sarcomere volume conservation (see below). Clearly, in order to account for these observations and to be consistent with the law of the fixed total volume of the myofibril it is necessary to assume that some of the cytoplasm shifts between the A-band and other parts of the sarcomere during the contraction.

2.1.6.2 Balance of forces determining the A-band spacing

The contribution of the basic interactions considered above to the radial forces within the A-band of intact striated muscle was recently measured (Millman, 1998). They consider that the net radial force in relaxed muscle is the sum of three components: osmotic (P_{om}), electrostatic (P_{es}) and passive structural (P_{st}) forces. Contraction and rigor state introduce an additional pressure from the cross bridges (P_{xb}). Under normal conditions, $P_{om}+P_{es}+P_{st}+P_{xb}=0$. To build up the outside pressure the "osmotic stress" technique was employed, which is based on the idea of adding inert, uncharged, nonpenetrating agents to the bathing solution. The electrostatic pressure P_{es} was measured by changing the ionic strength of the bathing solution. Thus, the measurements on relaxed skinned frog sartorius muscle (because these muscles are not active the P_{xb} component is absent) allowed these researches to estimate that electrostatic force is very small over most of the spacing range. In contrast, the force originating from structural elements (M-bridges) is significant at very large or very small spacings. At d_{10} between 33 and 37 nm corresponding to *in vivo* spacing (note that in order to calculate the thick filament distance this value has to be multiplied by 1.16) this structural force is near to zero. Further, after muscle activation the contribution from the cross bridge force could be measured and was found to be significantly larger than electrostatic and structural forces, at least for d_{10} larger than 32 nm.

Thus, we conclude that the role of M-bridges is to control excessive deformation of the lattice in relaxed muscle, providing the optimal distance between thick and thin filaments in the beginning of contraction. It is also conceivable that the elastic M-bridges contribute to even distribution of mechanical stress across the lattice in active muscle.

2.1.6.3 The M-band is responsible for the lateral alignment of thick filaments

The next structural role of M-bridges could be the lateral alignment of the thick filaments in the longitudinal direction. One of the consequences of the sliding filament model of muscle contraction is the inherent instability of the sarcomeric structure. If one of the thick filaments is displaced slightly towards one Z-band in active muscle, it will experience more force in the same direction due to the greater overlap it would have on that side with actin. According to the modern concepts, the titin linking the thick filament with the two adjacent Z-disks is counterbalancing this effect by supplying a centrally directed restoring force (Squire, 1997) and it is the main player, responsible for the lateral alignment of myosin filaments (Small et al., 1992). Let us consider, however, what is the value of the force exerted when the length of the elastic portion of titin is changed a little bit. Modern methods allowed the researchers to estimate the elasticity of single molecule of titin in vitro. These experiments show that at elongation about 200–300 nm from the relaxed length (here and below the data for skeletal muscle are given) titin behaves as a very compliant spring that is able to produce only weak force of the order of few pN (Rief et al., 1998). It is not surprising because in this interval the lengthening of the molecule is achieved mainly by straightening of the initially coiled Ig-region (Granzier et al., 1996; Trombitas et al., 1998). Concequently, the passive tension measurements on isolated skeletal fiber demonstrated that the significant passive force increase is not correlated with lengthening of the Ig domain region. Instead, it is correlated with extension of the PEVK element of titin that begins at elongation of about 400 nm per sarcomere (Linke et al., 1998). For comparison, the axial force exerted by a thick filament in active muscle might approach few hundred pN (Matsubara et al., 1984). Thus, titin with its extreme length is simply

incapable to correlate small displacements of the myosin filaments. At the same time, the M-bridges might accomplish this working as short connecting springs with a stiffness growing rapidly with elongation preventing thereby the myosin filaments escape from the highly ordered A-band.
There is an interesting experiment supporting this assumption: it was originally performed to check the importance of titin filaments for the centering of the A-band (Horowits and Podolsky, 1987). It showed that during the isometric contraction of the skeletal muscle, the A-bands can move from their central positions and the extent of their deviation depends on the length of the sarcomere (see Figure 2.1.4). This study suggested that this movement is due to a small initial disproportion in cross-bridge forces acting on different halves of the one of the thick filaments. However, it is not the separate thick filament alone, but the whole A-band with well defined A/I boundary that is displaced in the direction of one of Z-disks and this is clearly seen on electron micrographs (Horowits and Podolsky, 1987), and is schematically depicted on the Figure 2.1.4.

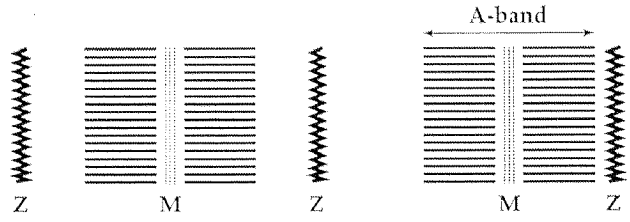

Figure 2.1.4: The A-band tends to deviate from the central position due to unbalances of cross-bridge forces. Schematical representation of the A-band movement during the isometrical contraction of skeletal muscle. Positions of the Z-disks (Z) and M-bands (M) are shown. Adapted from Horowitz, (1987).

This observation provides a strong argument that the thick filaments are tightly connected with each other. Thus, this connection is responsible for the perfect lateral alignment of thick filaments as seen in electron microscopic preparations. Titin, in its turn, provides the centering of the A-band as a whole and brings it back to the central position during the muscle relaxation.

2.1.7 M-band structure

2.1.7.1 M-band nomenclature

The M-band is a pronounced structure in the middle of the sarcomere. In the light microscope the M-band appears as dark line about 100 nm wide in the central light zone of A-band, where no myosin crossbridges are present (Sjostrom and Squire, 1977). The detailed analysis of electron micrographs revealed up to seventeen sublines, with five most prominent lines: M1, M4/M4', M6/M6' (according to the nomenclature of (Sjostrom and Squire, 1977), that were attributed to the so-called M-bridges. These filaments are supposed to link neighboring myosin filaments to each other, as seen in corresponding cross-sections of myofibrils (Luther and Squire, 1980). Secondary M-bridges in M3/M3' sublines and so-called M-filaments, which run in parallel to myosin filaments, are assumed to provide further stabilization of the M-band structure (Luther and Squire, 1978).

2.1.7.2 M-band structures vary in different muscle types

Electron microscopic studies have shown that M-band appearance correlates with the physiological performance of a particular muscle type. Generally, the slowest fibers have 4-line M-bands, the fastest have 3-line M-bands and fibers of intermediate speed have variations on 5-line pattern (Carlsson and Thornell, 1987; Edman et al., 1988; Sjostrom and Squire, 1977). The appearance of the M-band can change in the course of the development, for example, the M1 line disappear during the first four weeks from the differentiating slow fibers (Carlsson and Thornell, 1987).
In transverse sections, the M-band structure in the heart of higher vertebrates is quite similar to that of skeletal muscles. But difference is evident in the longitudinal sections, where the relative density of M1 seems to correlate with the heart beat frequency. Thus, rat cardiac M-bands show a 5-line pattern, whereas M-bands of larger animals (Guinea pig, rabbit, cow), which have lower heart beat frequencies, have a pattern known as 4+1; here the M1 line appears much stronger than the M4 or M5 lines (Pask et al., 1994).

2.1.7.3 M-band define the different symmetries of the A-band lattice

The thick filaments in vertebrate striated muscle might be arranged in two distinct A-band lattice structures (Luther et al., 1981). These types of the lattice can be distinguished because myosin filament has 3-fold rotational symmetry and has intrinsic orientation. In all skeletal and cardiac muscle of fish, studied to date the thick filament show the same orientation, forming a simple hexagonal A-band lattice (Luther, 1978). In all other vertebrates the thick filaments are arranged in a statistical superlattice. In this case, the filaments demonstrate various orientations that can be defined by a set of rules (Luther and Squire, 1980). It is assumed that the molecular interactions between the M-band proteins and myosin filaments are responsible for the formation two A-band lattice types (Luther et al., 1981). Furthermore, it was suggested that M4 bridges are the crucial for defining the A-band symmetry (Pask et al., 1994).

2.1.7.4 The muscle isoform of creatine kinase is responsible for M-band appearance on electron micrographs

The cytoplasmic isoform of creatine kinase is important for the energy supply in skeletal and cardiac muscle (Wallimann et al., 1992). Some part of this enzyme, in the form of M-CK subunit (MM-CK) is localized in the M-band in some muscle types (Stolz and Wallimann, 1998). The appearance of this enzyme in the M-bands of developing cardiac sarcomeres coincide with the ordering of the A-band lattice in both longitudinal and transverse planes (Carlsson et al., 1982). Thus, it was speculated that this enzyme might have a structural role in the M-band (Strehler, 1982, Walliman, 1983).
Several lines of evidence suggest that the MM-CK is the major component responsible for the M-band appearance in electron micrographs. Chicken cardiac muscles do not express MM-CK; they also lack the electron dense M-band (Walliman, 1977). The appearance of the M-band on the electron micrographs of newborn rat cardiac and skeletal muscles correlate with the MM-CK expression in these muscles (Carlsson et al., 1982; Carlsson and Thornell, 1987). Moreover, the extraction of the MM-CK by low salt buffer results in a loss of most of electron dense material from the M1 and M4 lines in the M-band (Strehler et al., 1983).

On the other hand there are many arguments showing that this enzyme is unlikely to play a structural role in the M-band. First, the M-band structural components must be both endurable and elastic in order to regulate A-band spacings during contraction (See section 2.1.6). These properties are difficult to reconcile with the enzyme function that needs a well-defined three-dimensional conformation of active center. Second, as already mentioned, the MM-CK is absent in some striated muscle types which does not prevent these muscles from having the ordered A-band lattice and functioning well (Walliman, 1977). Further, the MM-CK deficient mice is absolutely viable and show no pathological changes in the either cardiac or skeletal muscle (van Deursen et al., 1993).
Thus, although it is likely that the MM-CK gives the major contribution to the electron dense M-bridges that are visible in transverse and longitudinal sections of the M-band, these the strong arguments show that this protein does not play a significant structural role in this area. Rather, its localization at the M-band has strong advantages for muscle metabolism and ATP regeneration during contraction.

2.1.7.6 The structural components of the M-band

Thus, the actual observation of electron-dense M-bridges in electron microscopic pictures is due to the presence of MM-creatine kinase. This does not mean, however, that in muscles where these bridges are not seen the M-band is really absent. The effectiveness of the muscle contraction depends on the correct position of the thick filaments that can be supported only if these filaments are mechanically coupled in the M-band. Thus, it is reasonable to assume that there are proteins situated at the M-band region whose primary function is the cross-linking of the thick filaments, but these proteins are not visible as electron dense M-bridges. Naturally, the candidates for this role have to be looked for among M-band proteins that appear in all types of striated muscle.
The main structural proteins that might participate in establishing the M-band structure are N-terminal portion of titin (Labeit and Kolmerer, 1995), myomesin (Grove et al., 1984) and M-protein (Masaki and Takaiti, 1974). While titin and myomesin were found in all cross-striated muscle fibers starting from the early development (Bantle et al., 1996; Ehler et al., 1999; Grove et al., 1985; Grove et al., 1984), M-protein was found to be restricted to fast skeletal and cardiac muscle fibers in the adult animals, subsequent to a transient expression in all muscle fibers late in embryonic development (Furst et al., 1989; Grove et al., 1985). This suggests that myomesin together with titin is involved in a general mechanism controlling the assembly and maintenance of the A-band lattice, while M-protein is most likely involved in a fine-tuned structure that is needed to adsorb the greater strain in fast and cardiac muscle fibers. Additionally, it could be necessary for embryonic assembly of sarcomeres.

2.1.7.7 Current model of M-band structure

The cloning of M-band proteins made it possible to generate a number of antibodies that are directed against defined areas of these proteins and thus to accurately determine their location within the M-band. This has led researchers to the proposal of a detailed two-dimensional model of the M-band layout (Obermann et al., 1996). A reproduction is shown in Figure 2.1.5.

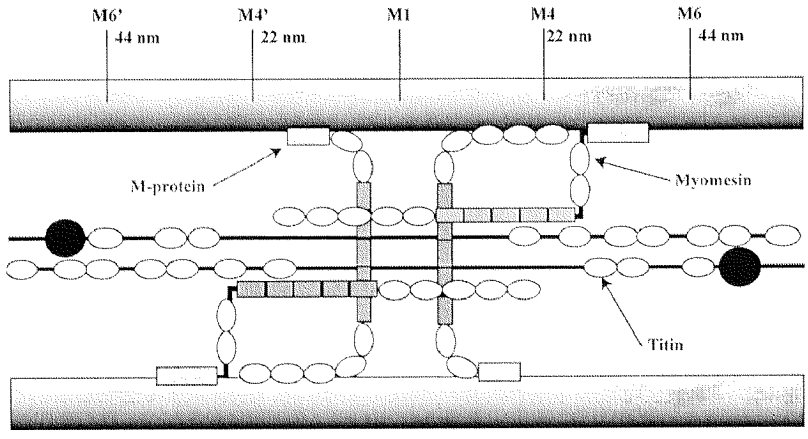

Figure 2.1.5: The current model of M-band structure. The model is based on a localization of antibodies, directed against defined regions of titin, myomesin and M-protein. Titin extends through the entire M-band, creating an antiparallel overlap with the titin strand from the opposite side of the sarcomere. The titin kinase domains are represented by a big black circles. Myomesin connects the thick filaments with titin and runs parallel to the thick filament axis for the most of its length. In contrast, M-protein is aligned orthogonal to the filament axis and contacts neighboring myosin molecules. Adapted from Obermann *et al.*, (1996).

According to Obermann model the titin molecules from opposite sides overlap in the M-band region, and are positioned in the middle between thick filaments. In this arrangement the titin-kinase domain (represented as the big black circle) is about 50 nm away from the central M1 line. M-protein is aligned perpendicular to the thick filament axis, at the level of M1 line. Both N- and C-terminal termini are organized along the thick filaments, whereas the intermediate section comprising eight domains connect the neighboring myosin filaments.

The bigger segment of the myomesin molecules runs parallel to myosin filament and is arranged in an antiparallel and staggered fashion. In this arrangement the myomesin fragment My4 - My6 is proposed to interact with the titin Ig-domain M5, as was shown by biochemical assays (Obermann et al., 1997). The model implies that titin, in complex with myomesin constitutes M-filaments that are observed in transverse section at a half distance between thick filaments (Luther and Squire, 1978). Further, it is assumed that two N-terminal part of myomesin are bent towards the thick filament and that they bind myosin via its head domain My1 at approximately M4-line level (Obermann et al., 1997). Experiments conducted in our group has shown, however, that although My1 binds myosin in solid phase assay, it requires the presence of the adjacent My2 domain, in order to be directed to the M-band in cultivated cardiomyocytes (Auerbach et al., 1999). This suggests that these domains bind cooperatively to myosin or another M-band component.

Although the predictions of the model are in a good agreement with the electron microscopic data, it fails to answer many important questions. First, it is striking that the model does not answer how the thick filament bridging is accomplished. The scheme implies that M-protein is the only linker but it is absent in many muscle types (Furst et al., 1989; Grove et al., 1985). Model also assumes that two or three myomesin domains connect myosin with titin filament. Likely, it implied that another myomesin molecule is attached on the other side thereby connecting neighboring thick filament. This, however, is difficult to reconcile with the length analysis. The length of each Ig-domain is about 4 nm, while the center-to center distance between thick filaments is about 45 nm and the surfaces are about 30 nm apart (Squire, 1981). Thus, 8 Ig-modules of M-protein and 3+3 of myomesin domains assumed by the model are not sufficient to bridge this distance. Moreover, the bridges connecting thick filaments have to be sufficiently elastic to survive the mechanical stress and allow for the significant changes in the lattice spacing during the

muscle contraction (see section 2.1.6). If one assumes that the Ig-stretch is in fact this elastic element, it needs to have a contour length much larger than the distance than it does cover. The Ig-stretch of titin elastic element, for instance, has a few times larger contour length than the interval that it occupies in slack sarcomeres (Gautel and Goulding, 1996; Linke et al., 1996).
The function of the C-terminal part of the myomesin molecule, My6-My13 also remains to be clarified: according to this model it does not participate in the myomesin-titin bridging and does not bind to any M-band component. However, the strong conservation of the amino acid sequence and domain layout of this myomesin fragment between species provides a strong argument for its functional significance. Moreover, the C-terminal myomesin epitopes are positioned in an orderly way in the M-band region (Obermann et al., 1996) indicating that they interact with some other structural elements. Clearly, the multi-component interactions can be involved in the M-band assembly; such interactions are difficult to identify by a simple biochemical assays. The question how different M-band proteins are involved in the thick filament bridging can be answered only by a combination of many approaches, including the knock-out studies and the ectopic expression of protein truncation mutants.

2.1.7.8 M-band assembly is regulated by phosphorylation

It was suggested that titin filaments in the M-band may interact with each other, since electron micrographs of isolated titin molecules often show dimers associated through their globular head (Nave et al., 1989). At present, it is not clear whether C-terminal ends of titin are able to dimerize directly or M-band proteins like myomesin or M-protein has to be also involved in this process. Both proteins are likely candidates for the involvement in this process because they consistently co-purify with titin and both are the components of the globular end of titin observed in electron micrographs (Nave et al., 1989; Vinkemeier et al., 1993). Interestingly, most of the described protein interactions between the M-band components are modified by phosphorylation. For example, the binding of My4-6 fragment of myomesin with the m4 domain of titin can be completely abolished by phosphorylation of a serine residue located in the linker connecting domains My4 and My5 of myomesin (Obermann et al., 1997). Another putative phosphorylation site was identified within the C-terminal 60 amino acids of the myomesin molecule (Obermann et al., 1995). Analogously the interaction of M-protein with myosin is modulated by the phosphorylation of the serine residue in the head domain (Obermann et al., 1998). The main player in the M-band interactions, the titin, contains in its sequence both phosphorylation sites and kinase domain (Labeit and Kolmerer, 1995).
The unique insertion is4, located in M-band portion of titin contains four KSP repeats. They can be phosphorylated by cdc2 kinase that is active in developing myoblasts but not in fully differentiated muscle (Gautel et al., 1993). Also, it seems likely that titin kinase participates in the control of myofibrillogenesis because, as it was shown recently, its activation requires a participation of another kinase that is present only in differentiating muscle cells (Mayans et al., 1998).

2.1.8 Myomesin isoforms

2.1.8.1 Myomesin is an essential component of M-band structure

Myomesin was initially described as cross-reacting antigen in the study of generating of monoclonal antibody against the M-protein (Grove et al., 1984). Subsequent studies established that this novel protein with molecular mass of about 185 kDa is an integral component of M-band and is more important than the M-protein itself (Grove et al., 1984; Perriard et al., 1986). Unlike the M-protein, the myomesin is expressed in all types of striated muscle and on all stages of development (Grove et al., 1989; Grove et al., 1985; Perriard et al., 1986). Studies of myofibrillogenesis in developing chicken heart have shown that myomesin becomes localized in its characteristic pattern simultaneously with the appearance of the first sarcomeres (Ehler et al., 1999).

Presently, the primary sequences for human myomesin (Vinkemeier et al., 1993), mouse skelemin (Price and Gomer, 1993), bovine myomesin (Obermann et al., 1995) and chicken myomesin (Bantle et al., 1996) are established. The analysis of these sequences revealed that myomesin is mainly composed of immunoglobulin-like and fibronectin type III domains arranged in a pattern that is identical with the domain arrangement of M-protein (Figure 2.1.6). The main difference between the two M-band proteins is in the structure of their unique N-terminal domains: the unique N-terminal domain of myomesin comprises 250 residues and is therefore much larger than the N-terminal domain of M-protein (Price and Gomer, 1993; Vinkemeier et al., 1993). Its most striking feature is a repeat of the amino acids KQSTAS that occurs in variable numbers in human, mouse and rat myomesin but is absent in chicken myomesin (Bantle et al., 1996; Price and Gomer, 1993; Vinkemeier et al., 1993).

It was observed in the early studies that myomesin has a strong affinity to the titin C-terminal end (Nave et al., 1989). Later biochemical assays allowed to localize precisely the binding sites of two proteins (Obermann et al., 1997). According to this study, the fragment My4-6 of myomesin interacts with domain m4 of titin, with the binding that can be completely abolished by phosphorylation of a serine residue located in the linker sequence connecting My4 and My5. The observation that the N-terminal unique domain of myomesin binds myosin led to the current model of M-band structure (Obermann et al., 1997; Obermann et al., 1998).

So, the ability of myomesin to bind both proteins suggests that its functional role is the anchoring of titin to the thick filaments in the M-band. This idea is supported by the study of early stages of myofibrillogenesis. These studies have shown that the integration of myosin filaments with the complexes containing actin, α-actinin and titin correlates with the localization of myomesin in the M-bands (Ehler et al., 1999; van Der Ven et al., 2000). Thus, it was assumed that myomesin might constitute a part of the myofibrillar scaffold that includes also titin and α-actinin, which provide the framework for the coordinated assembly of all other sarcomeric components (Ehler et al., 1999).

2.1.8.2 Myomesin has no analogs in the invertebrate muscle

Although myomesin was found in a number of vertebrate muscles, it seems to be absent from invertebrate muscles: no mRNA for myomesin was detected in muscles of insect *L.indicus* (Price and Gomer, 1993), and none of the antibodies directed against myomesin reacts with *Drosophila melanogaster* flight muscles (E. Ehler, unpublished observations).

Homology searches of genomic sequences of *Drosophila melanogaster* and *Caenorhabditis elegans* with cDNA sequences from either mouse or chicken myomesin do not result in any significant matches in the database. However, it was recently found that the switch-off the *unc*-89 gene in *C. elegans* leads to disappearance of the M-band and disorganization of the thick filaments (Benian et al., 1996). Interestingly, the 730 kDa product of *unc*-89 gene is another member of intracellular Ig-superfamily, and contains several other domains characteristic for proteins, involved in signaling pathway. The nematode sarcomeres are designed to transmit the force of contraction laterally to the cuticle, rather than longitudinally to the muscle ends, as do vertebrate sarcomeres (Burr and Gans, 1998). Thus, the nematode M-band proteins could connect the row of the thick filaments to the plasma membrane, providing the lateral force transmission. Therefore, the absence of homology with the vertebrate M-band components could be explained by quite different functions of these proteins.

2.1.8.3 Isoforms of myofibrillar proteins provide the functional diversity for sarcomeres

Despite the striking similarity at the level of the electron microscope (Small et al., 1992; Squire, 1975), the different types of striated muscle fibers are characterized by distinct contractile properties. These adaptations to specific physiological requirements are associated with the isoform diversity of sarcomeric proteins (Schiaffino and Reggiani, 1996). For example, the expression of different myosin heavy chain isoforms leads to differences in the rate of ATP hydrolysis and shortening velocity (Bottinelli et al., 1999; Buck et al., 1999; Reggiani et al., 1997) whereas different isoforms of the troponins and tropomyosins determine the variability in calcium sensitivity of the thin filaments (Pittenger et al., 1994; Schachat et al., 1987). Moreover, the occurrence of different isoforms is not restricted to proteins associated with force generation but has also been demonstrated for structural components of the sarcomere associated with force transmission. Different isoforms of titin are involved in controlling the elastic properties of different muscle types (Labeit and Kolmerer, 1995; Linke et al., 1997) and titin isoforms expressed in cardiac and skeletal muscle exhibit alternative splicing in their Z-disc and M-band regions (Kolmerer et al., 1996; Young et al., 1998). Different isoforms arise either from several genes (Weydert et al., 1985) or from different transcripts of the same gene generated by alternative splicing of the primary transcript (Bantle et al., 1996; Helfman et al., 1999; Kolmerer et al., 1996; Nadal-Ginard et al., 1991) or by alternative initiation of protein synthesis (Periasamy et al., 1984). Many isoforms show a tissue and developmental stage specific expression pattern (Sutherland et al., 1993) but so far, only a few of the regulatory sequences responsible for this specificity have been identified. The crucial puzzle concerning the isoforms of myoproteins is how to correlate the small differences in the amino acid sequences with their effects on the protein activity and function and to understand the molecular basis for physiological properties such as resting tension, elasticity or stretch activation.

2.1.8.4 Myomesin is expressed in several isoforms generated by alternative splicing

The first indication that myomesin might be expressed in several isoforms came from the observation that immunoblots of chicken heart and skeletal muscle show bands of different molecular weight (Grove et al., 1985). Subsequently, two transcripts of different sizes were detected in chicken heart and skeletal muscle (Bantle et al., 1996). These two isoforms

differ only at their respective C-termini, whereas the major part of the protein is identical (see Figure 2.1.6). The smaller skeletal muscle isoform (with a calculated molecular mass of 174 kD) is homologous to mammalian myomesin, whereas the bigger heart isoform (calculated molecular mass 182 kD) includes an additional unique segment at the C-terminus.

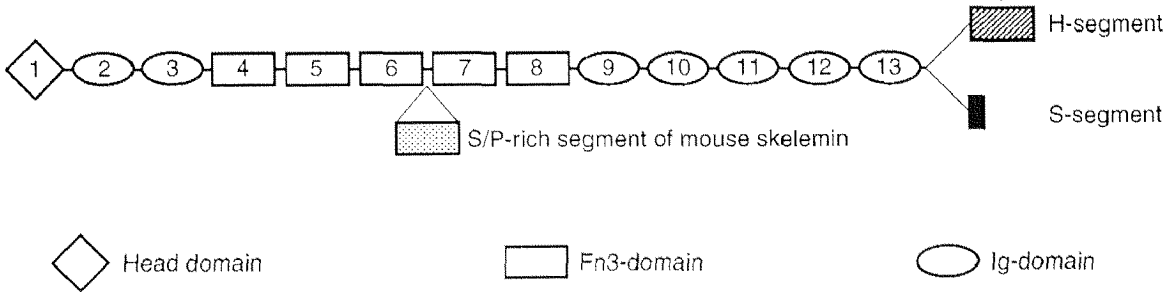

Figure 2.1.6: Schematic representation of the myomesin molecule. Myomesin consist mainly from the immunoglobulin (Ig) and fibronectin type III (Fn 3) domains. The N-terminal domain has no homologies to other known proteins. Alternative splicing on the C-termini generates two myomesin isoforms in chicken. The smallest S-myomesin is homologous to the mammalian myomesin, whereas the H-myomesin has an additional 100 residue H-segment after the last Ig domain. The mouse skelemin is characterized by the insertion of a serine/proline (S/P)-rich segment between domains My6 and My7.

Myomesin shares its modular structure with two other M-band associated proteins, M-protein and skelemin. All three proteins are closely related and have a common ancestor in evolution (Kenny et al., 1999). The nearest relative of myomesin is skelemin, which was originally described as a protein localized at the periphery of the M-band in mouse skeletal muscle (Price, 1987; Price and Gomer, 1993). The two skelemin isoforms, with molecular weights of 200 kDa and 220 kDa have been postulated, but no tissue-specificity has been shown (Price, 1987). Since the putative desmin core-like motifs were found in the skelemin sequence, it was proposed that it might be a link between the myofibrils and intermediate filaments (Price and Gomer, 1993). However, the recent determination of the complete gene structure of murine myomesin has unambiguously proven that skelemin is a splice variant of myomesin that is characterized by the insertion of a serine/proline (S/P)-rich domain between domains My6 and My7 (Steiner et al., 1999). However, the existence of an avian (chicken) counterpart to skelemin has not yet been confirmed and the functional role of this myomesin isoform remains obscure.

2.1.9 Aim of the project

The sarcomere of striated muscle is a natural machine that produces mechanical force. To guarantee its efficiency, it is very important that all components precisely fit each other, like wheels in a mechanical clock. The M-band in the center of the sarcomere is responsible for the maintaining the regular packing of the thick filaments. For this purpose, it must endure mechanical stress during sarcomeric contraction and also adjust to the changing physiological parameters of different muscle types. In order to understand the principle of its function one needs to analyze all its components and their mutual interactions.
The investigation of the M-band has a long history in the Institute of Cell Biology (Eppenberger et al., 1981; Eppenberger et al., 1982; Strehler et al., 1983; Strehler et al., 1980). One of the most evident successes of this study was the discovery of myomesin

((Grove et al., 1984). Follow-up work has shown that this essential sarcomeric component might be expressed in different isoforms (Grove et al., 1985). This was later confirmed by the study of (Bantle, 1997) who identified two different myomesin mRNAs transcripts in chicken striated muscle. Moreover, the study revealed the composition of these mRNA and indicated the differential expression in chicken heart and skeletal muscles. However, a comprehensive examination of the appearance and distribution of these isoforms on the protein level was lacking. For this reason, it was proposed to generate antibodies against the isoform-specific segments of chicken myomesin and use these to analyze the temporal and spatial expression of the myomesin isoforms in chicken. In this respect, this study is the direct continuation of the study done by Bantle *et al* .

Starting from its discovery in mouse skeletal muscle by Price et al. (Price, 1987) skelemin was a puzzling subject. When its primary sequence was determined (Price and Gomer, 1993) it became clear that this protein has a high homology to both human and chicken myomesin (Bantle et al., 1996; Vinkemeier et al., 1993). In chicken, however, no skelemin was found by immunostaining (Price, 1987) and no skelemin transcript was detected in Nothern blots of chicken RNA (Price and Gomer, 1993). At the beginning of this study in 1996 neither the structure of the putative skelemin gene nor the myomesin gene structure was known. The problem was further complicated by the fact that for a long time it was believed that skelemin is a distinct sarcomeric protein, with a function that is different from other M-band components. Nevertheless, it was proposed that skelemin could be a splice variant of myomesin. The findings presented here together with myomesin gene structure, published recently (Steiner et al., 1999) confirmed this unambiguously.

Furthermore, we planned to express recombinant isoform-specific segments of myomesin in cultured myocytes in order to investigate the myomesin isoform-specific functions. This strategy has been used successfully to investigate the role of myosin light chain and actin (Komiyama et al., 1996; Soldati and Perriard, 1991; von Arx et al., 1995).

Thus the main goal of our study was to establish how many myomesin isoforms are expressed in the striated muscle of higher vertebrates, and to investigate their composition and expression pattern.

Here, the issue of myomesin isoform diversity is reported. The expression pattern of different myomesin isoforms was analyzed using a combination of RT-PCR analysis and isoform-specific antibody. It was found that in chicken two alternative splicing events give rise to four myomesin isoforms, whereas in mammals and reptiles, a single splicing event leads only to two isoforms. The expression of the different isoforms is strictly regulated in a tissue-specific and developmental stage-specific manner. One of the splice variants proved to be an excellent marker for embryonic heart. In addition, it was established that the myomesin is an essential component of striated muscle sarcomere in all vertebrates from mammals to fishes.

2.2 Results

2.2.1 Expression of myomesin isoform mRNA in chicken is tissue and developmental stage specific

2.2.1.1 H-myomesin message is expressed exclusively in the heart

To study whether myomesin isoforms are expressed in a tissue and stage specific manner we performed RT-PCR analysis on total RNA isolated from chicken heart and skeletal muscles at different developmental stages (Figure 2.2.1). Three isoform-specific primer sets were derived from the published sequence of chicken myomesin (Bantle et al., 1996). The positions of the primers are shown in Figure 2.2.1.

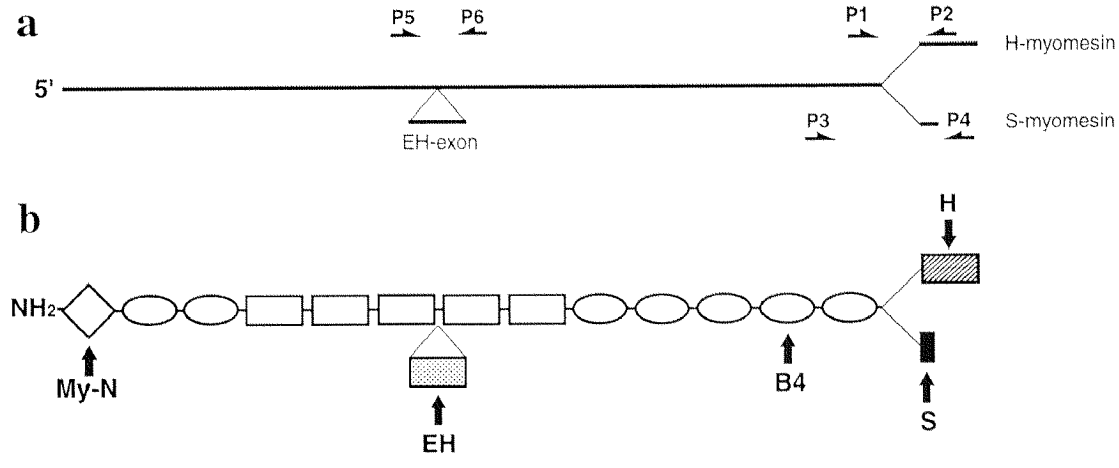

Figure 2.2.1: Schematic representation of myomesin isoforms.
a: Scheme of the chicken myomesin cDNA. The position of the alternative EH-exon is marked by a triangle. The alternatively spliced S- and H-exons are shown at the 3' end. Positions of P1-P6 PCR primers that were used in this study are indicated by halfarrows.
b: Diagram of the chicken myomesin protein. Chicken S- and H-myomesin isoforms differ in their C-terminus; the S-isoform has a short C-terminal sequence, which is very homologous to the mammalian variant of myomesin, whereas the H-isoform is characterized by an unique H-segment. The EH-isoform has an additional EH-segment inserted in the center of the molecule. Arrows indicate the positions of the epitopes of the antibodies, which were used in this study.

Control experiments carried out with cDNA, corresponding to either H- or S-myomesin isoforms confirmed the specificity of generated primers. The length of the fragments amplified from the cDNA serves as a control for the specificity of the bands, amplified from the total RNA extracts, further, to exclude all doubts we sequenced all the products. Using the primers P1 and P2 located in the C-terminal H-segment of myomesin, a 236 bp product was amplified from heart extracts of different embryonic stages, as well as from hatching-stage and adult hearts (Fig. 2.2.2 a, lanes 1-5).

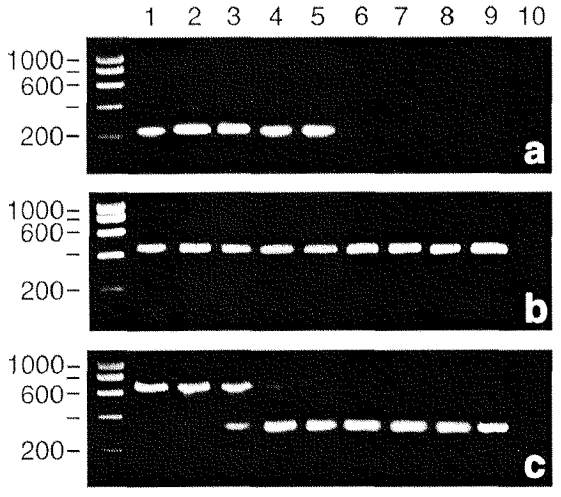

Figure 2.2.2: Expression of myomesin isoform mRNAs in chicken is tissue and developmental stage specific. RT-PCR analysis of total RNA extracted from chicken tissues of different developmental stages. Different sets of primers (see Fig.2.2.1) were used to detect the H-isoform (a, primers P1 and P2), the S-isoform (b, primers P3 and P4) and the EH-isoform (c, primers P5 and P6). Lane 1-5: heart extracts of HH stages 17, 29, 38, hatching and adult; lane 6-9: skeletal muscle extracts of HH stages 29, 38, hatching and adult; lane 10: brain from hatching-stage chicken. Fragment sizes are indicated on the left in bp. A single product of 236 bp is amplified in heart but not in skeletal muscle tissue using heart specific primers (a), while skeletal muscle specific primers give a single product of 434 bp in both kinds of striated muscle at all stages of development (b). Using primers specific for the domains flanking the optional domain in the central part of myomesin a product of 636 bp corresponding to the EH(+) splice variant can be amplified in embryonic heart, but not in adult heart or skeletal muscle of any stage (c). Although EH(+) is the only isoform found in heart at the earliest stages, it is rapidly replaced around birth by the EH(-) isoform; the latter is represented by the band of 327 bp. In skeletal muscle a product of 327 bp corresponding to EH(-) RNA is amplified at all developmental stages. No product is amplified from brain of hatching chicken with all sets of primers specific for chicken myomesin (a, b and c, lane 10). The amount of the total RNA loaded on the each line was normalized by RT-PCR using primers specific for chicken α-tubulin (data not shown).

By contrast, no product was observed in RNA samples prepared from identical stages of skeletal muscle or brain of hatching chicken (Figure 2.2.2 a, lanes 6-10). These results are consistent with earlier findings indicating that the expression of this isoform in chicken is restricted to the heart (Bantle et al., 1996). Therefore, we will refer to this isoform as H (heart)-myomesin, carrying the H-segment at the C-terminus.

2.2.1.2 S-myomesin message is accumulated in both types of striated muscle

Using a primer pair specific to the C-terminal sequence found in the skeletal isoform of myomesin (primers P3 and P4 in Figure 2.2.1), a product of 434 bp was amplified from both heart and skeletal muscle samples (Figure 2.2.2 b, lanes 1-5 and 6-9, respectively). However the intensity of the bands obtained from heart samples was found to be weaker as the ones from the skeletal muscle samples (Figure 2.2.2 b, lanes 1-5). Therefore, the isoform previously termed "skeletal muscle specific" (Bantle et al., 1996) is expressed in both types of striated muscle in chicken, but its expression level is much lower in the heart. This isoform is referred to as S (skeletal)-myomesin because it is mainly found in chicken skeletal muscle and the short sequence added to the C-terminus by alternative splicing is referred to as S-segment.

2.2.1.3 Inclusion of alternative EH-exon is characteristic for embryonic heart

The analysis of cDNA and genomic sequences of mouse myomesin has shown that alternative splicing of an exon located between fibronectin type III domains My6 and My7 gives rise to another isoform which has been termed skelemin (Price and Gomer, 1993; Steiner et al., 1999). However, no such isoform had been previously reported in chicken (Bantle et al., 1996) or human myomesin (Vinkemeier et al., 1993). To check this, we designed the primers P5 and P6, located in domains My6 and My7 of myomesin, which flank the alternatively spliced segment (Fig. 2.2.1 a). Surprisingly, we found that the alternatively spliced segment is not only present in chicken, but that its expression is developmentally regulated. While at early embryonic stages a product of 636 bp, corresponding to the myomesin isoform that includes the alternatively spliced exon was observed in heart, a product of 327-bp was found at later stages (Figure 2.2.2 c). The size of the latter product corresponds to a myomesin isoform lacking the alternatively spliced segment between domains My6 and My7 as previously described (Bantle et al., 1996). In the hearts of hatching stage embryos and in adult chicken, the 636-bp product was completely replaced by the 327-bp product (Figure 2.2.2 c). In order to confirm the presence of the alternatively spliced segment, the 636-bp product was cloned and sequenced, revealing a sequence stretch of 103 amino acids that was inserted between domains My6 and My7 of chicken myomesin. Sequence comparison with the alternatively spliced exon 17a of mouse skelemin (Steiner et al., 1999) showed a high homology (see below and figure 2.2.14), thus confirming the presence of this alternative splice variant in chicken. Interestingly, RT-PCR analysis of chicken skeletal muscle samples of different stages using the primer pair P5 and P6 gave rise to the 327 bp product only (Figure 2.2.2 c). Neither product could be amplified from adult brain. Thus, we postulated that the alternatively spliced fragment between My6 and My7 is only included in myomesin that is expressed in pre-natal stages of chicken heart. Therefore we termed this isoform EH (embryonic heart)-myomesin, since it contains the EH-insertion.

2.2.2 Generation of isoform-specific antibodies in rabbits

2.2.2.1 Expression of isoform-specific myomesin fragments in bacterial system

The RT-PCR analysis confirmed Bantle's conclusion that the expression of the chicken myomesin C-terminal splice variants is regulated in tissue-specific manner, further, it revealed the presence of a novel myomesin isoform that is restricted to embryonic heart. In order to investigate the myomesin isoform diversity in chicken at the protein level, we decided to generate the isoform-specific antibodies in rabbits.

Each myomesin isoform required a new strategy to produce antibodies against it. Because the S-segment differs from H- and EH-segments by its smaller size, the corresponding isoform-specific 20-mer amino acid residue peptide was synthesized and coupled to keyhole limpet hemocyanin (KLH) for rabbits immunization (for details, see M&M). KLH is a broadly used carrier protein for making hapten-carrier conjugates in antibody production (Schneider et al., 1983). Its high molecular mass ($4.5x10^5$-$1.3x10^7$), along with the fact that it is foreign to mammalian immune systems, make KLH highly immunogenic.

The isoform-specific H- and EH-segments of chicken myomesin consist of 89 and 103 amino acids, so we decided to produce them in a bacterial system. This method allows to get a large amount of recombinant protein that can be later used for immunization of rabbits and for biochemical studies. The nucleotides of the H-segment of chicken myomesin was amplified from the original cDNA clone (Bantle et al., 1996) and subcloned into the Bam HI site of the bacterial expression plasmid pGEX-2T (Pharmacia, Uppsala, Sweden). The EH-segment of chicken myomesin including parts of the surrounding fibronectin type III domains was amplified by RT-PCR from HH38 (Hamburger-Hamilton stage 38) embryonic chicken total RNA and subcloned into the Eco RI and Xba I sites of Bluescript II KS(+) (Stratagene, Amsterdam, Netherlands), and verified by sequencing. Subsequently, the EH-segment was amplified by PCR and subcloned into the Bgl II and Eco RI sites of pGEX-2T. The expression of polypeptides in frame with glutathione S-transferase (GST) allows purification of the fusion proteins from crude bacterial extracts under mild nondenaturing conditions by affinity chromatography on glutathione agarose, thus minimizing effects on antigenicity and functional activity of the expressed proteins (Smith and Johnson, 1988). Expression from a pGEX plasmid is controlled by the *tac* promoter, which is induced using the lactose analog isopropyl β-D-thiogalactoside (IPTG). Different E.coli strains were tried out to increase the level of protein expression and growth and induction conditions were varied in order to obtain the sufficient amount of soluble recombinant protein.
Finally, after a long series of trials the conditions were found, at which the fusion protein is at the same time highly expressed and remains soluble (Figure 2.2.3).

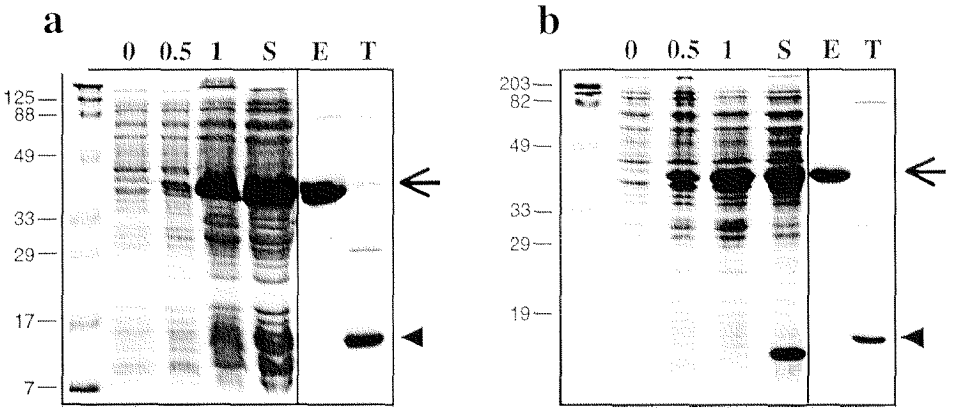

Figure 2.2.3: Expression and purification of chicken myomesin constructs from E. coli. The H-(a) and EH-segment (b) of chicken myomesin were expressed in BL-21 cells as GST-fusion proteins. Bacterial extracts were prepared after IPTG induction for the indicated periods of time (0, 0.5 and 1 hour). The bacterial lysates were cleared by centrifugation and the supernatants (S) were applied directly to Glutathione Agarose. Proteins were purified either as eluates (E) or as thrombin cleavage products (T). The fusion proteins and the cleaved recombinant fragments are indicated with arrows or arrowheads respectively. Proteins were separated in 15% SDS-PAGE followed by Coomassie Blue staining. Molecular weight markers are indicated in kDa.

An overnight culture of E.coli (strain BL-21) transformed with recombinant vectors IA3.3 and IA8.3, encoding the H-segment, accordingly EH-segment of chicken myomesin fused to GST was diluted 1:50 -1:100 in fresh medium and grown to log phase (OD_{600}≈0.6) before adding IPTG to a final concentration of 0.1 mM. The bacterial culture was incubated at 37°C, with intensive shaking and open lids in order to increase aeration, since high

oxygen transport can prevent the formation of inclusion bodies (Schein, 1990). For control of expression, bacterial extracts were prepared after IPTG induction for the indicated periods of time (0, 0.5, and 1 hour; Figure 2.2.3). After 2 hours of induction, the cells were pelleted and resuspended in 1/100-1/50 culture volume of STE-buffer containing 0.5 mg/ml lysozyme and protease inhibitors. After 15-minutes incubation on ice, DTT was added to 5 mM and the cells were lysed on ice using mild sonication. The bacterial lysate was cleared by centrifugation (Figure 2.2.3, lane S) and applied directly to a glutathion agarose column for purification. After the fusion protein was bound to the matrix, it was washed with buffer to remove non-specifically bound proteins. The desirable fusion protein was eluted with 10 mM glutathione and used for production of myomesin isoforms specific antibodies and in binding assays (Figure 2.2.3, lanes E). Alternatively, the fusion protein bound to the column matrix was cleaved with thrombin. After 1-2 hours of incubation with thrombin solution by room temperature, the eluate, containing the purified protein was collected (Figure 2.2.3, lanes T), while GST remained bound to the matrix. The purity and integrity of the recombinant proteins was monitored by SDS-PAGE.

2.2.2.2 Immunization of rabbits

We generated H- and EH-myomesin specific antisera by immunizing the adult female rabbits with the H- and EH-segments fused to GST. At the beginning of our work we did not find an example in the literature where GST was used as a carrier protein by immunization. However, we expected that that the pool of polyclonal serum that reacts with GST will not disturb the analysis of eukaryotic extracts and tissues because GST coming from the parasitic helminth *S. Japonicum* does not have close analogs among eukaryotic sarcomeric proteins. Our expectation was later proved to be correct. For the primary injection about 400 μg of fusion protein in PBS were emulsified with the same volume of complete Freund's adjuvant (Freund, 1956) and injected subcutaneosly (Vaitukaitis, 1981). The animals were successively boosted three times with 4-5 weeks interval with a mixture of 200-400 μg of fusion protein in PBS and the same volume of incomplete Freund's adjuvant.

After the booster-injections, small samples of blood were taken and the specificity of the response was checked by Western blot analysis. As soon as strong and specific responses were detected, the animals were sacrificed and the total sera were collected. The immunoglobulin fraction was prepared by ammonium-sulfate precipitation, and the antibody specificity further characterized.

2.2.2.3 Characterization of the polyclonal antibodies

In a number of preliminary experiments the immunosera obtained from rabbits that were immunized with the same antigen was compared and for following experiments only one antiserum showing the best specificity was retained. Accordingly, the antibodies were named anti-S, anti-H and anti-EH. The specificity of the antibodies was checked by immunoblot analysis of chicken tissue extracts (Figure 2.2.4).

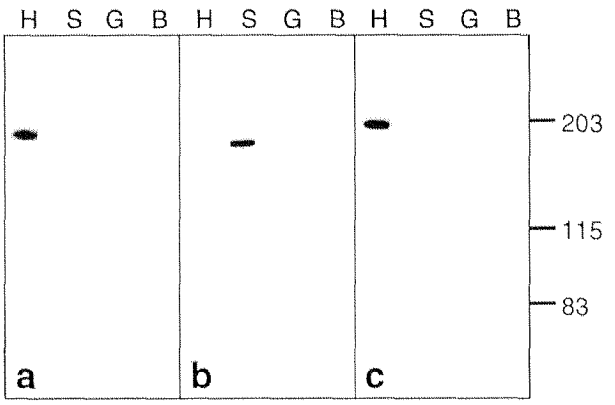

Figure 2.2.4: Specificity of polyclonal antibodies raised to different myomesin isoforms. Antibodies specific for chicken H-myomesin (a), S-myomesin (b) and EH-myomesin (c) isoforms were tested on SDS-samples of adult (a and b) and HH stage 45 embryonic (c) chicken tissues. Lane H: heart, lane S: skeletal muscle, lane G: gizzard, lane B: brain. Molecular weight markers are indicated in kDa. The anti-H antibody recognizes a band of about 190 kDa in the adult heart extract but not in skeletal muscle, gizzard or brain extracts. The anti-S antibody recognizes a band of about 180 kDa in skeletal muscle extracts but not in heart, gizzard and brain extract. The anti-EH antibody recognizes a band of about 200 kDa in the embryonic heart extract only: it does not react with embryonic skeletal muscle, gizzard, brain or any adult tissue extracts.

The anti-H antibody recognized a protein with a molecular weight of about 190 kDa in extracts of adult chicken heart and did not react with extracts of skeletal muscle (Figure 2.2.4 a). The anti-S antibody recognized a protein of about 180 kDa in skeletal muscle extracts but did not react with heart extracts (Figure 2.2.3 b). Although the RT-PCR analysis indicated that small amounts of the S-myomesin isoform mRNA are indeed accumulated in chicken heart, no protein product was detected suggesting that expression of S-myomesin protein in the heart is too low to be detected by immunoblotting. Note, that in contrast to anti-H and anti-S antibodies the anti-EH antibodies were characterized on the extracts of embryonic chicken tissues, since the results of RT-PCR analysis gave us the insight that the expression of the EH-myomesin stops after birth. This is confirmed by the fact that anti-EH antibody recognizes a protein of almost 200 kDa in extracts of embryonic chicken heart and does not react with skeletal muscle extracts (Figure 2.2.3 c). When preimmune sera are used at a similar dilution no reaction with the same chicken extracts is detected (data not shown). The apparent molecular weights of the myomesin isoforms determined by immunoblottting are in good agreement with the calculated sizes for S-, H- and EH-myomesin (Bantle et al., 1996; Price and Gomer, 1993). Note that the expression of all three myomesin isoforms is restricted to striated muscle and that none of the antibodies reacted with smooth muscle (gizzard extract) or non-muscle tissue (brain extract).

To further confirm their specificity, the antibodies were tested by immunofluorescence staining of cultured chicken embryonic cardiomyocytes (Figure 2.2.5 a-f) and skeletal muscle cells (Figure 2.2.5 g-l). All three isoform-specific antibodies label the M-band of the sarcomeres as is demonstrated by the antiperiodic staining obtained with a monoclonal antibody against sarcomeric α-actinin, which is located in the Z-disc of the sarcomere (Figure 2.2.5, insets). The anti-H antibody reacts strongly with the M-band of embryonic chicken cardiomyocytes (Figure 2.2.5 a), but an extremely weak M-band staining is also observed in skeletal muscle cells (Figure 2.2.5 g). The possible reason for it is cross-reaction of the anti-H antibody with S-myomesin, which is too weak to be observed in

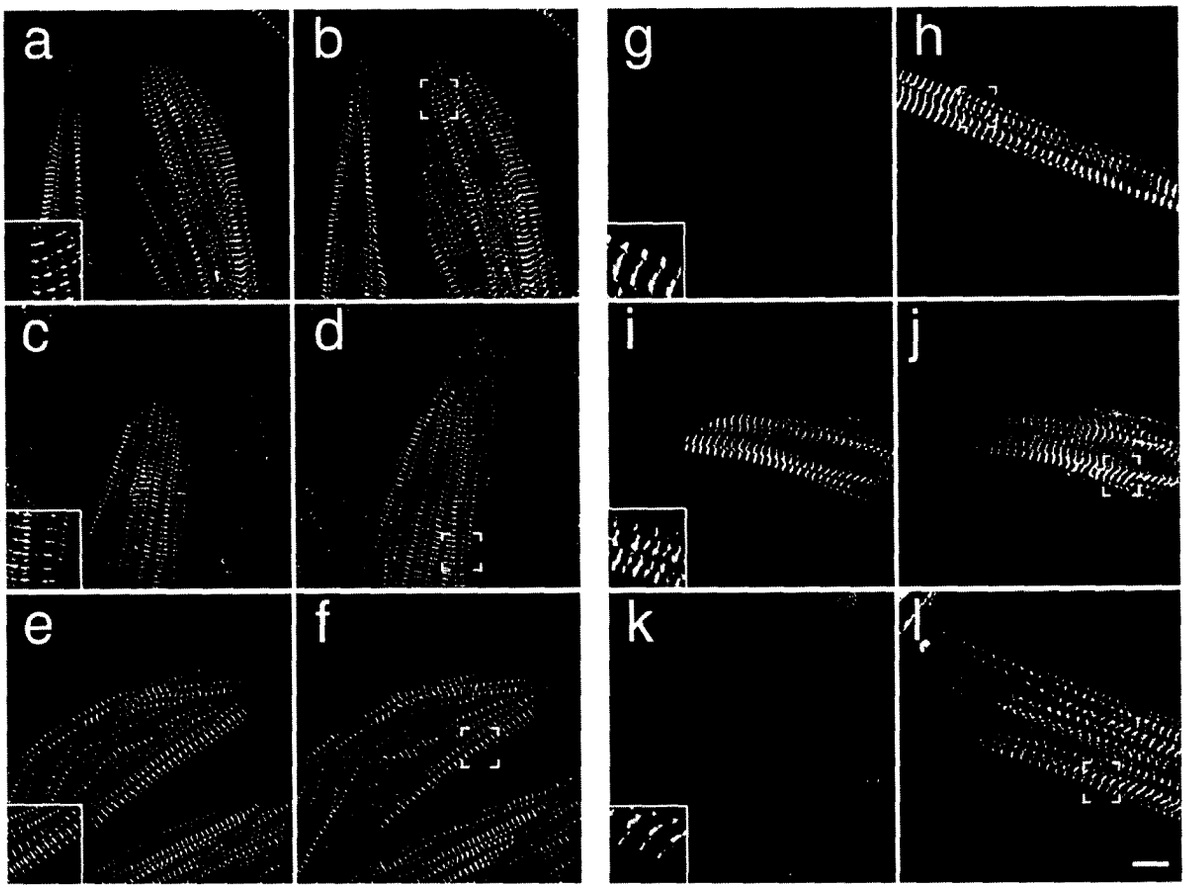

Figure 2.2.5: Immunofluorescent detection of myomesin isoforms in cultured chicken cardiomyocytes and skeletal muscle cells. Confocal images of cultured embryonic chicken cardiomyocytes (a-f) and embryonic chicken skeletal muscle myocytes (g-l) double-stained with anti-H (a, g), anti-S (c, i) or anti-EH (e, k) antibodies and an antibody against sarcomeric α-actinin (b, d, f, h, j and l). As shown by the superimposition of both signals in insets a, c, e, g, i and k all polyclonal antibodies specifically stain the M-band. The anti-H antibody reacts specifically with the chicken cardiomyocytes (a). A weak M-band staining can be seen in skeletal muscle cells (g) indicating a weak cross-reaction of anti-H antibody with S myomesin isoform possibly due to a shared epitope. The anti-S antibody reacts strongly with skeletal myocytes (i) and weakly with cardiomyocytes (c). The anti-EH antibody reacts exclusively with embryonic cardiomyocytes (e) and not with embryonic skeletal muscle cells (k). The inset pictures are two times magnified. Bar 10 μm.

immunoblots (see Figure 2.2.4). The possibility that the faint signal in skeletal muscle cells is due to weak cross-reactivity is also supported by RT-PCR results where no H-isoform mRNA could be detected in skeletal muscle (see Figure 2.2.2 a). Sequence comparisons between the H-segment and the S-segment identified several short elements consisting of three or four amino acids that occur in both sequences and that may lead to cross-reacting epitopes (Bantle et al., 1996).
The anti-S antibody specifically stains chicken skeletal myotubes (Figure 2.2.5 i) and, although more weakly, also cardiomyocytes (Figure 2.2.5 c). We believe that this staining is specific because the RT-PCR results already pointed to an expression of S-myomesin in chicken heart (see Figure 2.2.2 b). The staining obtained with the anti-S antibody on cardiomyocytes was very weak, so that the signal had to be amplified by image processing resulting in some non-specific background (e.g. weak nuclear staining in Figure 2.2.5 c).
The anti-EH antibody reacts exclusively with embryonic chicken cardiomyocytes (Figure 2.2.5 e) but not with embryonic chicken skeletal muscle cells (Figure 2.2.5 k).
These stainings confirm that all antibodies specifically recognize the respective myomesin isoforms in the M-band. In addition, it can be concluded that in cultured skeletal muscle cells only S-myomesin is present, whereas all three different isoforms are co-expressed in cultured embryonic cardiomyocytes. Since sarcomeric α-actinin is present in Z-discs throughout the sarcomere, it is also possible to investigate whether any of the myomesin isoforms is incorporated only in a subset of sarcomeres within a given cell by comparing the staining of sarcomeric α-actinin with that of the isoform-specific antibodies. Comparison of the two stainings in Figure 2.2.5 shows that regardless of the expression level, all three isoform specific antibodies uniformly stain the M-bands of all myofibrils in cultured cardiomyocytes. Thus, as judged by light microscopy, all myomesin isoforms appear to be incorporated equally well into the M-bands of myofibrils.

2.2.3 Isoform expression pattern is tissue-specific in chicken embryo

Having established the specificity of the generated antibodies and the localization of their corresponding antigens, we analyzed the distribution of myomesin isoforms in situ during embryonic development. Cryosections of stage 29 chicken embryos were stained using isoform specific antibodies in combination with a monoclonal antibody against sarcomeric α-actinin and phalloidin to visualize F-actin (Figure 2.2.6). As opposed to staining of cultured cells, the distribution and relative amounts of different myomesin isoforms can be assessed directly by comparing the staining intensities of isoform specific antibodies in cryosections containing both heart (arrowheads) and skeletal muscle anlagen (arrows). The anti-H and anti-EH antibodies stain embryonic heart (Figure 2.2.6 a, g) only, whereas the anti-S antibody strongly stains skeletal muscle tissue and, to a weaker extent, the heart (Figure 2.2.6 d). No difference in the intensity in which the different types of striated muscles were stained is observed with the antibody against sarcomeric α-actinin (Figure 2.2.6 b, e, h) or with F-actin staining (Figure 2.2.6 c, f, i). These findings confirm the conclusions drawn from the RT-PCR analysis and the stainings of isolated myocytes, namely, that all splice variants of myomesin can be detected in the embryonic chicken heart although the expression of S-myomesin is much weaker than that of H- and EH-isoforms. This is in contrast to skeletal muscles where the S-splice variant that has no EH-insertion is the only expressed myomesin isoform.

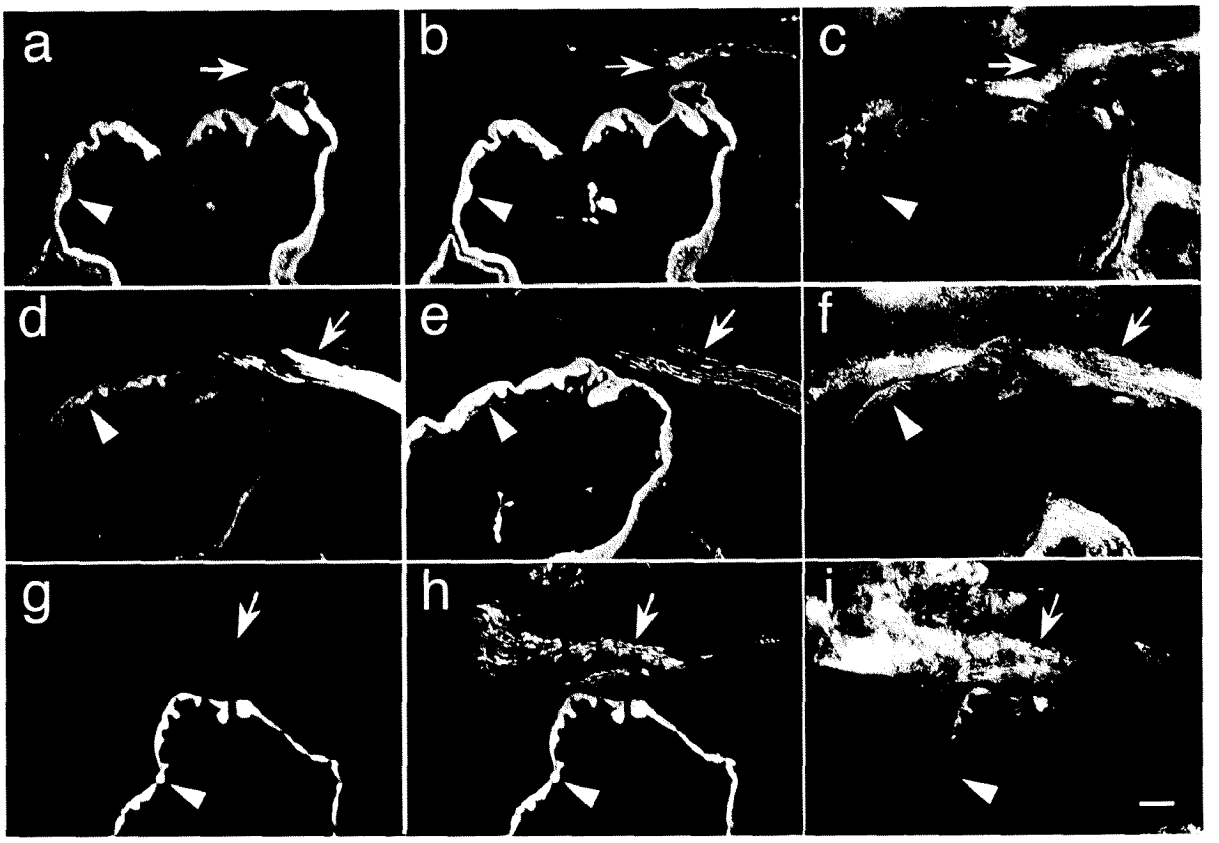

Figure 2.2.6: The expression of myomesin isoforms is tissue-specific in chicken embryos. CCD-camera images of HH stage 29 chicken embryo cryosections triple-stained with anti-H (a), anti-S (d) or anti-EH (g) antibodies together with antibodies to sarcomeric α-actinin (b, e and h) and phalloidin to visualize F-actin (c, f and i). Arrowheads indicate the position of the heart, arrows indicate the position of the skeletal muscle anlage in the vicinity of the heart. The anti-H antibody specifically stains the heart and no other tissue (a) while the anti-S antibody strongly stains the first skeletal muscle anlagen and to a smaller extent the heart (d). The anti-EH antibody specifically stains the heart and does not react with skeletal muscle or other tissue (g). Bar, 100 μm.

2.2.4 Expression of EH-myomesin is developmentally regulated in chicken

The results of our RT-PCR analysis indicate that there is change in myomesin isoform expression during embryonic heart development. In order to confirm that this is also the case at the protein level we performed immunoblots on chicken heart and skeletal muscle tissue of different developmental stages using our isoform specific antibodies (Figure 2.2.7).

With the anti-H antibody, we detected a shift of molecular weight for H-myomesin in heart extracts of different stages of development. While in embryonic hearts a high molecular weight band was predominant, at hatching stage, it becomes replaced by a lower molecular weight one (Figure 2.2.7, row H, lanes 1-6). A similar shift in molecular weight of S-myomesin is detected by the anti-S antibody on heart extracts (Figure 2.2.7, row S, lanes 1-6). Thus, at early stages, H-myomesin and S-myomesin are co-expressed in the developing heart, with the level of S-myomesin being significantly lower since the immunoblot had to be overexposed in order to reveal the signal for S-myomesin. A rough comparison of the band intensities obtained from heart and skeletal extracts indicates that the expression level of S-myomesin in heart is at least one order of magnitude lower than in skeletal muscle (data not shown). In skeletal muscle S-myomesin is the only isoform expressed at every developmental stage. Also, there is no transition in molecular weight (Figure 2.2.7, row S, lanes 8-11).

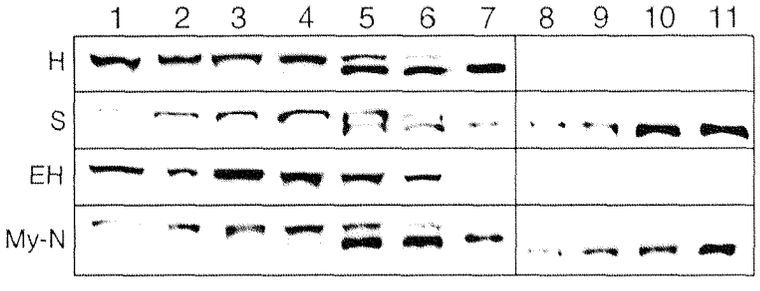

Figure 2.2.7: The expression of myomesin isoforms in chicken is regulated in a tissue and stage-specific manner. Striated muscle extracts of chicken at different developmental stages were probed by immunoblot with anti-H (H), anti-S (S), anti-EH (EH) or with an antibody My190-Nrt that recognizes all myomesin isoforms (My-N). Lanes 1-7: heart extracts of HH stages 17, 29, 34, 38, 44, hatching and adult; lanes 8-11: skeletal muscle extracts of HH stages 29, 38, hatching and adult. Note that the H and S isoforms are coexpressed in the heart but that the S isoform is expressed at much lower level. The panel S for the heart (lanes 1-7, row S) was exposed much longer as panel S for skeletal muscle (lanes 8-11, row S) in order to visualize a weak expression of the S myomesin isoform there. Comparison of the rows (H) and (S) shows that at early stages only the EH(+) variant is present (lanes 1-3) and that the double line corresponding to the alternative splicing event appears simultaneously in H- and S-isoforms (lanes 5-6). Thus, the splicing of the EH-segment is independent from the C-terminal extensions. After hatching, the EH(+) isoforms become downregulated and in the adult heart only the EH(-) isoforms are expressed (lane 7). In contrast, in skeletal muscle only the S isoform, which lacks the optional EH exon, is expressed throughout development and in adult stages (lanes 8-11). In agreement with these conclusions, the antibody against the EH domain shows the strong expression of EH isoform in the embryonic heart but only traces of the protein in the adult heart and it does not react with skeletal muscle extracts (row EH). Note that the EH and general myomesin antibody My190-Nrt detect only the heart isoform but no the skeletal muscle one because the latter is expressed at much lower level in the heart (row EH and My-N).

Immunoblots with the anti-EH antibody reveal that, at the early developmental stages, the upper band of the doublet is due to an inclusion of the EH-segment. Because of the low

abundance of the S-myomesin only the H-myomesin containing the EH-segment is visible on the blot (Figure 2.2.6, row EH, lanes 1-6). At the time of birth the reactivity with the anti-EH antibody decreases and only a very weak signal can be detected in the adult heart (Figure 2.2.6, row EH, lane 7). Comparison of rows H, S and EH suggests that the co-expressed isoforms, the highly abundant H-myomesin as well as the low-abundant S-myomesin include the EH-segment during early embryonic heart development but that this segment is spliced out at the time of hatching. No signal can be detected with the anti-EH antibody in skeletal muscle at any stage (Figure 2.2.6, row EH, lanes 8-11). Immunoblots with the general My190-Nrt antibody confirm these results, since a similar transition to lower molecular weight was detected in the same heart extracts (Figure 2.2.6, row My-N, lanes 1-7), but not in skeletal muscle (lanes 8-11). Note that this antibody, analogously to anti-EH-antibody reveals only the H-myomesin but not S-myomesin in the heart, since its expression is too low to be detected at normal exposure times. A number of tests which directly compare the reaction of anti-S-antibodies with the heart and skeletal muscle extracts, allowed us to estimate that the expression level of S-myomesin in the skeletal muscle is about one-two orders of magnitude higher than in heart (data not shown).

To summarize, we have performed a detailed developmental analysis of myomesin isoform expression in chicken. This analysis has shown that the H- and S-myomesin isoforms are the major myomesin species in the heart and skeletal muscles of chicken at all developmental stages while the inclusion of the EH-segment into the different myomesin isoforms is characteristic for embryonic chicken heart.

2.2.5 Expression of myomesin in early embryonic heart

2.2.5.1 All myomesin isoforms are co-expressed in the embryonic chicken heart during early developmental stages

The sensitivity of western blot analysis, described in previous chapter turns out to be insufficient to detect the expression of myomesin isoforms (especially, the low abundant S-isoform) in the embryonic chicken heart at early developmental stages. During these stages of embryogenesis, the important sequence of events leads to the appearance of the first functioning organ in the embryo, namely, the heart (Ehler et al., 1999). According to previous studies myomesin was clearly shown to be confined to the M-band (Bantle et al., 1996; Grove et al., 1985; Obermann et al., 1995). However, the problem of differential sorting of myomesin isoforms has not been addressed in these publications. In order to study the myomesin isoform expression and localization at the early developmental stages, the immunostaining of the whole mount preparations of embryonic chicken hearts (stage 12) was carried out (Figure 2.2.8). All specimens were stained with the combination consisting of one of the polyclonal isoform-specific antibodies (shown in green) and the general monoclonal myomesin antibody B4 (shown in red), which cross-reacts with all chicken myomesin isoforms.

First, the staining of each from myomesin isoforms specific antibodies coincides in the M-bands with the staining of general myomesin antibody. This indicates that the available antibodies against all myomesin isoform found their targets, confirming the presence of a corresponding isoforms in the embryonic heart. Note that the signal from the anti-S antibody was very weak, so we had to amplify it by image processing (Figure 2.2.8, b and

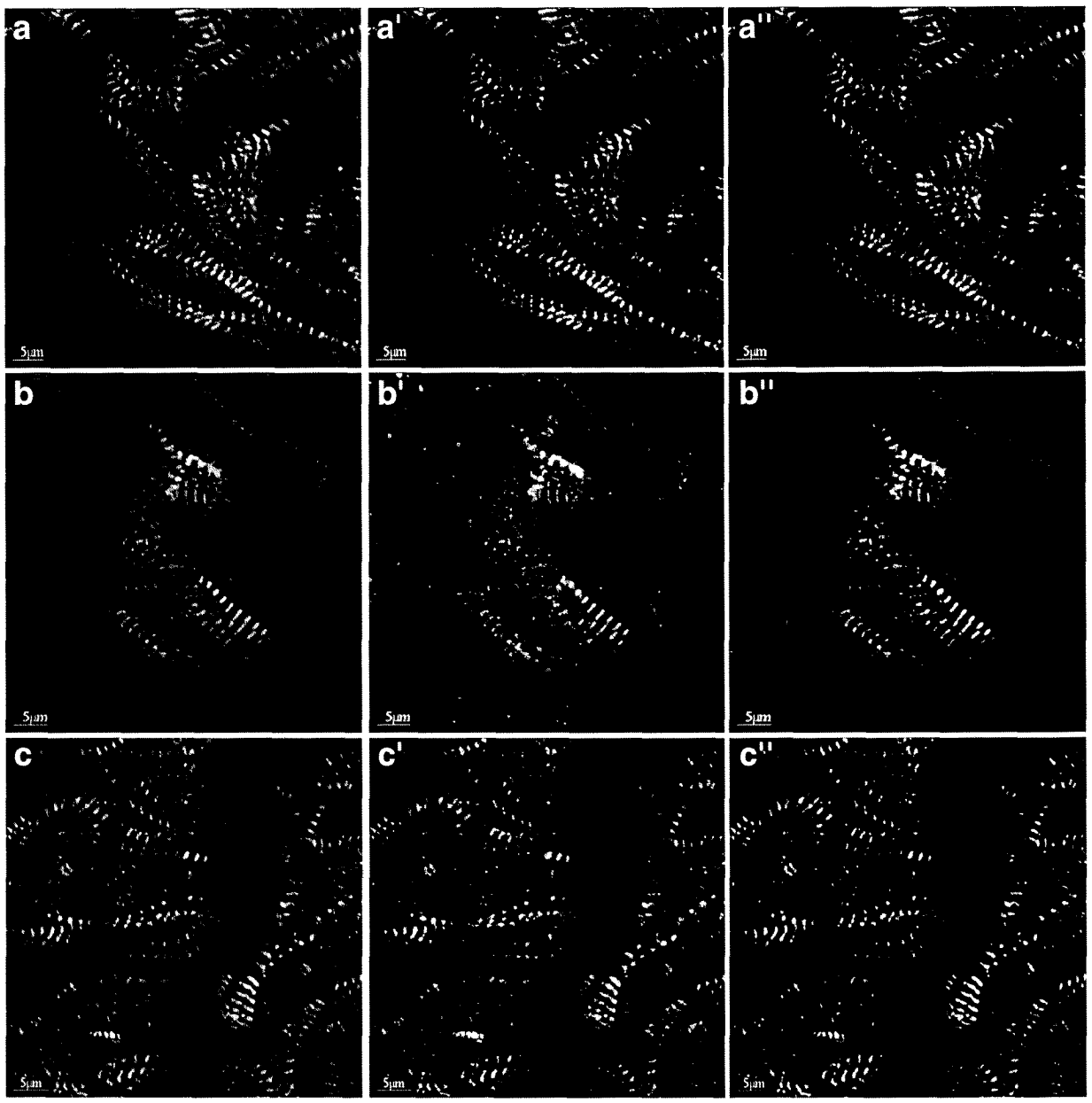

Figure 2.2.8: All myomesin isoforms can be detected in chicken heart at early developmental stages. Confocal sections taken from double-labelled chicken heart whole mount preparations at the 13 somite stage stained with anti-H (a'; green in a), anti-S (b'; green in b) and anti-EH (c'; green in c) antibodies together with mM antibody B4 (a'', b'', c''; green in a, b, and c), which crossreact with all myomesin isoforms. The superimposed images are shown in a, b and c. The staining obtained with the anti-S antibody was very weak, so that the signal had to be amplified resulting in some non-specific background (e.g. the green dots in b, correspondingly white dots in b'). The stainings with anti-H, anti-S and anti-EH antibody overlapped with the staining with general myomesin antibody B4 (a, b and c) demonstrating that non of the myomesin isoforms are sorted to the special locations but incorporated uniformly into the M-bands of the first sarcomeres.

b'). It is likely that an insufficient amount of corresponding antigen, present in this tissue, combined with a long incubation time used in immunostaining of whole mount preparations results in the antibody sticking to unspecific sites in the specimen. This leads to the appearance of unspecific background, consisting of a quantity of green dots, which superimpose the specific staining (b', green in b). However, the specific signal from the anti-S antibody is localized in M-band, analogously to the signals from the anti-H and anti-EH antibodies, demonstrating that all myomesin isoforms are co-expressed in the embryonic chicken heart in the course of the first sarcomere assembly.
The appearance of some M-band signals only in one picture (i.e. only in one color) would be the evidence of specific localization of the corresponding isoform. However, the signals from all polyclonal antisera overlapped with the staining with general myomesin antibody B4, resulting in yellow color of the superimposed image (Figure 2.2.8, a, b and c). This coincidence lead to the second important conclusion that the myomesin isoforms are not sorted to special locations but are incorporated uniformly into all M-bands of the first sarcomeres in the embryonic chicken heart.

2.2.5.2 Myomesin becomes localized in periodic pattern simultaneously with the appearance of the first sarcomeres

In our study we have found that the dominating myomesin isoform in the early embryonic heart is the H-myomesin with the inserted EH-segment. Thus, both anti-H and anti-EH antibody can be used for the study of the myofibrillogenesis process in the embryonic chicken heart. Further, due to their origin from rabbits they can be conveniently combined with monoclonal antibodies against other myofibrillar proteins.
Observations made during embryonic heart development showed that assembly of myoproteins into functional sarcomeres occurs fast and well coordinated (Ehler et al., 1999). The first contractions are observed in the 9-somite chicken heart. At this moment all sarcomeric proteins, including myomesin are already expressed (naturally this should happen before the heart starts to beat) while myofibril assembly is going to happen within a few hours. In order to study the involvement of myomesin in this process we used the isoform-specific myomesin antibodies for immunofluorescent analysis of embryonic chicken heart. By using the triple labeling technique we were able to compare localization of myomesin with the localization of the major sarcomeric proteins within the same myofibril (Figure 2.2.9). The whole mount preparations of embryonic chicken heart, taken at the stage 12, were stained with the anti-H antibody (a''', b''', green in a and b), together with the monoclonal antibody against sarcomeric myosin heavy chain (a'', red in a), or antibody against sarcomeric α-actinin (b'', red in b), combined with the phalloidin to visualize F-actin (a', b', blue in a and b). Among all stained proteins the myomesin appear to be localized exclusively in sarcomeric pattern, while other proteins are also observed in diffuse distributions. Most likely, this apparent absence of myomesin in diffuse state can be explained by the fact that the signal from an individual myomesin molecule drifting in cytoplasm is too weak whereas a number of molecules forming highly-ordered structure (such as in M-band) produced a signal observable by confocal microscope. The detailed comparison of myomesin organization with other components reveals that regions where actin and myosin show periodicity typical for sarcomeric organization are always associated with regularly arranged myomesin dots (shown by arrows). As was shown in earlier studies, myomesin becomes localized in a periodic pattern simultaneously with the

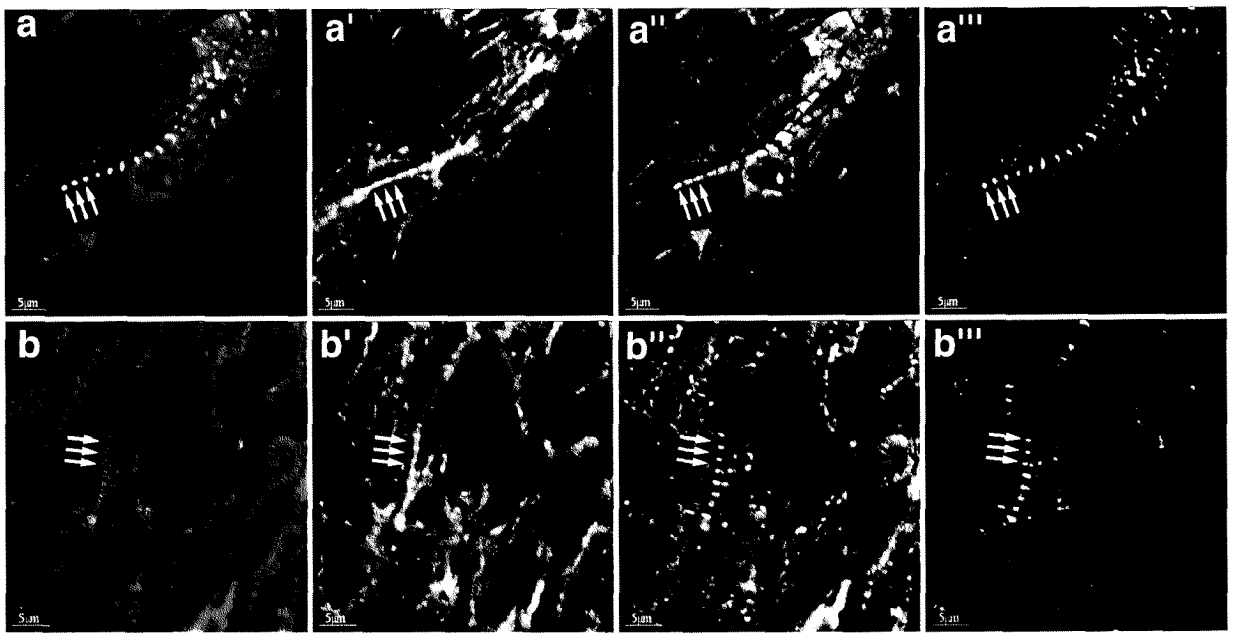

Figure 2.2.9: Myomesin is part of the basic framework in the sarcomere. Confocal sections taken from triple-labelled chicken heart whole mount preparations at the 12 somite stage (a-a''') and of cultured embryonic chicken myoblasts (b-b''') stained with anti-H (a', b'; green in a and b) antibodies together with mM antibodies IgG to sarcomeric myosin heavy chain (a''; red in a), or mM IgM antibodies to sarcomeric α-actinin (b'''; red in b) and phalloidin to visualize F-actin (a''', b'''; blau in a and b). The superimposed images are shown in a and b.

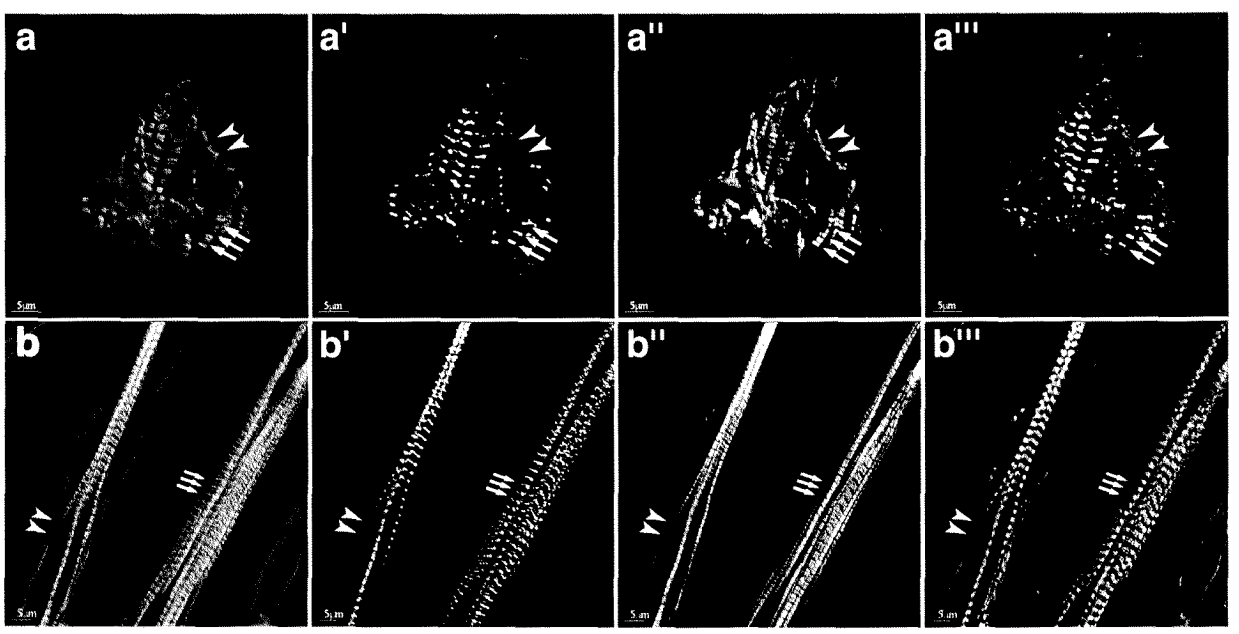

Figure 2.2.10: Myomesin is required for the integration of thick filaments and titin during myofibrillogenesis. Confocal sections taken from triple-labelled chicken heart whole mount preparations at the 12 somite stage (a-a''') and of cultured embryonic chicken myoblasts (b-b''') stained with anti-EH (a'; blau in a), anti-S (b'; blau in b) antibodies together with mM antibody IgG to sarcomeric myosin heavy chain (a'', b''; red in a and b) and mM IgM antibodies to titin , clone 9D10 (a''', b'''; green in a and b). The superimposed images are shown in a and b. Each mature double band of myosin and titin is associated with the myomesin, which is localized in the M-band (arrows), whereas no myomesin spots can be detected in non-sarcomeric accumulations, containing myosin and titin (arrowheads).

appearance of the first sarcomeres in the embryonic heart (Auerbach et al., 1997; Ehler et al., 1999). Taken together with the fact that the myomesin is present in all types of striated muscle without a single exception (Grove et al., 1985), these observations suggest that myomesin is an essential building block of the sarcomeric structure.
Some investigators proposed that in the process of sarcomeric construction the thick filaments might be assembled independently and only become incorporated later into myofibrils (Schultheiss et al., 1990; Wang and Wright, 1988). Although the some diffusive aggregations of myosin was observed separately from actin structures, bipolar thick filaments, fasten by myomesin in the middle, are always associated with actin filaments (Figure 2.2.10, a, arrows). Analogously, all myomesin spots are co-localized with actin filaments that display regularly spaced Z-disks, revealed by α-actinin staining (Figure 2.2.10, b). Thus, myomesin might play an important role in association of myosin filaments with actin filaments based complexes, containing titin and α-actinin, that seem to be the first building blocks for myofibrillogenesis (Ehler et al., 1999; Furst et al., 1989; Tokuyasu and Maher, 1987).

2.2.5.3 Myomesin is required for the integration of thick filaments and titin during myofibrillogenesis

In order to build a sarcomeric structure out of many different proteins one needs a template that determines the positions of different elements of this structure. The most probable candidate for this role is titin, which extends from the Z-disk (N-terminus) to the M-line (C-terminus). The important role of this protein during myofibrillogenesis was demonstrated in many studies (Tokuyasu and Maher, 1987; Turnacioglu et al., 1997; van der Ven et al., 1999). It was also shown that titin participates in dense body-like structures, which later transform into Z-disks (Tokuyasu and Maher, 1987). To perform as a sarcomeric ruler, the titin have to unfold their C-terminus, attach to the corresponding titin strand from the opposite side and put the myosin filaments in register. The mechanism of this process remains unclear. Myomesin, that shows binding to both myosin and titin in vitro might be a candidate for the role of integrating molecule in the M-band.
To compare the localization of myomesin, sarcomeric myosin and titin during early stages of sarcomere assembly, we performed triple staining of whole mounts preparations of embryonic chicken heart at the 12 somite stage or of cultured embryonic chicken myoblasts, isolated at HH stage 36 (Figure 2.2.10). The anti-EH antibody was used for the detection of myomesin in the heart sample (Figure 2.2.10 a', blue in a), whereas the anti-S antibody was employed in skeletal myoblasts (Figure 2.2.10 b', blue in b). The 9D10 antibody, which recognizes an epitope in the PEVK region in the I-band of titin (Figure 2.2.10 a''', b''', green in a and b) and antibody against sarcomeric myosin heavy chain (Figure 2.2.10 a'', b'', red in a and b) were used for visualization of titin and myosin respectively. Comparing to heart muscle, the skeletal sarcomeres were fixed in a more relaxed state which is shown by the doubling of titin antibody bands (Figure 2.2.10 b'''). Despite this difference in these two tissues we may note one general feature–in both cases all double bands of myosin are associated with myomesin and the position of the mature A-band complexes coincides with the regions where titin bands are arranged in regular periodic pattern (arrows). However, myomesin is absent from the regions of diffuse accumulation of myosin and titin (arrowheads). This suggest that although myosin filaments are assembled independently as shown by electron microscopy (Hiruma and

Hirakow, 1985; Manasek, 1968), their integration into sarcomeres can only happen together with the M-band structure composed of the antiparallel C-termini of titin and of myomesin.

2.2.6 Myomesin isoform diversity in vertebrates

2.2.6.1 High molecular weight isoform was detected in the cardiac extracts of all tested birds, but the reactivity with anti-H antibody depends from the evolutionary distances

The analysis of the myomesin isoforms expression revealed that H-myomesin is expressed in the heart of chicken throughout all stages of development. To investigate whether the presence of this distinct isoform in heart is a common feature of avian species, we performed immunoblotting on heart and skeletal muscle extracts of several bird species that are at different evolutionary distances from chicken (Figure 2.2.11).

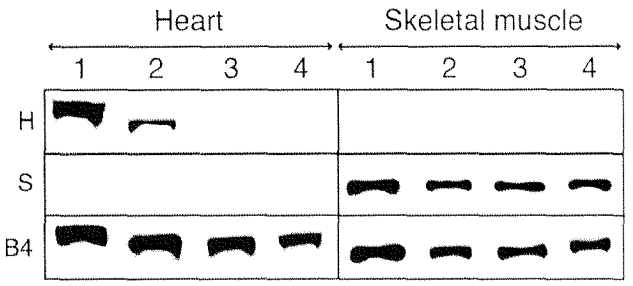

Figure 2.2.11: Different bird species express the H-isoform of myomesin in the heart. Striated muscle extracts of different avian species were probed by immunoblot with either anti-H (H), anti-S (S) antibodies or with an antibody that recognizes all myomesin isoforms (B4). Equal amounts of muscle proteins from chicken (lane 1), goose (lane 2), pigeon (lane 3), and ostrich (lane 4) were loaded on a SDS gel. The chicken anti-H antibody does not react with the heart extracts of other birds with the exception of goose with which they react, albeit very weakly (row H). The anti-S antibody reacts with skeletal muscle extracts of all tested birds, indicating that the skeletal epitope is conserved to a much higher degree than the heart epitope among avian species (row S). The general antibody against myomesin B4 reacts with both myomesin isoforms in all avian species; it shows that the mobility of the heart and skeletal myomesin isoforms is different. Thus, it seems that all birds have the C-terminal heart domain but its sequence is not conserved between distantly related avian species.

The anti-H and anti-S antibodies were used together with the antibody B4 which recognizes an epitope in the domain My12 near the C-terminus (see Figure 2.2.1 b) and therefore cross-reacts with all myomesin isoforms. Surprisingly, the anti-H antibody does not react with the heart extracts of the majority of the birds that were tested, with the notable exception of a weak reaction visible in the extract from goose, which is closely related to chicken (Figure 2.2.11, row H, line 2). In contrast, the anti-S antibody reacts with the skeletal muscle extracts of all birds investigated, indicating that among avian species, the S-segment is much more conserved than the H-segment. However, the fact that the anti-S antibody does not react with any of the heart extracts clearly shows that the C-terminus of avian H-myomesin differs from that of S-myomesin. This observation is confirmed by immunoblots with the B4 antibody that demonstrates that the mobility of heart and skeletal muscle myomesin are different in all avian species investigated (Figure 2.2.10, row B4). These results indicate that all birds express an isoform of higher molecular weight in the heart, and that the higher molecular weight is probably due to the presence of an

alternatively spliced domain at the C-terminus. Nevertheless, the sequence of this H-segment is not conserved between distantly related avian species as shown by the lack of cross-reactivity with the anti-H antibodies.

2.2.6.2 Only S-myomesin is found in the heart and skeletal muscles of mammals and reptiles, while the amphibians and fishes exhibit high molecular weight isoform in cardiac muscle

The finding that a heart-specific isoform of myomesin is present in all avian species that we investigated raises the question whether such an isoform may also be present in the hearts of mammalian species. We consequently analyzed the reactivity of heart and skeletal muscle extracts of several vertebrates using all available antibodies against myomesin (Figure 2.2.12).

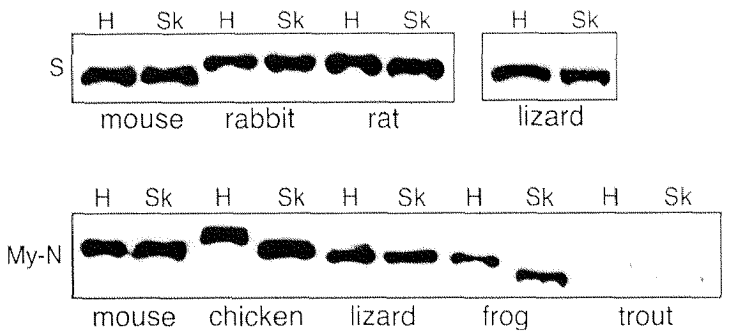

Figure 2.2.12: The H-myomesin isoform is not present in all vertebrates. Striated muscle samples of different vertebrate species were probed by immunoblot with anti-S antibody (S) or an antibody My190-Nrt that recognizes all myomesin isoforms (My-N). H: proteins extracted from heart; Sk: proteins extracted from skeletal muscle. In contrast to birds, only one myomesin isoform can be found in adult mammalian and reptilian tissues because the anti-S antibody recognizes myomesin in both heart and skeletal extracts of mammals and reptiles (row S). The analysis of the heart and skeletal extracts of different animals with the general myomesin antibody My190-Nrt (row My-N) shows that mammals and reptiles have only one myomesin isoform in the heart and skeletal muscle. In contrast, the heart myomesin in birds, amphibians and fishes has a lower mobility than the skeletal myomesin from the same species. This suggests that also some lower vertebrates may possess a heart-specific C-terminal segment.

Of these extracts, only chicken heart showed a specific reaction with the anti-H antibody (data not shown). This had to be expected since the epitope is not even conserved between birds (see Figure 2.2.11, row S). In contrast, the anti-S antibody reacts strongly with both heart and skeletal extracts of several mammals and a reptile species (lizard), yielding bands of the same apparent molecular weight (Figure 2.2.12). From these results, we conclude that in these species, only S-isoform appears to be expressed in both adult heart and skeletal muscle. We also tested two lower vertebrates, frog and fish, but no specific staining was observed when using the anti-S antibody (data not shown). Obviously, these species have C-termini that differ from those found in higher vertebrates. For the study of evolutionary distantly related species, the antibody My190-Nrt, which was generated against the head domain of human myomesin (Obermann et al., 1996), proved to be more effective. Despite the fact that the head domain sequence is rather heterogeneous between vertebrates (Bantle et al., 1996), the antibody My190-Nrt recognizes myomesin in all vertebrate muscle extracts tested, although very weakly in fish (Figure 2.2.12, row My-N). In heart and skeletal muscle extracts of mammals and reptiles, the antibody recognized a band of

identical molecular weight, which suggests that these species express only one isoform in their heart and skeletal muscles. However, in skeletal muscle extracts of chicken, frog, and trout, the myomesin isoform detected was apparently smaller than in the corresponding heart extracts. Since none of the antibodies generated against the alternatively spliced segments of myomesin reacts with extracts of these species, we do not know whether the difference in mobility is due to a splicing event or due to a posttranslational modification of myomesin. In spite of the fact that the C-terminal sequence appears to be variable among lower vertebrates, the molecular weight of myomesin remains roughly the same from fish to mammalian muscles.

2.2.6.3 EH-myomesin is expressed in embryonic heart of mammals, too

As was discussed in the preceding sections, the novel myomesin isoform, containing an alternatively spliced EH-segment in the middle part of the molecule, is expressed in embryonic chicken heart. To determine whether the EH-myomesin isoform is also expressed in embryonic hearts of mammalian species we analyzed mouse hearts of different developmental stages by RT-PCR (Figure 2.2.13 a) and immunoblotting (Figure 2.2.13 b). In embryonic mouse heart two amplification products were observed with primers located in domains My6 and My7 of myomesin (Figure 2.2.13 a, lanes 1, 2).

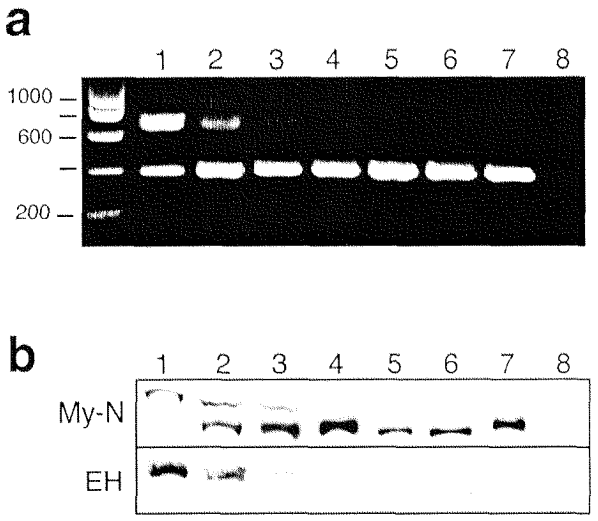

Figure 2.2.13:The inclusion of the EH segment in the central part of the myomesin molecule characterizes the embryonic heart of mammals, too.
a: RT-PCR analysis of total RNA from different mouse tissues with primers derived for the domains flanking the embryonic heart specific domain. Lanes 1-4: heart of embryonic stages 14.5, 18.5, newborn and adult; lanes 5-7: skeletal muscle of embryonic stage 18.5, newborn and adult; lane 8: brain of newborn mouse. Fragment sizes are indicated on the left in bp. The upper product of 687 bp, corresponding to the EH(+) splice variant is predominant at early stages in embryonic mouse heart (lane1), but is rapidly replaced around birth by the EH(-) isoform represented by a product of 395 bp (lanes 2 and 3). Only the lower band, corresponding to the EH(-) isoform can be amplified in adult heart and skeletal muscle extracts of all developmental stages (lanes 4-7). No signal was amplified from brain from newborn mouse (lane 8).
b: Striated muscles of mouse at different developmental stages were probed by immunoblot with anti-S (S) or anti-EH antibody (EH). The lanes are the same as in a. In accordance with the RT-PCR analysis the chicken skeletal myomesin specific antibody (S) recognizes the upper band, corresponding to EH(+) isoform at early stages in heart (lane 1), then the doublet of both bands can be seen in the heart around birth (lanes 2 and 3) and finally, only the lower band, corresponding to the EH(-) isoform appears in adult heart and in skeletal muscle extracts at all developmental stages (lanes 4-7). The anti-EH antibody recognizes only the upper band of embryonic heart extracts (lanes 1-3). This confirms the suggestion that the upper band in panel S

corresponds to the mouse EH(+) myomesin isoform. Both antibodies do not react with brain tissue from newborn mouse (lane 8).

The upper band completely disappears at the time of birth and at adult stages (Figure 2.2.13 a, lane 3 and 4, respectively) and also can not be detected in skeletal muscles of any stage. Immunoblot analysis confirms that the upper band is due to the inclusion of the EH-segment. In embryonic mouse heart a high molecular weight band is recognized both by the antibody My190-Nrt and the anti-EH antibody (Figure 2.2.13 b, lane 1, 2). Around birth, a second band of lower molecular weight appears (Figure 2.2.13 b, lane 3). In adult heart, as well as in skeletal muscle this is the only detectable isoform (Figure 2.2.13 b, lanes 4 and 5-7). This isoform does not contain the EH-segment since the anti-EH antibody does not recognize it. Thus, we conclude that the presence of an embryonic isoform of myomesin in heart, termed EH-myomesin, is characteristic for avian as well for mammalian species and is therefore a universal marker for embryonic heart.

2.2.6.4 The sequence of human EH-segment reveals a high homology to the mouse EH-segment

By searching the EST database (Boguski et al., 1993) using the sequence of the mouse EH-segment we were able to identify a human EST clone (accession number AA248352) which was originally isolated from a cDNA-library of human fetal heart. Sequencing indicates that this clone represents the complete sequence of the human myomesin EH-segment. The deduced amino acid sequence is aligned with the mouse and chicken EH-segments (Figure 2.2.14).

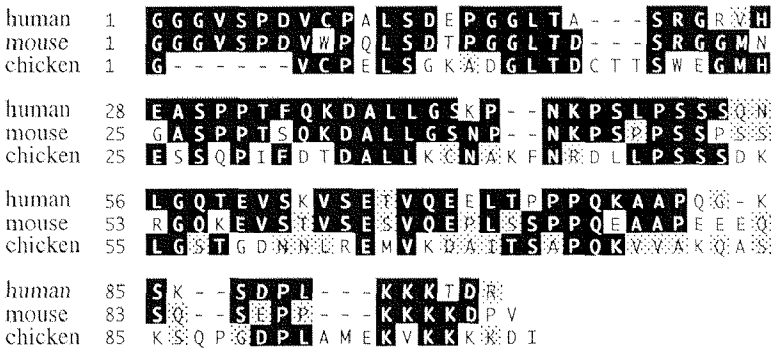

Figure 2.2.14: Comparison of mouse, human and chicken EH-segments sequences. The deduced amino acid sequences of the human (GenBank accession number AF185573), mouse (fragment of the myomesin/skelemin sequence available under accession number AJ012072), and chicken (GenBank accession number AF185572) EH-segments were aligned using the Clustal W method. Black boxes indicate identical residues and dotted boxes indicate conservative exchanges.

The highest homology occurs between the human and mouse EH sequences (65% identity, 76% similarity), whereas the chicken sequence is more divergent (36% identity, 48% similarity compared to mouse). Both mouse and human EH-segments are rich in serine/proline residues, hence the original name serine/proline rich domain, but this feature does not seem to be essential since the chicken counterpart contains fewer serine and proline residues. The presence of the EH-segment in a human EST clone originating from a fetal heart library clearly confirms our RT-PCR and immunoblot data for chicken and mouse and suggests that the expression of EH-myomesin can indeed serve as a marker for embryonic heart.

2.2.6.5 EH-myomesin can be detected in the heart of newborn lizard

Birds and reptiles are in close proximity on the evolutionary tree (Remane, 1979). The comparison of cytochrom-C sequences confirms the close relationships of these two species at the genes level (Kaempfe, 1985). Thus, the absence of the C-terminal splice variants of myomesin in the striated muscle of lizard (see section 2.6.2) was quite unexpected. To find out whether the EH-splice variant of myomesin appears in reptilian muscles, we checked the reactivity of heart and skeletal muscle extracts of newborn lizard with chicken myomesin isoform-specific antibodies (Figure 2.2.15).

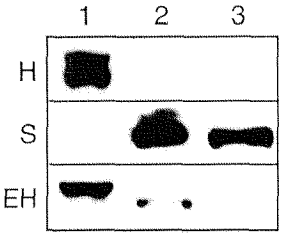

Figure 2.2.15: EH-myomesin is expressed in the heart of newborn lizard. Equal amounts of proteins from the heart of hatching chicken (lane 1), heart of newborn lizard (lane 2) and skeletal muscle of newborn lizard (lane 3) were loaded on a SDS gel. These extracts were probed by immunoblot with either anti-H (H), anti-S (S) or with anti-EH (EH) antibodies. The chicken anti-H antibody does not react with the heart and skeletal muscle extracts of lizard (row H, lines 2 and 3), thereas the anti-S antibody reacts with both lizard extracts (row S, lines 2 and 3), indicating the absence of H-splice variant from the lizard myomesin. However, the anti-S antibody reveals the dublet of bands in the newborn lizard heart extract (row S, line 2), similar to the one, detected by the anti-H antibody in the heart of hatching chicken (row H, line 1). The anti-EH antibody reacts with the upper bands in both chicken and lizard extracts, confirming the presence of EH-insertion in the lizard myomesin. A significant difference in motility between chicken and lizard EH-myomesin can be explained by the absence of H-segment at the C-terminus of lizard myomesin.

The heart extract of hatching chicken was used as a control (lane 1). Both lizard muscle extracts react only with anti-S antibody, but not with the anti-H antibody, confirming the conclusion made in 2.6.2, that only one myomesin isoform is expressed in adult reptilian muscle. However, the staining of the heart of newborn lizard with the anti-S antibody reveals the doublet (lane 2), analogously to the one appearing in the heart of hatching chicken (lane 1). Thus, we may assume that the upper band corresponds to the lizard counterpart to EH-myomesin. Indeed, the anti-EH antibody recognizes this upper band in the lizard heart extract, confirming the presence of this isoform in reptiles. We have also observed that reaction of anti-EH antibody with the lizard heart extract is stronger and much more specific than the reaction with the mouse heart extract. We assume that the sequence of reptilian EH-segment is closer related to chicken EH-segment than the mammalian one (compare with Figure 2.2.13 b). A significant difference in motility between chicken and lizard EH-myomesin (Figure 2.2.15, row EH) can be explained by the absence of the H-segment at the C-terminus of lizard myomesin.

2.2.6.6 Higher molecular weight myomesin isoform is expressed in the embryonic Xenopus heart

Thus, all higher vertebrates (amniotes), including mammals, birds and reptiles express the EH-myomesin in the embryonic heart. To determine, whether this also holds true for lower vertebrates (anamnia), the extracts of Xenopus tadpole (stage 59), and adult Xenopus were analyzed by immunoblot (Figure 2.2.16). As was noted above, none of our myomesin

isoform-specific antibodies reacts specifically with Xenopus extracts, thus for this assay we had to use general myomesin antibody My190-Nrt, that recognizes the epitope in the head domain of myomesin.

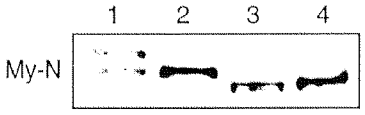

Figure 2.2.16: Expression of the myomesin isoforms in Xenopus muscle seems to be tissue- and developmentally-regulated. Equal amounts of proteins from the heart of xenopus tadpole (lane 1), heart of adult Xenopus (lane 2), skeletal muscle of Xenopus tadpole (lane 3) and skeletal muscle of adult Xenopus (lane 4) were loaded on SDS gel. These extracts were probed by immunoblot with My190-Nrt antibody, which recognizes the epitope in the head domain of myomesin. The pattern of myomesin isoform expression in Xenopus resembles the one in chicken. Namely, the high molecular weight isoform appear in the embryonic heart (lane 1) and additionally, the myomesin in heart extract demonstrates the slower motility as in skeletal muscle.

Interestingly, the expression of myomesin isoforms in Xenopus muscle seems to be tissue and developmentally regulated. The anti-myomesin antibody recognizes two bands in the heart of Xenopus tadpole, while the upper band disappears in the adult Xenopus heart and is not observed in skeletal muscle extracts. Whether the high molecular weight is due to inclusion of the EH-segment is unclear because specific antibody is not available. However, the general pattern of Xenopus myomesin isoform expression is similar to the one in chicken. The resemblance is enforced by the fact that myomesin in adult Xenopus heart extract has slower motility than the one in skeletal muscle. As was already noted, the reason for this difference remains unknown.

2.2.7. EH-myomesin is reexpressed in mouse models showing phenotype of dilated cardiomyopathy

Re-expression of the fetal isoforms of several sarcomeric proteins has been described in deceased hearts (for review see (Chien, 1999)). To investigate whether the EH-myomesin isoform is re-expressed in the adult heart in some pathological situations, several rodent models for cardiomyopathy were examined (Figure 2.2.17). In each case for control we have used adult heart extracts from the mouse strains that were used to create mutant animals and heart extract from the newborn mouse.

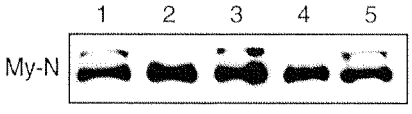

Figure 2.2.17: EH-myomesin is reexpressed in the adult cardiomyocytes of mouse models, showing the phenotype of dilated cardiomyopathy. Equal amounts of proteins from the heart of newborn control mice (lane 1), heart of adult control for tropomodulin-overexpressing transgenic (TOT) mice (lane 2), adult TOT mouse (lane 3), adult control for muscle LIM protein (MLP)-deficient mice (lane 4) and adult MLP-deficient mouse (lane 5) were loaded on a SDS gel. These extracts were probed by immunoblot with general myomesin antibody My190-Nrt. The upper band, corresponding to EH-myomesin appear in the heart of newborn mice (lane 1), but disappear in both adult controls (lanes 2 and 4). However this isoform is reexpressed in the heart extracts of adult TOT and MLP-knockout mouse, showing the phenotype of dilated cardiomyopathy (Lines 3 and 5).

In order to compare the relative amounts of EH(+) and EH(-) myomesin species, the immunoblot analysis was performed using the antibody My190-Nrt that recognizes both isoforms. The upper band, corresponding to the EH(+) variant appears in the cardiomyocytes extracts from the tropomodulin-overexpressing transgenic (TOT) mouse ((Arber et al., 1997), lane 3) and the muscle LIM protein (MLP) knockout mouse ((Sussman et al., 1998), lane 5). In both cases the expression level is roughly the same as in newborn mouse (lane 1). Interestingly, both strains show a phenotype of dilated cardiomyopathy (Arber et al., 1997; Sussman et al., 1998). On the other hand, the expression of the EH-myomesin was detected neither in rats that develop hypertrophy due to hypertension (SHR strain, compared to control stain WKY), nor in cultivated adult rat cardiomyocytes, which were frequently used as a model of hypertrophy in vitro (data not shown). This suggests that the re-expression of EH-myomesin could serve as a novel marker for dilated cardiomyopathy.

2.2.8 The isoform-specific fragments of chicken myomesin do not have capacities for sorting to specific sarcomeric sites

2.2.8.1 Expression of H-segment in embryonic chicken cardiomyocytes

As was shown in our lab, the exogenously expressed C-terminal fragment of chicken myomesin is accumulated in the M-bands in the cultivated embryonic chicken cardiomyocytes (Dani Auerbach, personal communication). In order to study whether this sorting capacity is associated with the H-segment, we cloned the H-segment into the eukaryotic expression vector in frame with the epitope tag encoding 11 amino acids from vesicular stomatitis virus (VSV tag, [Gallione, 1985 #118; Soldati, 1991). The fusion with the tag allowed distinguishing exogenously expressed myomesin from endogenous myomesin present in the cardiomyocytes. Details of the construction are described in the "Materials and Methods" Section. In the cardiomyocytes that express the whole C-terminal part of chicken heart myomesin (including the H-segment) recombinant protein is associated with myofibrils and accumulated mainly in the M-bands (Figure 2.2.18, a) while H-segment alone is distributed diffusely in cytoplasm or accumulated in the nucleus (Figure 2.2.18, c). Note that the nuclear staining is often observed in cardiomyocytes expressing chicken myomesin head domain cMy1 and can be explained by the fact that over-expressed protein is taken up unspecifically by some nuclear structures (Auerbach et al., 1997). Further, the α-actinin staining demonstrate that the myofibrillar apparatus is intact in cells transfected with both constructs (Figure 2.2.18, b and d). Therefore, we conclude that the diffuse localization of the H-segment is due to a lack of interaction with the myofibrils.

2.2.8.2 Expression of EH-segment in embryonic chicken cardiomyocytes

The EH-segment is included in the myomesin molecule only in the embryonic heart. For performing its specific function this segment might need to interact with some sarcomeric element that appears only during embryonic development. To investigate the function of the EH-segment on the basis of this hypothesis, this fragment was ectopically expressed as fusion to the GFP tag in embryonic chicken cardiomyocytes. The GFP tag allows the observation of transfected cells in vivo. In order to estimate whether the over-expression of

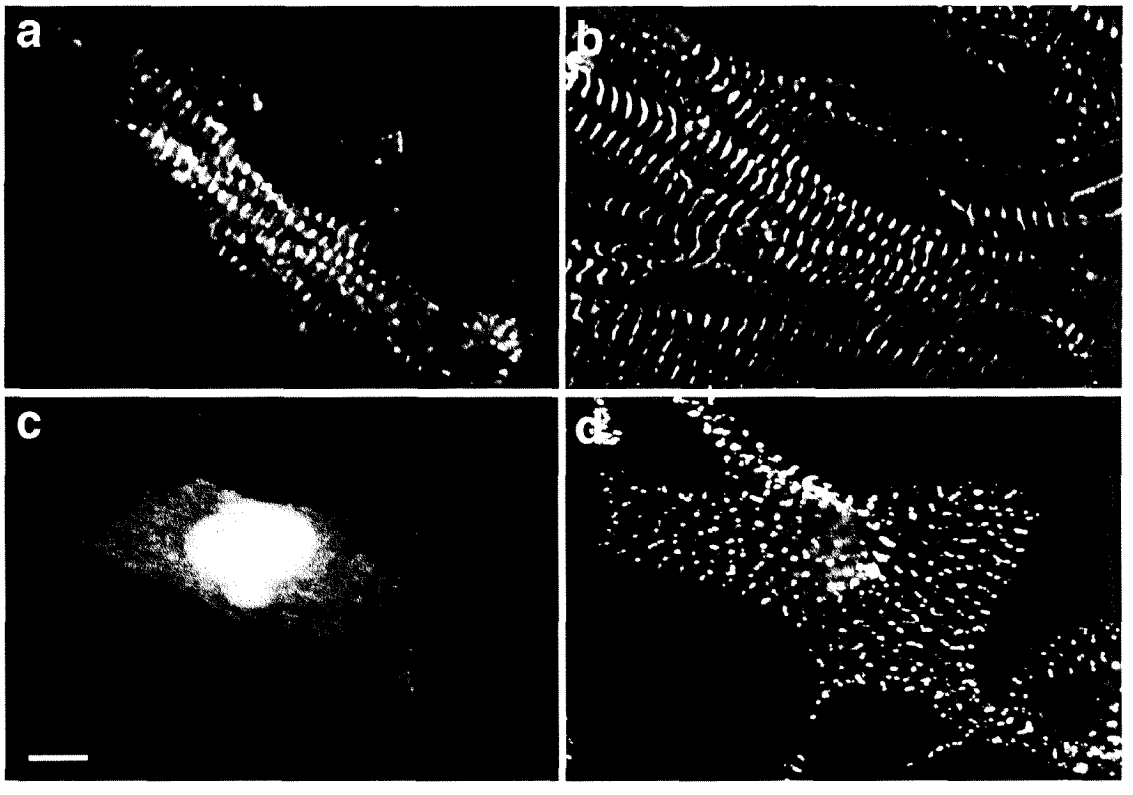

Figure 2.2.18: Expression of C-terminal fragments of chicken myomesin in embryonic chicken cardiomyocytes. Constructs chMy9-14 and chMy14 (H-segment alone) were expressed as fusions to VSV-tag. Cells were stained with antibodies against VSV-tag (a,c) or against sarcomeric α-actinin (b,d). Protein, containing six C-terminal domains of chicken H-myomesin is accumulated mainly in the M-bands of the sarcomere, whereas H-segment alone is distributed diffusely in the cytoplasm. Bar: 5 μm.

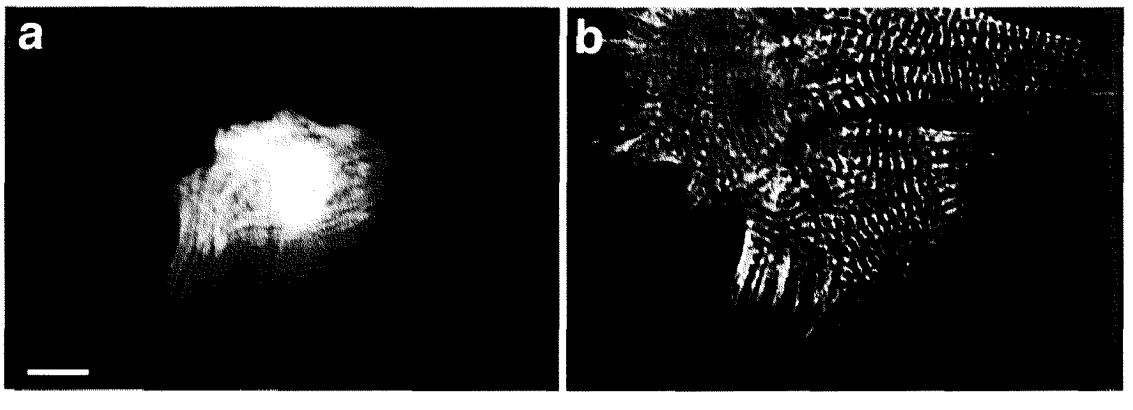

Figure 2.2.19: Expression of EH-segment of chicken myomesin in embryonic chicken cardiomyocytes. Constructs, encoding the cEH-segment was expressed as fusions to GFP-tag. Cells were stained with antibodies against GFP-tag (a) or against sarcomeric α-actinin (b). The fusion protein is not targeted to the M-bands of the sarcomeres, but is localized in typical 'cable-like' pattern, most likely due to the affinity of GFP for some sytoskeletal structures present in the cardiomyocytes. Bar: 10 μm.

this fragment affects the sarcomeric structure the cells were fixed and stained with antibodies against GFP tag (Figure 2.2.19 a) and against sarcomeric α-actinin (Figure 2.2.19 b). In the cell, expressing EH-GFP, the recombinant protein is not targeted to the M-bands of the sarcomere but is localized diffusely in cytoplasm and accumulated in typical 'cable-like' pattern along the filaments in the cell (Figure 2.2.19 a). It was shown that the paraformaldehyde fixation leads to unspecific stacking of GFP to some cytoplasmic structures in cardiomyocytes (Leu, 1996). Therefore, in this case we can not establish whether in our case the localization of fusion protein is controlled by GFP tag or by the EH-segment alone. Thus, these experiments allow us to conclude that EH-segment does not have strong capacity to sort into some sarcomeric site, however, weak affinity to myofibrils can not be excluded.
The staining of fixed cells with antibody against sarcomeric α-actinin revealed no defects in myofibrilla structure (Figure 2.2.19 b). Also, no difference was observed in the contractile properties between the transfected and neighboring untransfected cells (living cell observations). Therefore, the over-expression of the EH-segment has no obvious antimorphic effects on the cardiomyocytes and affects neither the sarcomere structure nor the contractile ability of these cells.

2.2.9 EH-segment shows the characteristics of largely unfolded protein

2.2.9.1 Computer analysis predicts an increased flexibility of the EH-segment

The finding of the human EST clone containing the sequence of EH-segment of myomesin gave an opportunity to compare and analyze EH-segments from mouse, human and chicken. This region is unlike any other sequence in the databases, so its structure cannot be reliably predicted by comparison to other proteins. As was discussed in Section 2.6.4, the three EH-sequences differ from each other more than Ig-like domains from the same species. This suggests that EH-segment has a less stringently organized structure than Ig-like domain because such structure requires the presence of conservative residues in well defined positions (Improta et al., 1996). Despite a rather low sequence homology between mammals and birds, analysis of the secondary structure of all three sequences with the Protean program (DNASTAR Inc., Wisconsin, USA) showed the features that are common to all EH-sequences and that distinguish them from Ig domains (domain My2 was used for this comparison). First, the Garnier-Robson algorithm predicted a significantly smaller part of β-sheet conformation in the EH-segment, second, the Karplus-Schulz algorithm predicts an increased flexibility of the EH-segment and finally, the Kyte-Doolittle algorithm predicts a much larger solubility of the EH-segment comparing to the Ig domain. The latter prediction is borne out by the observation that in the course of expression of EH-segment in E.coli practically all of the recombinant protein remains in a soluble fraction (see Figure 2.2.3 b). Usual Ig-like domains are largely composed of a set of interconnected β-sheets. Such regular secondary structures are favored because it permits extensive hydrogen bonding between backbone atoms, which is essential for stabilizing the hydrophobic interior of the domain. The dominating of hydrophilic residues in the sequence of the EH-segment, taken together with the predictions of increased flexibility and reduced quota of β-

sheet conformation leads to assume that the folding of this fragment could be less stable as the folding of Ig domains making the major part of the myomesin molecule.

2.2.9.2 CD-spectrum of recombinant chicken EH-segment reveals the absence of a definite secondary structure

Circular dichroism (CD) spectra of the myomesin (Obermann et al., 1995) corresponds to the classical spectra of Ig-like domain, which can be explained by dominant presence of this pattern in the molecule. In order to study the structural properties of the isoform-specific H- and EH-segments of chicken myomesin, the CD spectra of these fragments were measured. Both recombinant proteins were produced in *E.coli* as GST fusion and cut from the GST tag by trombin digestion, as described in section 2.2.1. The CD-spectra were measured by room temperature in a physiological buffer solution. Results are shown in Figure 2.2.20. Usually, three basic curves corresponding to three main conformations: β-sheet, α-helix and random coils allow analysis of the secondary structure. To estimate the contribution from each of the basic conformations the positions of main positive and negative peaks in the measured spectrum should be compared to the position of the peaks in the basic curves. The CD-spectrum of H-segment (Figure 2.2.20 a) shows one positive peak at about 195 nm and two negative peaks at about 212 nm and between 230 nm and 240 nm, respectively, this is an evidence of a secondary structure with dominant β-sheet conformation.

In contrast to this, the spectrum of EH-segment (Figure 2.2.20 b) contains a weak positive peak at 195 nm and one strong negative peak at about 200 nm, this CD corresponds to a mostly unfolded protein with residual secondary structure.

These results, obtained by CD-measurements of recombinant protein, strongly support the hypothesis, based on the computer predictions that the EH-segment has no definite secondary structure and is present in a mostly unfolded state, while the H-segment has a more stringent structural organization.

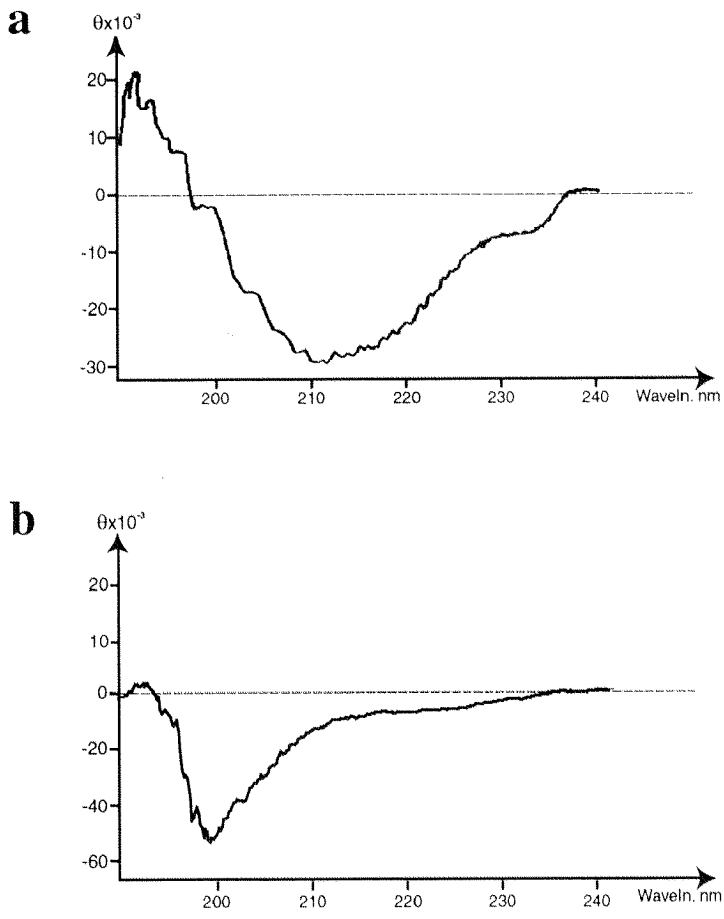

Figure 2.2.20: The recombinant chicken EH-segment shows the characteristics of largely unfolded protein. Circular dichroism spectra for the recombinant chicken myomesin H-segment (a) and EH-segment (b) were measusred in a limited spectral region from 190 nm to 250 nm, by 20°C. Both fragments were dissolved in PBS of pH 7.2. The spectrum of H-segment (a) shows one strong peac at 195 nm, two negative peaks at 212 nm and between 230 nm and 240 nm, indicating the presence of secondary structure with dominant β-sheet conformation. In contrast, the spectrum of EH-segment (b) contains one weak positive peak at 195 nm and one strong negative peak at about 200 nm, this corresponds to a structure of mainly unfolded protein with residual secondary structure.

2.3 Discussion

2.3.1 Myomesin isoforms diversity in vertebrates

2.3.1.1 The expression of myomesin isoforms in chicken is regulated in a both tissue- and stage-specific manner

This study continues the work of Stefan Bantle who had shown that two different myomesin transcripts that are generated by alternative splicing at the C-terminus can be found in chicken heart and skeletal muscle (Bantle et al., 1996). The RT-PCR analysis confirmed the difference in the expression pattern of these two isoforms and revealed a novel splice isoform that appears only in embryonic heart (see Figure 2.2.2). This EH-myomesin isoform corresponds to the mouse splice variant, previously called "skelemin" (Price and Gomer, 1993). Thus, two splicing events are possible in the chicken myomesin; further, it is remarkable that one of them is regulated in a tissue-specific manner and the other in a stage-specific manner. The generation of myomesin isoform-specific antibodies allowed analysis of the isoform expression on the protein level starting from the early embryonic to adult state (see Figure 2.2.6). The results are summarized in Table 2.2.

	Embryonic heart	*Adult heart*	*Embryonic skeletal muscle*	*Adult skeletal muscle*
S-myomesin	+/-	+/-	+++	+++
H-myomesin	+++	+++	-	-
EH-myomesin	+++	-	-	-

Table 2.2: Expression of myomesin isoforms in chicken.

The splicing event at the C-terminus is unique to avian myomesin. It results in two splice variants, termed H-myomesin and S-myomesin, representing the major myomesin species in heart and skeletal muscle of birds, respectively. Further, the expression of H-myomesin is strictly restricted to the heart, whereas some amount of S-myomesin canbe detected in heart by both immunoblot and immunostaining assays (see Figures 2.2.5 and 2.2.7). Arguing from RT-PCR data, previous investigators believed that the S-myomesin dominates over H-myomesin in the early embryonic heart, but is down regulated before hatching (Auerbach et al., 1997). However, the immunoblot analysis with isoform specific antibodies does not confirm the abrupt switch in the S-myomesin expression in the heart during embryonic development, on the contrary, it shows weak and stable expression level in all developmental stages (see Fig 2.2.7). The direct comparison of the staining intensities of heart and skeletal tissues obtained with the anti-S antibody in the thin sections of chicken embryos also confirms that the expression of S-myomesin in heart is much lower than in skeletal muscle (see Fig 2.2.6). Western blot analysis of adult heart and skeletal muscle with the anti-S antibody (data not shown) allowed us to estimate that the difference in the expression level between the two muscle types is about one or two orders of magnitude. Therefore, we believe that the minor expression of S-myomesin in the heart is due to the

leakage of the splicing mechanism and that S-myomesin does not play a major functional role in cardiac muscle of the chicken.

2.3.1.2 S-myomesin meets the minimal requirements for myomesin molecule

We have found that the closest relatives of chicken, namely, the adult mammals and reptiles express only S-myomesin in both heart and skeletal muscle indicating that this isoform is able to fulfil the basic function of the myomesin molecule. This smallest myosin isoform contains all myosin and titin binding sites that have been identified so far (Auerbach et al., 1999; Obermann et al., 1997). Therefore it seems to meet the minimal requirements for the function of the myomesin molecule, proposed to act as a bridge between the thick and the elastic titin filaments in the M-band. Interestingly, the C-terminal sequence of S-myomesin is much more conserved than the one of H-myomesin because chicken anti-S antibody recognizes myomesin even in mammals and reptiles, whereas anti-H antibody failed to react even with the distant avian species.

2.3.1.3 The role of the C-terminal part of myomesin molecule

Our study also addresses the question of the significance of the C-terminal part of myomesin molecule. According to the model of Obermann *et al.* (1996) it does not participate in myosin-titin bridging, and it does not contain identifiable binding sites (Auerbach et al., 1999; Obermann et al., 1996). However, comparison of part of the C-terminal immunoglobulin like domain My13 from human, mouse, chicken and zebrafish shows strong conservation of its amino acid sequence (see Figure 2.3.1).

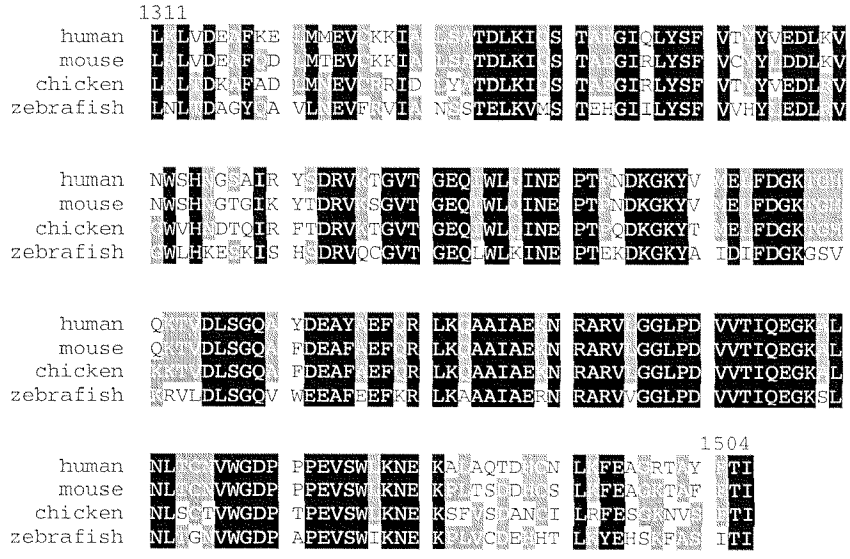

Figure 2.3.1 Comparison of the C-terminal sequences of human, mouse, chicken and zebrafish myomesin. The alignment of human (GenBank accession number AF185573), mouse (fragment of the myomesin/skelemin sequence available under accession number AJ12072), chicken (GenBank accession number AF185572) and zebrafish (EST clone AI658181) myomesin C-terminal fragments was performed using MULTITALIN programm (see M&M). Black boxes indicate identical residues and gray boxes indicate conservative exchanges. Numbers correspond to the chicken myomesin sequence. The C-terminal sequence of myomesin is conserved in all vertebrates, indicating for the functional significance of this part of the molecule.

Furthermore, the number and order of domains is preserved in all known myomesin sequences (Bantle et al., 1996; Obermann et al., 1995; Steiner et al., 1999). Our data confirm that despite the existence of isoforms the length of myomesin remains approximately the same in all vertebrates from mammals to fishes (see Figure 2.2.12). All these arguments taken together indicate for functional significance of the C-terminal part of the myomesin molecule.

2.3.1.4 The H-myomesin isoform may represent an evolutionary adaptation to specific physiological conditions in avian heart

This study established that the C-terminal splice variant H-myomesin is expressed in hearts of all tested bird species. This isoform has a higher molecular weight and does not react with the anti-S antibody that detects S-myomesin in skeletal muscle extracts from the same species. Quite surprisingly the anti-H antibody generated against the H-segment of chicken myomesin did not react with the heart extracts of other birds except with the closely related goose. Thus the primary sequence of the H-segment is not entirely conserved between different avian species, but the heart-specificity of the splice machinery must remain intact and thus allow the successful splicing. We speculate that the presence of the H-segment determines some mechanical or biochemical properties of myomesin in avian cardiac muscle that are preserved in the diverging primary sequences. A similar observation was made in the case of the myomesin head domain. According to biochemical data the head domain contains a myosin binding site (Auerbach et al., 1999; Obermann et al., 1997), but at the same time its sequence differs significantly from one species to another (Bantle et al., 1996).
Surprisingly, the reptiles that are the closest relatives of birds do not have a special H-myomesin in the heart although they react well with other anti-chicken myomesin antibodies. Thus the H-myomesin splice variant appeared after the birds evolved from reptiles and is likely to be the result of the evolutionary adaptation to physiological conditions in avian heart.

2.3.1.5 Lower vertebrates express diverse myomesin isoforms in the adult heart and skeletal muscle, but the composition of these isoforms is not clear

Thus, birds express different isoforms of myomesin in adult striated muscles whereas in mammals and reptiles one isoform appears to be sufficient. However, going further down the evolutionary tree we find that myomesin isoforms of heart and skeletal muscle in amphibian and fish differ in their apparent molecular weights (Figure.2.2.12). Unfortunately, we could not establish whether this difference is due to an additional C-terminal segment because neither the anti-S antibody nor the anti-H antibody reacts with extracts from these species. The different mobility may also be due to other splicing events or due to posttranslational modifications, such as phosphorylation. To clarify whether the difference in molecular weight is indeed due to an additional C-terminal segment one has to compare the sequences of the myomesin in heart and skeletal muscles of amphibian and fish species.

2.3.1.6 Does EH-myomesin appear in the embryonic heart of lower vertebrates?

Using RT-PCR and immunoblot analysis we established that EH-myomesin formed by inclusion of the alternative EH-exon dominates in the embryonic heart of chicken and mouse. The sequence of human EH-segment was found in an EST clone that originates from a fetal heart library. Employing the crossreaction of chicken antibodies with the reptilian samples we could establish that heart of newborn lizard also contains EH-myomesin in the proportion corresponding to the hatching chicken (Figure 2.2.15). Taken together, these findings lead to the conclusion that the expression of the EH-myomesin isoform is specific to the embryonic heart of all higher vertebrates. The analysis of lower vertebrates, such as amphibian and fishes is made more difficult by the absence of appropriate isoform-specific antibodies. However, in Xenopus tadpole heart the general myomesin antibody reacts with an additional band that has a higher apparent molecular weight than the myomesin band in the adult heart (Figure 2.2.16). It is tempting to assume that this band corresponds to the Xenopus counterpart of EH-myomesin. To clarify this issue one might try to generate primers from the most conserved fragments of domains My6 and My7, flanking the putative EH-insertion and perform RT-PCR analysis of total RNA from amphibian muscles.

2.3.2 The EH-myomesin corresponds to mouse splice variant, previously called "skelemin"

2.3.2.1 "Skelemin" was initially cloned from adult skeletal muscle

We cloned the EH-myomesin isoform from the embryonic chicken heart. A seach in the database showed that EH-myomesin corresponds exactly to a mouse splice variant of myomesin, previously called "skelemin" (Price, 1987; Steiner et al., 1999) including a serine-proline rich sequence between domains My6 and My7, which we have termed EH-segment. We could now show that this splice variant exists also in chicken, lizard and man. However, we were unable to detect myomesin isoforms containing the EH-segment either by RT-PCR or by immunoblotting in skeletal muscle at any developmental stage, which is in contradiction with the fact that the mouse "skelemin" cDNA was cloned from adult skeletal muscle (Price and Gomer, 1993). A possible explanation might be the insufficient sensitivity of our RT-PCR analysis to detect minor amounts of EH-segment containing transcripts present in skeletal muscle or that there is some expression of EH-myomesin in regenerating muscles.

2.3.2.2 The principal functional role of "skelemin" should be the same as for conventional myomesin

Several functions have been proposed for "skelemin": first it was suggested that it might act as a linker between intermediate filaments and the M-band (Price and Gomer, 1993); second an interaction of "skelemin" and β-integrin was proposed, based on an interaction between these proteins in a yeast two-hybrid assay (Reddy et al., 1998). Thus, it was suggested that the function of "skelemin" in the M-band might be different from that of myomesin. Here, we provide strong evidence that "skelemin", or EH-myomesin, is the only isoform of myomesin that is present in the M-band of early embryonic heart. Therefore, the

principal role of EH-myomesin must be the same as of conventional myomesin, e.g. the maintenance of an ordered thick filament lattice in the M-band. Confusingly, the anti-"skelemin" antibody used by Reddy and co-workers recognizes a protein not only in muscle tissue but also in Chinese hamster ovary cells, platelets and even endothelial cells. A possible explanation for these conflicting results may be the binding of the antibody to a crossreacting antigen. Indeed, their antibody recognizes a protein with a molecular weight of 205-210 kDa (Reddy et al., 1998), which is in contradiction to the calculated molecular mass of 174 kDa and the mobility of myomesin as observed in previous studies (Bantle et al., 1996; Grove et al., 1985; Grove et al., 1984; Obermann et al., 1995; Vinkemeier et al., 1993). A cross-reacting antibody would also explain the detection of "skelemin" in smooth muscle (Price, 1987). Previous investigations on myomesin expression by several laboratories have characterized myomesin as a sarcomeric protein and also reported its expression exclusively in striated muscle (Auerbach et al., 1997; Bantle et al., 1996; Grove et al., 1985; Grove et al., 1984; Steiner et al., 1999; Vinkemeier et al., 1993). In the present study we confirm by means of RT-PCR and immunodetection that the expression of all myomesin isoforms is restricted to heart and skeletal muscle.

2.3.2.3 In contrast to its mouse counterpart, the chicken EH-segment is not serine/proline-rich

Sequence analysis showed that the EH-segments of mouse and human are rather similar, whereas the chicken EH-segment amino acid sequence is more divergent with only 36% of identity and 48% similarity between the chicken and mouse EH segments (Table 3). This is a relatively small value as opposed to the 75 % identity of the rod portion of myomesin, consisting of Ig-like and Fn3 domains (Bantle et al., 1996).

	mouse	*human*	*chicken*
mouse		**65**	**36**
human	**65**		**40**
chicken	**36**	**40**	

Table 2.3: Homology between EH-segments of myomesin from different species. Numbers correspond to percents of amino acid identity.

Both mouse and human EH-segments are rich in serine/proline residues, hence the original name serine/proline rich domain. However, this feature does not seem to be essential since the chicken counterpart contains fewer serine and proline residues, making it resemble an Ig-like domain My2 much more closely (See Table 2.4).

	mouse EH	*human EH*	*chicken EH*	*chicken my2*
proline	**17.0**	**13.3**	**5.8**	**7.3**
serine	**18.0**	**13.3**	**10.7**	**7.3**

Table 2.4. Comparison of the serine/proline content of EH-segments of myomesin from different species. Numbers correspond to percents by frequency.

2.3.3 Different aspects of EH-myomesin isoform expression

2.3.3.1 EH-myomesin is the perfect marker for embryonic heart

In contrast to H-myomesin, which was found only in avian cardiac muscle, the EH-isoform of myomesin is present in the developing heart of mammals, birds and reptiles. The high molecular weight isoform of myomesin was detected also in the heart of the Xenopus tadpole, and this isoform may represent the amphibian counterpart to EH-myomesin. Therefore EH-myomesin could serve as a valuable marker for the embryonic vertebrate heart, because no other myofibrillar protein expression is restricted to embryonic heart in such a tightly controlled manner (Schiaffino and Reggiani, 1996).

2.3.3.2 Reexpression of EH-myomesin could serve as a novel marker for dilated cardiomyopathy

Cardiomyopathies are defined as primary disorders of cardiac muscle and include three specific types: hypertrophic cardiomyopathy, dilated cardiomyopathy and restrictive cardiomyopathy (Towbin, 1998). Very often the development of this disease is accompanied by the reexpression of embryonic or fetal isoforms of some sarcomeric proteins (Clement et al., 1999; Komuro and Yazaki, 1993; Schiaffino et al., 1989). Cardiomyocytes from hypertrophic hearts are often characterized by myofibril disarray and the sarcomeres are not as strictly registered as they are in the healthy heart, possibly indicating the reversion to more embryonic sarcomeric structures. Preliminary experiments have shown re-expression of EH-myomesin in adult cardiomyocytes from MLP-knock-out mice (Arber et al., 1997) and from tropomodulin overexpressing mice (Sussman et al., 1998). Interestingly, both mouse strains show a phenotype of dilated cardiomyopathy (DCM). This myocardial disorder is characterized by left ventricular dilation with increased left ventricular volume and systolic dysfunction (Towbin, 1998). The pathophysiology of DCM is well known, but the underlying cause of this disorder is elusive. Several reports, however, have indicated that weakening of the myocyte cytoskeleton, especially elements associated with the force transducing apparatus, may cause this cardiac disorder (Chien, 1999).

Interestingly, we were not able to detect the EH-myomesin neither in rats that develop hypertrophy due to hypertension (SHR strain), nor in cultivated adult rat cardiomyocytes which are frequently used as a model of hypertrophy in vitro (Rothen-Rutishauser et al., 1998; Schaub et al., 1997). Therefore, we suggest that the reexpresion of embryonic EH-isoform of myomesin could serve as a novel marker for dilated cardiomyopathy. The generation of an antibody directed against the mammalian EH-fragment is under way, and will hopefully allow the investigation to which extent the re-expression of EH-myomesin can be associated with myofibrillar disarray in the failing heart.

2.3.3.3 Purine-rich nucleotide stretch is conserved in all known EH-sequences

Alternative splicing of the EH-exon is regulated in a both developmentally- and tissue-specific manner, i.e., the exon is included only in embryonic heart and skipped in adult heart and skeletal muscle of any stage. This regulatory pattern is conserved between birds and mammals. It is very likely that the skipping of EH-exon is the default splicing pattern that results from a balance of several features that make this exon an intrinsically poor

splicing substrate. Therefore, there should be a splicing factor(s) that promote the inclusion of the EH-exon in the embryonic heart. Despite a low conservation at both amino acid and nucleotide sequence levels (see Figure 2.2.13) the stretch GAAAAAGAAGA is conserved in all known EH-sequences. It is likely that this stretch represent the purine-rich exonic splicing enhancer. Similar sequences have been identified in many regulated and constitutively spliced pre-mRNAs (Lavigueur et al., 1993; Lopez, 1998; Ryan and Cooper, 1996). In general they activate splicing of the upstream intron by promoting the use of a weak 3' splice site (Xu et al., 1993). Biochemical evidence indicates that these elements function as binding sites for SR (splicing regulators) proteins. The observation that several different regulatory programs for alternative splicing run concurrently within individual cells makes it unlikely that all regulated splicing in vertebrates are mediated by changes in the nuclear concentrations of constitutive splicing factors. Certainly, alternative splicing is regulated by programs that utilize distinct sets of *cis* elements and *trans*-acting factors, similar to a process occurring in *D.melanogaster* (Lopez, 1998). Thus, most likely, the fate of the EH-exon is determined not only by already described exonic enhancer but also by several elements that are located in the adjacent introns. Similar muscle-specific splicing enhancers were identified recently in the upstream and downstream introns of the cardiac troponin T alternative exons (Ryan and Cooper, 1996).

2.3.3.4 Removal of the intron, following the EH-exon occurs later

A search of the EST databases using the sequence of mouse EH-segment resulted in a human EST clone (see section 2.2.6.4) and three mouse EST clones, that originate from the human and mouse fetal hearts, respectively. On one hand, this confirms the conjecture that EH-myomesin is expressed in embryonic heart but on the other hand it raises the question how its sequence could have gotten into EST databank. There are two puzzles, all related to the way in which EST clones are produced: it is usually obtained by the purification of the mRNA, which is then reverse transcribed into cDNA using oligo dT adapter-primer technique. One thus expects that EST library should be composed of clones containing the C-terminal portions of the proteins and that these clones do not contain introns. The first puzzle is that, contrary to these expectations, the sequence comparison reveals that none of these four clones contain the C-terminal sequences of myomesin. The second is that, as we have found, the three mouse clones contain a partial sequence of EH segment together with the intron following it. The fact that it is indeed intron can be established with a high degree of confidence because this part of mouse myomesin gene was partially sequenced before (Steiner et al., 1999). Because these features are common to all mouse and human clones the puzzle demand an explanation. Analysis of the sequence of the human EST clone is shown in Figure 2.3.1.

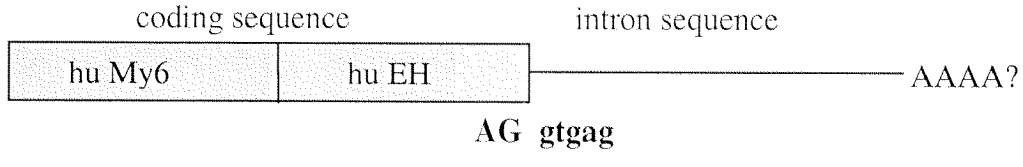

Figure 2.3.1. Schematic representation of the EST clone AA248352 containing the EH-segment of human myomesin. The sequencing reveals that the sequence of the human EH-segment (found by a high homology to the EH-segment of mouse myomesin) directly follows the sequence of domain My6 of human

myomesin. In the 3' half of the clone no coding sequence was found. This part of the clone clearly belongs to the intron. Approximately, the beginning of the intron sequence was determined by alignment with the mouse EH-sequence and then was positioned precisely at the location of splicing consensus sequence AG/atgag. A putative poly A sequence is shown at the 3' end of the clone.

Comparison of the of EST clone with human myomesin (Vinkemeier et al., 1993) and with mouse myomesin (Price and Gomer, 1993) shows that this clone contains a full EH-sequence that directly follows the domain My6 of human myomesin. However, the analysis of the 3' end of the clone sequence shows the presence of a non-coding sequence that has no homology to known myomesin sequences. The 3' boundary of the EH-segment was established using the homology with the mouse counterpart and then elaborated using the position of splicing consensus AG/gtgag. Furthermore, the position of this splice site shows that the non-coding sequence belongs to a phase-1 intron, since the frame is broken after the first nucleotide of the affected codon. The analysis of the mouse myomesin gene also demonstrates that the mouse EH-exon is flanked by phase-1 intron (Steiner et al., 1999). Thus, we assume that this EST clone is the product of reverse transcribed, partially unspliced message, which was subcloned in the process of the EST library generation most likely because it contains a long A-rich stretch in the upstream intron. This pseudo-poly A stretch is likely to be present also in the mouse intron, which flanks the EH-exon and is responsible for the appearance of its sequences in EST libraries.
Usually, the splicing of pre-mRNA takes place in nucleus and only RNA, freed from the intronic sequences is released from nuclear pores into the cytoplasm (Alberts et al., 1994). Thus it is not at all clear how a partially unspliced myomesin sequence can get into the library. We speculate that due to unknown reason the removal of the intron following EH exon occurs later, it might be that this process is completed only in cytoplasm. This conjecture is supported by the fact that the 3' end of the same intron was found in the sequence of chicken myomesin clone SB 13 containing the domain My7 (Bantle et al., 1996).

2.3.4 The functional significance of EH-myomesin expression in embryonic heart

2.3.4.1 The isoform-specific EH-segments of chicken myomesin do not participate in myomesin targeting to the M-band

According to *in vitro* studies, the head domain of myomesin is responsible for the interaction with myosin, whereas the fragment containing the domains My4-My6 binds to titin (Obermann et al., 1997). The transfection experiments show, however, that the chicken My2 domain is sufficient to target sarcomeric M-bands, possibly due to interaction with some unknown protein (Auerbach et al., 1999). We have found that the novel myomesin isoform, different by EH-segment inserted between domains My6 and My7, is expressed in embryonic hearts of many species. Because the appearance of this EH-myomesin correlates with the time of active sarcomere construction, it is natural to assume that the isoform specific EH-fragment helps the myomesin molecule to get sorted to the proper place within the growing myofibril. We checked this hypothesis by expressing the EH-fragment as a GFP fusion in chicken cardiomyocytes, but found that this construct does not have M-band

targeting capacity (see Figure 2.2.19). Thus, it is unlikely that it participates in targeting of myomesin to the M-band and must therefore perform a different function in the embryonic heart.

2.3.4.2 The EH-segment could function as an extendable and elastic element in the middle of the myomesin molecule

Despite a rather low sequence homology between the EH-segments of mammals and birds, analysis of the amino acid sequences using the Karplus-Schulz algorithm allowed to find characteristic features that are present in all EH-sequences. Computer simulations predict an increased flexibility of the EH segment and also a significantly lower probability of β-sheet conformation, as compared to Ig-like domains that make up the major part of the molecule. These results indicate that the EH-segment is not as well folded as an Ig-like domain. In agreement with this prediction we found that the circular dichroism spectra of the recombinant chicken EH-segment shows the characteristics of a largely unfolded protein with residual secondary structure (see Figure 2.2.20). Therefore, this segment could function as an extendable elastic stretch in the middle part of the myomesin molecule. In this sense the structure of EH-myomesin resembles the structure of titin, which is also composed of two principally distinct regions with stretches of Ig modules separated by unique segments of elusive secondary structure: the PEVK domain and the N2A or N2B sequence insertions.

The unique N2A and N2B sequence insertions are differentially expressed in heart and skeletal muscles (Labeit and Kolmerer, 1995; Trombitas et al., 1999). As was noted previously, the N2B insertion, characteristic for cardiac muscle, has a lower conservation and less probability of β-sheet conformation than the Ig-like domains (Siu et al., 1999). The elasticity of these segments allows titin to extend fully reversibly at physiological forces, without the need to unfold the Ig domains, which would be catastrophic in beating cardiomyocytes (Linke et al., 1998; Linke et al., 1999; Tskhovrebova et al., 1997).

According to current notion titin is responsible for the elasticity of the sarcomere in the longitudinal direction. Further, the stiffness of different muscles correlates with the presence of distinct titin isoforms there (Linke et al., 1996). We speculate that myomesin works as a "mini" analog of titin. Namely, it may be responsible for elasticity of the M-band in the transverse direction, and, correspondingly, the inclusion of the EH-segment may modulate the elastic properties of the myomesin isoform expressed in embryonic heart.

2.3.4.3 EH-myomesin may serve as a safety device by absorbing mechanical stress applied to sarcomeric M-band during cardiomyocyte cell division

What may be the physiological need for additional M-band elasticity in embryonic heart? Embryonic cardiomyocytes differ in principle from skeletal muscle cells and adult cardiomyocytes by their ability to divide, despite the possession of contractile machinery. Presently, it is not clear what happens exactly to the myofibrillar apparatus during cell division, although there are some indications of partial disassembly of myofibrils, particularly the Z-bands (Goode, 1975). However, it was unequivocally demonstrated that some sarcomeres within isolated cardiomyocytes persist throughout mitosis (Kelly and Chacko, 1976; Rumyantsev, 1977). Moreover, a recent study indicates that most myosin filaments remain bundled with myomesin in mitotic myocytes (Li et al., 1997). This suggests that the M-bands in sarcomeres may be exposed to rather strong mechanical stress

during the formation of the cleavage furrow and separation of the dividing cells. The additional elastic element in the center of myomesin molecule would therefore serve as a safety device, analogous to the PEVK domain and N2B insertion of titin, but in the perpendicular direction, thus preventing the irreversible unfolding of Ig domains or even the disruption of the M-bands in the dividing cardiomyocytes.

2.3.4.4 The lateral alignment of thick filaments correlates with the disappearance of EH-myomesin from the M-bands in embryonic heart

Although our understanding of the functional significance of EH-myomesin is still incomplete, electron microscopic studies of the developing heart provide interesting insights. They reveal that cardiac sarcomeres acquire their characteristic morphology, including an electron dense M-band and stringently aligned thick filaments, only some days after birth (Smolich, 1995). Neither the M-bridges, nor the five band periodicity characteristic of the adult M-band can be seen in the new born rat atrial and ventricular myocytes (Carlsson et al., 1982). The first M-bridges appear in small areas of myofibrils about 11 days after birth (Anversa and Olivetti, 1981). The appearance of the M-bands coincides with the alignment of the thick filaments into well-organized A-bands. This observation led to the conclusion that M-bridges help to order thick filaments and register the A-band (Carlsson et al., 1982). However, it is important not to confuse the terms "visible M-band" and "real M-band". The "visible" electron-dense M-band has been ascribed to the presence of muscle-creatine kinase (M-CK) (Wallimann and Eppenberger, 1985). Indeed, the appearance of M-CK is correlated with the appearance of an electron dense M-bands in electron microscopic preparations but M-CK does not seem to play an essential structural role in the M-band since the M-CK deficient mice exhibit no obvious abnormalities in sarcomere structure (van Deursen et al., 1993). Moreover, M-CK is absent from chicken heart, that, however, doesn't prevent appearance of the regular assembly of thick filaments there.

At the same time, myomesin is absolutely necessary for sarcomeric assembly and participates in the "real" M-band, which is present in all cardiac sarcomeres starting from early embryonic development (Ehler, 1999; this study). These observations provide a strong argument that myomesin, rather than M-CK, is implicated in the positioning of myosin filaments in the sarcomere. Moreover, the switch in myomesin isoform expression correlates precisely with the appearance of well-organized A-bands in the postnatal myocardium. Therefore, the increasing order of the thick filaments can be explained by the replacement of the longer and flexible EH-myomesin isoform by the rigid adult myomesin, reducing the imprecision of the thick filament alignment in the M-band. This hypothesis is corroborated by studies of developing chicken skeletal muscle where no EH-myomesin is expressed and perfectly aligned thick filaments in sarcomeres were observed in muscle of day 12 embryos (Fischman, 1967).

2.3.5 Myofibrillogenesis in the embryonic chicken heart

2.3.5.1 Titin serves as molecular scaffold during sarcomeric assembly

Myofibrillogenesis is a fast and well coordinated process: it results in the 'self-assembly' of dozens of proteins into a quasi-crystalline sarcomeric structure within only few hours during early cardiac development (Ehler et al., 1999). The current models of myofibrillogenesis suggest that this self-assembly occurs according to the plan encoded by giant titin molecule (Dabiri et al., 1997; Ehler et al., 1999; Rhee et al., 1994; van Der Ven et al., 2000). The functional knock-out of titin provided recently the direct evidence for the crucial role of titin in both thick filament formation and in the coordination of sarcomeric assembly (van Der Ven et al., 2000). It seems likely that in the first step of myofibrillogenesis the N-terminus of titin binds to α-actinin and membrane associated actin filaments. These complexes, which have been termed "dense body–like structures" seem to play a role of organizing centers for myofibrilla assembly (Fürst et al., 1989; Tokuyasu and Maher, 1987). Initially, the spaces separating these structures are about 1 μm but gradually they increase (according to yet unspecified mechanism) to 2 μm that is the distance between mature Z-bands (Hiruma and Hirakow, 1985). It is supposed that in the course of this process the titin molecules unfold and finally the C-termini of the titin molecules, attached to the neighboring dense bodies begin to interact with each other in an anti-parallel fashion according to current M-band model ((Obermann et al., 1996).
The few things however, remain puzzling. First, molecules larger than 200 kDa can not move freely in cytoplasm (Luby-Phelps, 1987), so it is unclear how many giant titin molecules of about 3000 kDa are able to get together in the nascent Z-disk. Second, it is mysterious how it is possible to avoid irregular pairing of C-temini of titin molecules that point in arbitrary directions from adjacent dense-body-like structures. Of course, one can imagine that parallel packing of synthesized titin molecules with already existing one occurs in a zip-zap fashion and this process culminates in a formation of M-band. However, the linking of adjacent titin molecules in all their length is very difficult to reconcile with their elastic behavior in the sarcomere.

2.3.5.2 Titin mRNA could participate in regular packing of titin strands

We suggest a plausible mechanism how a colossal titin mRNA may help to pack titin strands in a parallel fashion It is known that developing myocardial and skeletal muscle cells contain huge amounts of ribosomes that provide fast synthesis of myofibrillar proteins. At the early stages of development a large pool of ribosomes may bind to either the plasma membrane or to actin filaments associated with this membrane. One of these ribosomes may catch the titin mRNA molecule, beginning the titin protein synthesis. It is known that the Z-portion of titin forms ternary complexes with α-actinin and F-actin *in vitro* (Young et al., 1998), thus it is reasonable to assume that a freshly synthesized part of the titin molecule will be immediately anchored to the preexisting α-actinin dimers associated with actin filaments. As the polypeptide chain grows, the first ribosome moves away and leaves the 5' end of the mRNA free for the next ribosome that is usually attached at a distance about 50 nm from the first (Alberts et al., 1994). Thus, the N-terminus of nascent titin peptide produced at this ribosome gets a good chance to react with the opposite ends of α-actinin dimers of about 35 nm length (Blanchard et al., 1989), attached

to the first titin chain in accordance with a recent model of interaction between titin and α-actinin (Young et al., 1998). In this way the formed polyribosome allows the successive synthesis of multitude of titin molecules and their simultaneous co-translational assembly into the growing tetragonal lattice of Z-disks. This hypothesis is borne out by the observation that titin becomes incorporated into insoluble structures during translation (Isaacs et al., 1989). The estimate shows that up to a thousand ribosomes may simultaneously work on one titin mRNA. This is more than sufficient to completely form small myofibrils that are observed in the developing heart at the early stages of myofibrillogenesis (see (Chacko, 1976; Fischman, 1967; Komiyama et al., 1993). Evidently, in order to inflate the plane of the Z-disk, the next titin molecules have to attach to the existing lattice either in a helical manner enveloping the existing strands or in a zigzag pattern. This conjecture is supported by many independent studies, reporting that ribosomes often form complexes with growing myofibrils (Chacko, 1976; Manasek, 1969). Moreover, long zigzag-like or helical polyribosomes closely associated with the myofibrils are often observed in the electron microscopic pictures of developing myocardium of rat (Chacko, 1976), chicken (Przybylski and Blumberg, 1966), and frog (Huang, 1967). Large polyribosomes associated either with myofibrils or with titin strands were observed in embryonic chicken cardiomyocytes (Komiyama et al., 1993).

Clearly, the titin molecules will be held together with in a bundle by a long messenger molecule only until the producing ribosomes reache the 3' end, after this the free C-terminal ends of titin have to be immediately jointed by M-band proteins. As new portions of the titin sequence appear from the ribosomes they are ready to attach other myofibrillar proteins, providing a basic lattice for ordered packing of other sarcomeric components. The bundle of titin strands grows until it meets another one growing from the neighboring dense-body-like structure. It is tempting to assume that it is the force of simultaneous polymerization of many titin molecules that is responsible for the increase in distance between the adjacent dense body like structures.

This hypothesis can be verified by the following experiment: one needs to separate the polyribosome fraction isolated from the embryonic heart by centrifugation in the sucrose gradient (Nikcevic et al., 1999) and check by hybridization with titin specific probe which fractions contain titin message. This method was used recently to show the shift from small to large polysomes, synthesizing the MHC, in response to increased contractility (Ivester et al., 1995). Hopefully, this strategy will allow estimating the approximate size of polyribosomes, producing titin molecules and thereby testing the hypothesis.

2.3.5.3 The myomesin is a part of the basic cytoskeletal lattice of the sarcomere

Thus the C-terminal end of titin is likely to be fasted together by M-band proteins, and the first candidate for this protein is myomesin because it appears in all types of striated muscle. It is observed in a periodic pattern simultaneously with the appearance of the first sarcomeres in embryonic heart (Auerbach et al., 1997; Ehler et al., 1999), this study). Recent observations have suggested that myomesin concentration at the M-band might even precede final thick filament assembly, as marked by MyBP-C incorporation (van der Ven et al., 1999). Myomesin was shown to interact with both titin and myosin in vitro and thus is a good candidate for the role of integrating molecule in the M-band ((Obermann et al., 1997). How exactly the myosin is attached to M-band and to what degree titin and myomesin are involved in this process is not known. However, there are a several

indications that myosin filaments might independently assemble in cytoplasm. Isolated myosin molecules are able to form bipolar filaments even in the test tube (Goldfine et al., 1991), and electron microscopy revealed the presence of separate myosin filaments in intact tissue (Hiruma and Hirakow, 1985; Manasek, 1968) and in cultured cardiomyocytes (Schultheiss et al., 1990). However, the recent study demonstrated that the cells are unable to form the thick filaments in the absence the C-terminal parts of titin molecules (van Der Ven et al., 2000).

In the present study has shown that all double bands of myosin are always associated with myomesin, located in the M-band. This is true not only in the embryonic heart but also in the developing skeletal cells those actively build new sarcomeres (see Figure 2.2.10). Furthermore, it was not possible to discern the myosin-myomesin complexes separately from actin filaments. These observation provide a strong argument that myomesin is an essential intermediate for the association of bipolar myosin filaments with actin and titin-based I-Z-I complexes that are formed at the early stages of the myofibrillogenesis. Our observations also confirm the assumption that the function of the myomesin in the M-band could be analogous to the function of α-actinin in the Z-band, namely that it links contractile elements, in this case myosin, to titin (Ehler et al., 1999). These three proteins may form the basic cytoskeletal lattice that keeps actin and myosin filaments in the positions that are optimal for the interaction. Hopefully, the current project running in our lab (which goal is to switch off the myomesin gene) will allow checking whether myomesin plays a key role in A-band assembly.

2.3.6 Outlooks

This study reports a significant progress in our understanding of myomesin isoform diversity in vertebrates. Many problems were resolved but, as usual, even more new puzzles appear, as the saying goes: "Our knowledge is like a circle, the more we increase its area the bigger is the unknown surrounding it".

Present study thoroughly analyzed the expression of myomesin isoforms in high vertebrates but the situation in lower vertebrates, such as amphibian and fishes was not clarified completely. Although the appearance of multiple myomesin isoforms in striated muscle of these species is established, the composition of these isoforms remains unclear. We propose additional experiments to continue the investigation of myomesin isoforms diversity in lower vertebrates in the chapter 2.3.1. It is likely that the good starting point for this study is EST clone AI658181. This clone originates from the cDNA of zebrafish and contains the sequence of C-terminal end of myomesin. The primers generated from this sequence will help to clarify whether the C-terminal splicing is indeed responsible for different isoforms in heart and skeletal muscle in fishes as it is in chicken muscle.

One of most important result of this study seems to be the resolution of a skelemin puzzle which dates back to the discovery of this protein in 1987 (Price, 1987). For along time it was regarded as independent protein with a function different from the another M-band components. The correct picture was revealed in the study of (Steiner et al., 1999) and finalized in our work. The result can be summarized in a sentence: "skelemin" is nothing but EH-myomesin isoform that is specific for the embryonic heart.

Given the importance of the unique EH-segment that gives rise to EH-myomesin in embryonic heart of all higher vertebrates, we believe that its structure and the molecular

mechanism of its extensibility are worth studying in detail. For this purpose the most promising seems to be the strategy that was recently employed for the investigation of the elastic properties of titin (Rief et al., 1998; Tskhovrebova et al., 1997). These studies make use of recent technical innovations: the atomic force microscope and optical tweezers that make it possible to record force and extension accurately in single polypeptide molecule. This approach can prove the hypothesis that EH-myomesin is a softer spring than conventional myomesin and might damp strong mechanical stresses incurred by cell division. Clearly, this conjecture requires a revision of the existing M-line model that does not involve the participation of the C-terminal part of myomesin molecule in the titin-myosin bridging. However, the mere fact of the appearance of EH-isoform in all high vertebrates provides a strong argument in favor of functional significance of this part of the molecule.

Of course before one can make any conclusions regarding isoprotein function one has to understand basic function of myomesin and this problem is addressed by the running myomesin knock-out project. Most likely, the elimination of myomesin would lead to embryonic death. Thus one plans to investigate the consequences of knock out in the system of differentiating ES-cells. Moreover, this system might be used for the investigation what fragment of myomesin molecule is able to restore normal sarcomeric structure. Ectopic expression of the of different myomesin truncations in the myomesin deficient ES-cells could be the key experiment to define the functional roles of different parts on myomesin molecule and hopefully, to establish the new model of sarcomeric M-band structure.

On the other hand, it appears very interesting to continue the study of EH-myomesin involvement in the development of dilated hypertrophy in the heart. For this purpose one has first to generate antibody against mammalian myomesin. The work in this direction has already been started. The EH-segment of human myomesin is expressed as GST fusion and immunization of rabbits is currently under way. Because of a high similarity between the mammalian EH-segments, it is highly probable that the obtained antibody might be used in mouse and rat models.

We believe that the detailed analysis of the structure and function of myomesin that is an important building block of a sarcomere will bring us closer to the full understanding of mechanisms underlying muscle assembly and contraction.

Chapter 3:

MATERIALS AND METHODS

3.1 Cloning procedures

3.1.1 Polymerase chain reaction (PCR)

PCR reactions were carried out in 50 µl volumes with the following components: 100 pg-1ng template DNA, 1X Pfu polymerase buffer (containing $MgCl_2$), 1 µM each primer, 0.2 mM dNTPs, 2 units Pfu polymerase. Reactions were overlayed with mineral oil and run on a Hybaid Omnicycler (MWG Biotech, Lausanne, Switzerland) using the following conditions: 95°C 2 minutes followed by 30 cycles of 95°C 45 seconds, annealing at 45-65°C 45 seconds, extension at 72°C for 1-10 minutes and a final elongation at 72°C for 10 minutes. Usually, the polymerase was added after the initial denaturation step.

3.1.2 Plasmid digestion

For preparative digestions, 3-10 µg plasmid DNA were digested with 10-30 U of enzyme in the appropriate 1X restriction buffer for 2 hours. Alternatively, DNA was digested with 10 U enzyme for 1 hour, another 10 U of enzyme were added and the digest was continued for another hour. For difficult plasmids or for digesting close to the ends of the DNA fragment, digests were carried out with 1-5 U of enzyme over night. A list of enzymes that can be used in over night digests can be found in the New England Biolabs catalogue. When needed, digestion mixes were supplemented with 1X bovine serum albumin (BSA, supplied by the enzyme manufacturer). Enzymes were from Boehringer Mannheim (Rotkreuz, Switzerland), Angewandte Biotechnologie Systeme (AGS, Axon Lab, Wallisellen, Switzerland) and New England Biolabs (NEB, Bioconcept, Allschwil, Switzerland).

3.1.3 Isolation of DNA fragments from agarose gels

Digests were run on preparative 1-2% agarose gels in 0.5X Tris-borate EDTA (TBE) buffer according to (Ausubel et al., 1987). Bands were visualized by a long-range ultraviolet light source, excised using a scalpel and purified using the Nucleospin extract kit (Macherey Nagel, Düren, Germany) according to the manufacturers specifications. Yield and purity of the isolated fragments was judged by running them on a 1-2% agarose gel and comparing the band intensity to a standard 1 kb DNA ladder (purchased from Eurogentec, Seraing, Belgium).

3.1.4 Dephosphorylation of 5'ends

When cloning into a single site of a vector, 5' ends were dephosphorylated to inhibit self-ligation of the vector. Dephosphorylation is commonly performed using calf intestine

alkaline phosphatase (CIAP). CIAP cannot be heat-inactivated and may modify the ends of the vector during subsequent incubation steps, sometimes leading to serious cloning problems. To circumvent this problem, alkaline phosphatase from arctic shrimp was used (SAP, Amersham Pharmacia Biotech). Dephosphorylation was done by incubating maximally 2 µg of linearized vector with 1X SAP buffer and 1 U of SAP for 30 minutes at 37°C, followed by an inactivation step at 75°C for 10 minutes. After inactivation, an additional unit of SAP was added, incubation was continued at 37°C for 30 minutes and the reaction was terminated by incubation at 75°C for 10 minutes. In most cases, dephosphorylation was carried out directly after digestion in the restriction enzyme buffer since SAP is active in all restriction buffers.

3.1.5 Ligation of DNA fragments

DNA fragments were quantitated on agarose gels as described above and the amount of insert DNA needed for a given amount of vector DNA was calculated using the following formula:

ng insert = ((ng vector * insert size in kb) / vector size in kb) * insert:vector ratio

Generally, ligations were performed in 10 µl volumes using 20-50 ng of vector and insert: vector ratios of 3:1, 1:1 and 1:3. As a control, vector without insert was ligated. For ligations involving overhangs, the incubation was carried out either at room temperature for 2 hours or at 16°C over night. For blunt ligations, incubations were always done at 16°C over night. Vector DNA, insert DNA, 1X ligation buffer and 0.5-1 µl of T4 DNA ligase (NEB) were mixed and incubated as described above. For blunt ligations, a cycling protocol was sometimes used: the ligation mixture was assembled as described above and incubated over night in a PCR machine programmed to run the following cycles: 30 seconds at 10°C, 30 seconds at 30°C (Lund et al., 1996).

3.1.6 Linker ligation

In some experiments, short linkers consisting of two complementary overhangs were inserted into the vectors to add sequences encoding epitope tags or containing additional sites for restriction enzymes. The oligonucleotides were designed so as to form a complementary double-stranded linker fragment with single-stranded overhangs at the ends. The plasmid was digested with the respective enzymes and gel purified. The method can be used both for cloning into a single site and for forced cloning using two different sites. 100 pmol of each oligonucleotide was mixed, heated to 90°C for 2 minutes and left at room temperature to cool down for 30 minutes. A ligation reaction was set up containing 50 ng vector and 1 µl of the oligonucleotide mix, 1X T4 DNA ligase buffer and 1 µl T4 DNA ligase (NEB) in a volume of 10 µl. The reaction was incubated for 2 hours at room temperature and 5 µl were transformed using either Protocol 1 or Protocol 2 (see below). It is important not to dephosphorylate the ends of the vector since the oligonucleotides are not phosphorylated. The reaction is driven by the large excess of linker over vector and has the advantage that no concatemers of linkers will occur. Usually, 6 clones were picked for analysis and in all cases, the majority of the clones contained the correct linker.

3.1.7 Transformation of plasmid DNA

For the propagation of plasmid DNA, two *E. Coli* strains were used, namely XL-1 Blue and DH5α. XL-1 Blue were made competent using Protocol 1, whereas DH5αwere made competent using Protocol 2 (see below). Transformations using Protocol 1 cells: XL-1 Blue cells were thawed on ice and divided into 50 µl aliquots. Subsequently, 5 µl of ligation mix or 1-10 ng of supercoiled plasmid was added and the cells were incubated on ice for 5 minutes. 450 µl of SOC medium was added and the cells were incubated at 37°C with shaking for 15 minutes (for plasmids carrying the ampicilline resistance gene) to 1 hour (for plasmids carrying the kanamycine resistance gene). 50-200 µl aliquots were spread on plates with the appropriate antibiotic and incubated over night at 37°C. Transformations using Protocol 2: DH5α cells were thawed on ice, divided into 100 µl aliquots and 5 µl ligation mixture or 1 ng supercoiled plasmid DNA was added. The transformation mix was incubated on ice for 30 minutes, heat-shocked at 42°C for 90 seconds, incubated on ice for 3 minutes, and 500 µl SOC medium was added. Subsequent steps were carried out as for Protocol 1.

3.1.8 Transformation by electroporation

For electroporation, XL-1 Blue or SURE strains (Invitrogen) were used. Cells were thawed on ice, 40 µl aliquots were transferred to ice-cold electroporation cuvettes (0.2 mm gap width, BTX, Axon Lab), 1 µl of the ligation reaction was added and incubated on ice for 30 minutes. Cells were electroporated in a BTX electroporator model ECM 600 at 1.5 kV, 2.5 kV/resistance, 129 Ohm. Directly after the electroporation step, 1 ml of SOC medium was added into the cuvette, mixed and transferred to a Falcon tube. Cells were incubated at 37°C for 1 hour with shaking and 200 µl aliquots were spread on plates with the appropriate antibiotic.

3.1.9 Plasmid DNA isolation.

For the analysis of recombinant clones, a standard miniprep protocol was used (Ausubel et al., 1987). For the preparation of large amounts of plasmid DNA suitable for transfection, maxiprep kits from Quiagen (Quiagen, Hilden, Germany) or Macherey Nagel were used. The preparations were done according to the protocols supplied by the manufacturer, with minor modifications: the centrifugation step after lysis was shortened to 10 minutes and the supernatant was additionally filtered through a standard folded filter (Schleicher und Schüll, Dassel, Germany). The centrifugation step after plasmid DNA precipitation was carried out in a HB-4 swing-out rotor to avoid smearing of the DNA pellet along the walls of the glass tube. Plasmid DNA was dissolved in water at an approximate concentration of 1 µg/µl. Quantitation was done by agarose gel electrophoresis and UV measurement. For UV measurement, the plasmid DNA was diluted 1:40 in 5 mM Tris-Cl buffer pH 8.5. Absorption at 260 nm and at 280 nm was measured. Plasmid DNA was considered to be clean if the ratio 260:280 was above 1.8. The amount of plasmid DNA was calculated using 1 OD_{260} unit = 50 µg/ml DNA. Plasmid DNA for transfections was aliquoted and stored at –20°C. Working aliquots were kept at 4°C and discarded after 1 month.

3.1.10 Protocol 1 for competent cells

XL-1 Blue cells were streaked out on LB+tetracycline plates from a glycerol stock and incubated over night at 37°C. 5-10 single colonies were transferred into 500 ml and grown

at room temperature over night with shaking. In the morning, cells were diluted back to an OD_{600} of 0.1 and grown at room temperature to an OD_{600} of 0.4-0.5. Cells were incubated on ice for 30 minutes, centrifuged at 4000 g for 10 minutes and resuspended in 10 ml 1X TSS by gentle swirling. Cells were dispersed in 200 µl aliquots, snap-frozen in liquid nitrogen and stored at –80°C. This protocol yields approximately $5x10^5$ to 10^6 transformants per µg.

3.1.11 Protocol 2 for competent cells

DH5α cells were streaked out on LB plates from a glycerol stock and incubated over night at 37°C. 5-10 single colonies were transferred into 200 ml Medium A and incubated at 18°C with shaking until they reached an OD_{600} of 0.5 (usually 2-3 days). Cells were incubated on ice for 10 minutes and pelleted at 4000 g for 10 minutes and resuspended in 80 ml ice-cold Medium B, followed by 10 minutes on ice. Cells were pelleted again, resuspended in 20 ml ice-cold Medium B and slowly stirred on ice. While stirring, 1.4 ml dimethyl sulfoxide (DMSO) was added dropwise and cells were incubated on ice for another 10 minutes. 400 µl were made, snap-frozen in liquid nitrogen and stored at –80°C. This protocol yields approximately $5x10^6$ to 10^7 transformants per µg.

3.1.12 Electrocompetent cells

XL-1 Blue or SURE were streaked onto LB+tetracycline plates from glycerol stocks and incubated over night at 37°C. Several single colonies were picked into a pre-culture of LB+tetracycline and grown over night at 37°C with shaking. 1 liter of LB was inoculated 1/100 with the pre-culture and grown to an OD_{260} of 0.8-0.9. Cells were aliquoted into pre-cooled flasks, incubated on ice for 20 minutes and centrifuged at 4000 g for 15 minutes. Pellets were resuspended in a total volume of 1 liter of ice-cold water by slight vortexing and centrifuged again. Pellets were resuspended in a total volume of 0.5 l of ice-cold water, resuspended by vortexing and centrifuged again. Pellets were resuspended in a total volume of 20 ml ice-cold water/10% glycerol by swirling, transferred to a single ice-cold 50 ml Falcon tube and centrifuged again. Finally, cells were resuspended in 2 ml of ice-cold water/10% glycerol and dispersed into 120 µl aliquots that were snap-frozen in liquid nitrogen and stored at –80°C. This protocol yields approximately 10^9 transformants per µg.

3.2 RT-PCR analysis

Chicken embryos were staged according to Hamburger and Hamilton (Hamburger and Hamilton, 1992). Timed pregnant mice were obtained from the C57Bl strain (BRL, Füllinsdorf, Switzerland). The day of the detection of the vaginal plug was considered as embryonic day 0.5. Total RNA was isolated from heart, leg and brain of chicken and mouse embryos using the SV Total RNA isolation system (Promega, Wallisellen, Switzerland). RT-PCR was carried out on approximately 1 µg of total RNA with the Access RT-PCR system (Promega). Primers specific for different chicken myomesin isoforms were derived from the chicken myomesin sequence (Bantle et al., 1996). The approximate positions of all primer sets are shown in Fig. 1*a*. Primer sequences were as follows and are denoted 5'-3'. Forward primers used: P1- GGAAGAACGTCAGCTTCACC, P3- TTTGATGAAGCCTTTGCCGAGTTCC, P5- GGGAACCATGCAACAACAATC.

Reverse primers used: P2- TTCCTGTTGTGGTTTGCTC, P4- CCAAAATCTCCCCCACGCTTTTGTT, P6- TCCCAGGAACACCACCAATC. Primers used for the amplification of the central fragment of mouse myomesin were derived from the mouse skelemin sequence (Price and Gomer, 1993). Forward primer-GGCAAAATCATCCCAAGTAG; reverse primer-ATAATAGCCTGTAATCTCTGC. Primers specific for chicken and mouse α-tubulin were used to standardize the amount of RNA used in the RT-PCR.

3.3 Expression of recombinant proteins and generation of polyclonal antibodies

3.3.1 Purification of GST-fusions using glutathione-agarose.

If not noted otherwise, all recombinant proteins were expressed in *E. Coli* BL21 (Novagen, Madison, WI, USA). For the soluble expression of GST-cH and GST-cEH, 1 liter of LB+ampicilline was inoculated with 25 ml of an overnight culture and grown at room temperature to an OD_{600} of 0.6. Protein expression was induced with 0.2 mM IPTG and the cells were grown for an additional 2 hours with open lids for increased aeration. Cells were pelleted by centrifugation at 4000 g for 15 minutes, the pellet was resuspended in 40 ml STE buffer (10 mM Tris, 150 mM NaCl, 1 mM EDTA, 0.1 % Triton X-100, pH 8) containing 1.6 ml of a 25x stock solution of the „Complete" protease inhibitor mix (Boehringer Mannheim, Rotkreuz, Switzerland) and lysozyme was added to a final concentration of 100 µg/ml and the suspension was incubated on ice for 20 minutes. Cells were disrupted by sonification (3-5x 10 second bursts in a Branson Sonifier 250, 50% duty cycle) and cell debris was pelleted by centrifugation at 20000 g for 20 minutes. The supernatant was incubated with 1 ml of 50% glutathione sepharose 4B (Pharmacia Biotech) for 4-6 hours at 4°C. Washing was done overnight with STE buffer. The purified protein was eluted in 2 ml elution buffer (100 mM reduced glutathione (Sigma) in STE buffer) and the purity and integrity of the recombinant protein was checked by SDS-PAGE.

3.3.2 Removal of GST by thrombin digestion

Thrombin (isolated from human plasma, T-6884, Sigma) was dissolved in phosphate buffered saline (PBS) to a specific activity of 1 NIH unit/µl, aliquoted and stored at –80°C. Aliquots were thawed maximally twice and were then discarded. Approximately 100 µl glutathione-resin were washed twice with PBS, excess liquid was removed with a 23 gauge needle and 50 µl thrombin mix (0.5 µl thrombin stock and 49.5 µl PBS) was added to the resin and incubated at room temperature on a shaker for 3 hours. The resin was pelleted by centrifugation and the supernatant was transferred to a new tube. The resin was washed twice with 50 µl PBS and the wash fractions were added to the supernatant. Protein concentration was measured using the BCA kit (Pierce) and by SDS-PAGE.

3.3.3 Generation of polyclonal antibodies in rabbits

Antibodies against recombinant myomesin fragments were generated by immunizing adult female rabbits either with the H-segment or the EH-segment fused to Glutathione S-transferase. Antibody against the S-segment was generated by immunizing rabbits with a

synthesized 20-mer peptide coupled to keyhole limphet hemocyanin (ANAWA, Zurich, Switzerland; immunization performed by Eurogentec, Seraing, Belgium). A standard immunization scheme was used for all rabbits (Harlow and Lane, 1988). As soon as strong and specific responses were detected, the animals were sacrificed and sera were collected. The IgG fraction was prepared by ammonium-sulfate precipitation, and the specificity of the antibodies was further characterized.

3.4 Cell culturing

3.4.1 Neonatal rat cardiomyocytes (NRC)

Primary cultures of neonatal rat cardiomyocytes (NRC) were prepared as described(Komiyama et al., 1996). Cells were seeded at a density of $0.4x10^6$ cells per 35 mm dish in plating medium. The plating medium consisted of 68% Dulbecco's MEM (Amimed AG, Basel, Switzerland), 17% Medium M199 (Amimed), 10% horse serum (Gibco), 5% fetal calf serum (Gibco), 4 mM glutamine (Amimed) and 1% penicilline-streptomycine (Amimed). Prior to transfection, cells were grown for 24 hours in 10% CO_2.

3.4.2 Adult rat cardiomyocytes (ARC)

Ventricular cardiomyocytes of 2 month-old Sprague-Dawley-Javonas rats were isolated according to (Eppenberger-Eberhardt et al., 1990). The culture dishes were coated with 0.1% gelatine (Fluka, Buchs, Switzerland) and the cells were grown in Medium M199 without L-glutamine, containing 20% fetal calf serum (FCS, Readysystem AG, Zurich, Switzerland), 20 mmol/L creatine (Sigma), 1% penicillin streptomycin (Gibco). Cytosine arabinoside (10 µmol/L, Sigma) was added throughout the culture period to inhibit fibroblast overgrowth. The medium was changed after 2 and 7 days.

3.4.3 Embryonic chicken cardiomyocytes (ECC) and skeletal cells (ECSC)

Hearts from 11 days-old chicken embryos were digested with collagenase (108 units/ml, Worthington Biochemical Corp., Freehold, NJ, USA) in ADS buffer (116 mM NaCl, 20 mM HEPES, 0.8 mM NaH_2PO_4, 1 g/l glucose, 5.4 mM KCl, 0.8 mM $MgSO_4$; pH 7.35) and cultured as described (Sen et al., 1988). Cells were plated onto dishes coated with fibronectin in plating medium (67% Dulbecco's MEM, 17% Medium M199 (Amimed AG, Basel, Switzerland), 10% horse serum, 5% fetal calf serum and 1% penicillin/streptomycin (Gibco, Life Technologies, Basel, Switzerland)). After one day the medium was replaced with the maintenance medium (78% Dulbecco's MEM, 20% Medium M199, 1% penicillin/streptomycin, 1% horse serum and 10^{-4} mol/l phenylephrine (Sigma)). To reduce the number of contaminating fibroblasts, glutamine was left out and cytosine arabinoside (10 µmol/l, Sigma) was added to the culture media.
For preparation of the skeletal muscle cell cultures the breast muscles of 11 days old chicken embryos were dissociated mechanically in the absence of $Ca^{2+}$by using a vortex. Cells were plated with a density of 10^5/ml of medium onto dishes coated with 0.1% gelatin in plating medium (M199, 10% horse serum, 2% chicken embryo extract, 1% L-Glutamin and 1% penicillin/streptomycin).

3.4.4 Transfection of cultivated cardiomyocytes

Two hours before transfection, the cells were changed to transfection medium (78% Dulbecco's MEM, 20% M199, 4% horse serum, 4 mM glutamine, 1% penicilline-streptomycine). Transfections were carried out using a modified CaPO4 transfection protocol (Komiyama et al., 1996). 1-2 µg plasmid DNA was adjusted with water to 135 µl, 15 µl 2.5 M $CaCl_2$ was added and mixed by vortexing briefly. While slowly vortexing, 150 ml BBS buffer (50 mM BES, 1.5 mM Na_2HPO_4, 280 mM NaCl, pH 6.7) was added dropwise and the mixture was incubated for 12 minutes at room temperature. The cells were incubated at 37°C, 3% CO_2 for 6 hours, washed twice for 5 minutes in 1 X TBS and kept in maintenance medium for 72 hours, followed by fixation and staining. Maintenance medium consisted of 78% Dulbecco's MEM, 20% Medium M199, 1% horse serum, 1% penicilline-streptomycine, 4 mM glutamine and 10^{-4} M phenylephrine (Sigma). For live observations, cells were plated on laminin-coated glass-bottom culture dishes (MatTek Corp., Ashland, MA, USA) and treated as described above.

3.5 Immunohistochemistry

3.5.1 Immunostaining

For immunofluorescence staining, 4 days-old cultures were fixed with 4% paraformaldehyde in PBS for 15 minutes at room temperature, blocked with 0.1 M glycine in PBS for 5 minutes and permeabilized in 0.2% Triton X100/PBS for 10 minutes. After blocking with 5% normal (pre-immune) goat serum and 1% bovine serum albumin in PBS for 20 minutes, primary antibodies were added and incubated for 1 hour at room temperature. After washing with PBS, secondary antibodies were added for 45 minutes. The specimens were washed in PBS and mounted in 0.1 M Tris-HCl (pH 9.5) /glycerol (3:7) containing 50 mg/ml n-propyl gallate as anti-fading reagent (Messerli et al., 1993).

3.5.2 Chicken whole mount heart preparation

Preparations of specimens was carried out as discribed in (Tokuyasu and Maher, 1987). The hearts of fertilized white Leghorn chick embryos ranging from 8 to 12 somite-stage (Hand Ham, 19519 were dissected and rinsed several times in PBS. Trasferring of the hearts was done with a Gilson Pipette plastic tip.The hearts were fixed in 3% paraformaldehyde in PBS for 1 hour, washed several times in PBS and treated with 0.1% Triton X-100 in PBS for 30 min.The specimens were when washed in PBS and treated with hyaluronidase solution (330 Units/mg, Sigma) in PBS for 30 min. After blocking with 5% normal (pre-immune) goat serum and 1% bovine serum albumin in PBS for 1 hour, primary antibodies were added and incubated over night at 4°C. After 4x30 min.washing with PBS, secondary antibodies were added for 6 hours at room temperature. The specimens were washed in PBS (4x30 min) and mounted sa discribed above.

3.5.3 Frozen sections of chicken embryos

Fertilized eggs from white Leghorn hens (Hungerbühler, Flawil, Switzerland) were incubated at 37°C for about 7 days. Embryos were removed from the eggs, transferred into cold PBS and staged according to Hamburger and Hamilton (Hamburger and Hamilton,

1992). After an overnight incubation in 30% sucrose in PBS the embryos were frozen in liquid nitrogen and stored at -70°C until sectioning. 10 µm thick sagittal sections through the whole embryos were cut on a cryostat (Reichert, Vienna, Austria) and collected on gelatin-coated glass slides. For immunofluorescence experiments, the sections were fixed, stained and mounted as described above.

3.5.4 SDS-PAGE and Immunoblotting

Tissue samples (brain, gizzard, heart and skeletal muscle) were carefully dissected from the animal, homogenized by freeze-slamming and resuspended in a modified version of SDS-sample buffer (3.7 M urea, 134.6 mM Tris pH 6.8; 5.4% SDS; 2.3% NP-40; 4.45% β-mercaptoethanol; 4% glycerol and 6 mg/100 ml bromophenol blue (Laemmli, 1970) and boiled for 1 minute. SDS-samples were run on 6% polyacrylamide minigels (Biorad, Glattbrugg, Switzerland) together with broad range molecular weight standards (Biorad). Equal amounts of protein were loaded for the different tissue extracts as judged by Coomassie blue staining of a twin gel. Blotting was carried out over night onto nitrocellulose Hybond-C extra (Amersham, Zurich, Switzerland). Unspecific binding sites were blocked with 5% non-fat dry milk (w/v) in washing buffer (PBS, pH 7.4, 0.3% Tween-20) for 1 hour at room temperature. Primary and secondary antibodies were diluted in washing buffer supplemented with 1% non-fat milk powder and incubated for 1 hour respectively with intermittent washing in washing buffer. Chemiluminescence reaction was performed according to the manufacturer's instructions (Amersham and Pierce, Socochim, Lausanne, Switzerland, respectively) and visualized on Fuji Medical X-Ray films.

3.5.5 Antibodies

F-actin was stained for immunofluorescence microskopy with rhodamine-labeled phalloidin. The antibodies against chicken myomesin isoforms were generated in rabbits as discribed in section 3.3.3. The following primary antibodies agains other proteins have been used for indirect immunofluorescence and immunoblotting:

Antigen	Antibody	Dilution	Source
sarcomeric α-actin	mAb 5C5	1:100	Sigma
cardiac α-actin	mAb Ac-1	1:10	Progen
smooth muscle α-actin	mAb 1A4	1:100	Sigma
cytoplasmic γ-actin	pAb G2	1:100	gift from J.C. Bulinski
cytoplasmic β-actin	mAb A5441	1:100	Sigma
cytoplasmic β-actin	poRaβcyto	1:100	gift from Chaponnier, (Yao et al., 1995)
sarcomeric α-actinin	mAb EA-53	1:1000	Sigma
myomesin	mAb B4	1:1	raised in our lab, (Grove et al., 1984)
myomesin	poAb My190-Nrt	1:100	gift from M. Gautel (Obermann et al., 1996)

titin	mAb T12	1:100	Boehringer Mannheim
titin	mAb (IgG) 9D10	1:3	DHSB
myosin	mAb (IgM) 1025	1.10	Alexis

Table 3.1: The summary of the primary antibodies, which were used in the study. For immunodetection on the western blot the antibodies were diluted about 10 times more. DHSB denote Developmental Studie Hybridoma Bank, Jowa.

For immunofluorescence secondary antibodies were FITC-conjugated goat anti rabbit IgG (Cappel, West Chester, PA, USA) and Cy3-conjugated goat anti mouse IgG (Jackson Immunoresearch, West Grove, PA, USA). Cy5-conjugated phalloidin was a generous gift of Prof. H. Faulstich (Heidelberg, Germany). For immunoblotting, horse radish peroxidase-conjugated anti mouse Igs (DAKO, Zug, Switzerland), anti rat Igs (DAKO) and anti rabbit Igs (Calbiochem, Luzern, Switzerland) were used as secondary antibodies.

3.6 Microscopy

Analysis of the stained cells was carried out using a Leica confocal unit equipped with a DM/IRB E inverse microscope, an argon/krypton mixed gas laser and a Leica PL APO 63x/1.4 NA objective lens. Image processing was done on a Silicon Graphics Workstation using the image processing software Imaris (Messerli et al., 1993), distributed by Bitplane AG, Zürich, Switzerland). Conventional fluorescence microscopy was done on a Zeiss Axioplan fitted with a Plan-Neofluar 63x/1.4 NA objective lens. Images were recorded using a Hamamatsu CCD camera and processed using Photoshop software (Adobe Systems, San Jose, CA, USA).
Images were recorded with a Leica inverted microscope DM IRB/E connected to a Leica true confocal scanner TCS NT. Leica PL APO 100x/1.4 oil or PL APO 63x/1.4 oil immersion objectives were used.The fluorescence images of the frozen sections were recorded using an Achrostigmat 5x/0.12 objective.

3.7 Sequence analysis

GenBank release 112.0 was searched using the Blast program (Altschul et al., 1990) at the National Center for Biotechnology Information (http://www.ncbi.nlm.nih.gov). Sequence alignments were performed using the MegAlign software (DNASTAR Inc, Madison Wi, USA). Protein motif predictions were done with the software Motif (http://www.motif.genome.ad.jp). The EST clone AA248352 was a kind gift of Dr. C.C. Liew (Toronto, Canada). The sequences of chicken and human EH segments are available from GenBanc/EMBL/DDBJ under accession numbers AF185572 and AF185573, respectively.

References

Alberts, B., Dennis, B., Julian, L., Martin, R., Keith, R., and D., W. J. (1994). Molecular biology of the cell, 3 Edition (New York: Garland Publishing).

Allen, P. G., Shuster, C. B., Kas, J., Chaponnier, C., Janmey, P. A., and Herman, I. M. (1996). Phalloidin binding and rheological differences among actin isoforms. *Biochemistry* 35: 14062-14069.

Almenar-Queralt, A., Lee, A., Conley, C. A., Ribas de Pouplana, L., and Fowler, V. M. (1999). Identification of a novel tropomodulin isoform, skeletal tropomodulin, that caps actin filament pointed ends in fast skeletal muscle. *J. Biol. Chem.* 274: 28466-75.

Alonso, S., Garner, I., Vandekerckhove, J., and Buckingham, M. (1990). Genetic analysis of the interaction between cardiac and skeletal actin gene expression in striated muscle of the mouse. *J. Mol. Biol.* 211: 727-738.

Altschul, S. F., Gish, W., Miller, W., Myers, E. W., and Lipman, D. J. (1990). Basic local alignment search tool. *J. Mol. Biol.* 215: 403-410.

Arber, S., Hunter, J. J., Ross, J. J., Hongo, M., Sansig, G., Borg, J., Perriard, J. C., Chien, K. R., and Caroni, P. (1997). MLP-deficient mice exhibit a disruption of cardiac cytoarchitectural organization, dilated cardiomyopathy, and heart failure. *Cell* 88: 393-403.

Auerbach, D., Bantle, S., Keller, S., Hinderling, V., Leu, M., Ehler, E., and Perriard, J. C. (1999). Different domains of the M-band protein myomesin are involved in myosin binding and M-band targeting. *Mol. Biol. Cell* 10: 1297-1308.

Auerbach, D., Rothen-Ruthishauser, B., Bantle, S., Leu, M., Ehler, E., Helfman, D., and Perriard, J. C. (1997). Molecular mechanisms of myofibril assembly in heart. *Cell Struct. Funct.* 22: 139-146.

Ausma, J., Wijffels, M., van Eys, G., Koide, M., Ramaekers, F., Allessie, M., and Borgers, M. (1997). Dedifferentiation of atrial cardiomyocytes as a result of chronic atrial fibrillation. *Am J Pathol* 151: 985-97.

Ausubel, F., Roger, B., Kingston, R. E., Moore, D. D., Smith, J. A., Seidman, J. G., and Struhl, K. (1987). Current protocols in molecular biology: New York: John Wiley & Sons).

Ayscough, K. R. (1998). In vivo functions of actin-binding proteins. *Curr Opin Cell Biol* 10: 102-111.

Bandman, E. (1992). Contractile protein isoforms in muscle development. *Dev. Biol.* 154: 273-283.

Bantle, S. (1997). The molecular biology of chicken myomesin, *Diss*ertation (Zürich: Swiss Federal Institute of Tecnology).

Bantle, S., Keller, S., Haussmann, I., Auerbach, D., Perriard, E., Muhlebach, S., and Perriard, J. C. (1996). Tissue-specific isoforms of chicken myomesin are generated by alternative splicing. *J. Biol. Chem.* 271: 19042-19052.

Benian, G. M., Tinley, T. L., Tang, X., and Borodovsky, M. (1996). The Caenorhabditis elegans gene unc-89, required fpr muscle M-line assembly, encodes a giant modular protein composed of Ig and signal transduction domains. *J. Cell. Biol.* 132: 835-848.

Bennett, P., Craig, R., Starr, R., and Offer, G. (1986). The ultrastructural location of C-protein, X-protein and H-protein in rabbit muscle. *J Muscle Res Cell Motil* 7: 550-67.

Bergsma, D. J., Chang, K. S., and Schwartz, R. J. (1985). Novel chicken actin gene: third cytoplasmic isoform. *Mol. Cell. Biol.* 5: 1151-1162.

Blanchard, A., Ohanian, V., and Critchley, D. (1989). The structure and function of alpha-actinin. *J. Muscle Res. Cell. Motil.* 10: 280-289.

Blinks, J. R. (1965). Convenient apparatus for recording contractions of isolated heart muscle. *J. Appl. Physiol.* 20: 755-757.

Boguski, M. S., Lowe, T. M., and Tolstoshev, C. M. (1993). dbEST-database for "expressed sequence tags". *Nat. Genet.* 4: 332-333.

Boheler, K. R., Carrier, L., de la Bastie, D., Allen, P. D., Komajda, M., Mercadier, J. J., and Schwartz, K. (1991). Skeletal actin mRNA increases in the human heart during ontogenic development and is the major isoform of control and failing adult hearts. *J Clin Invest* 88: 323-330.

Bottinelli, R., Pellegrino, M. A., Canepari, M., Rossi, R., and Reggiani, C. (1999). Specific contributions of various muscle fibre types to human muscle performance: an in vitro study. *J. Electromyogr. Kinesiol.* 9: 87-95.

Buck, S. H., Konyn, P. J., Palermo, J., Robbins, J., and Moss, R. L. (1999). Altered kinetics of contraction of mouse atrial myocytes expressing ventricular myosin regulatory light chain. *Am. J. Physiol.* 276: H1167-1171.

Burr, A. H., and Gans, C. (1998). Mechanical significance of obliquely striated architecture in nematode muscle. *Biol. Bull.* 194: 1-6.

Caplan, A. I., Fiszman, M. Y., and Eppenberger, H. M. (1983). Molecular and cell isoforms during development. *Science* 221: 921-7.

Caravatti, M., Minty, A., Robert, B., Montarras, D., Weydert, A., Cohen, A., Daubas, P., and Buckingham, M. (1982). Regulation of muscle gene expression. The accumulation of messenger RNAs coding for muscle-specific proteins during myogenesis in a mouse cell line. *J. Mol. Biol.* 160: 59-76.

Carlsson, E., Kjorell, U., Thornell, L. E., Lambertsson, A., and Strehler, E. (1982). Differentiation of the myofibrils and the intermediate filament system during postnatal development of the rat heart. *Eur. J. Cell. Biol.* 27: 62-73.

Carlsson, E., and Thornell, L. E. (1987). Diversification of the myofibrillar M-band in rat skeletal muscle during postnatal development. *Cell. Tissue Res.* 248: 169-180.

Carlyle, W. C., Toher, C. A., Vandervelde, T. R., Mcdonald, K. M., Homans, D. C., and Cohn, J. N. (1996). Changes in beta-actin mRNA expression in remodeling canine myocardium. *J. Mol. Cell. Cardiol.* 28: 53-63.

Carrier, L., Boheler, K. R., Chassagne, C., de la Bastie, D., Wisnewsky, C., Lakatta, E. G., and Schwartz, K. (1992). Expression of the sarcomeric actin isogenes in the rat heart with development and senescence. *Circ. Res.* 70: 999-1005.

Cazorla, O., Freiburg, A., Helmes, M., Centner, T., McNabb, M., Wu, Y., Trombitas, K., Labeit, S., and Granzier, H. (2000). Differential Expression of Cardiac Titin Isoforms and Modulation of Cellular Stiffness. *Circ. Res.* 86: 59-67.

Chacko, K. J. (1976). Observations on the ultrastructure of developing myocardium of rat embryos. *J. Morphol.* 150: 681-709.

Chaponnier, C., Goethals, M., Janmey, P. A., Gabbiani, F., Gabbiani, G., and Vandekerckhove, J. (1995). The specific NH2-terminal sequence Ac-EEED of alpha-smooth muscle actin plays a role in polymerization in vitro and in vivo. *J. Cell. Biol.* 130: 887-95.

Chien, K. R. (1999). Stress pathways and heart failure. *Cell* 98: 555-558.

Claycomb, W. C., and Palazzo, M. C. (1980). Culture of the terminally differentiated adult cardiac muscle cell: a light and scanning electron microscope study. *Dev. Biol.* 80: 466-482.

Clement, S., Chaponnier, C., and Gabbiani, G. (1999). A subpopulation of cardiomyocytes expressing alpha-skeletal actin is identified by a specific polyclonal antibody. *Circ. Res.* 85: e51-58.

Dabiri, G. A., Turnacioglu, K. K., Sanger, J. M., and Sanger, J. W. (1997). Myofibrillogenesis visualized in living embryonic cardiomyocytes. *Proc. Natl. Acad. Sci. USA* 94: 9493-9498.

DeNofrio, D., Hoock, T. C., and Herman, I. M. (1989). Functional sorting of actin isoforms in microvascular pericytes. *J. Cell Biol.* 109: 191-202.

Dlugosz, A. A., Antin, P. B., Nachmias, V. T., and Holtzer, H. (1984). The relationship between stress fiber-like structures and nascent myofibrils in cultured cardiac myocytes. *J. Cell. Biol.* 99: 2268-2278.

Edman, A. C., Lexell, J., Sjostrom, M., and Squire, J. M. (1988). Structural diversity in muscle fibres of chicken breast. *Cell. Tissue Res.* 251: 281-289.

Ehler, E., Rothen, B. M., Hammerle, S. P., Komiyama, M., and Perriard, J. C. (1999). Myofibrillogenesis in the developing chicken heart: assembly of Z-disk, M-line and the thick filaments. *J. Cell. Sci.* 112: 1529-1539.

Elliott, G. F., Lowy, J., and Millman, B. M. (1965). X-ray diffraction from living striated muscle during contraction. *Nature* 206: 1357-8.

Eppenberger, H. M., Eppenberger-Eberhardt, M., and Hertig, C. (1995). Cytoskeletal rearrangements in adult rat cardiomyocytes in culture. *Ann N Y Acad Sci* 752: 128-30.

Eppenberger, H. M., Perriard, J. C., Rosenberg, U. B., and Strehler, E. E. (1981). The Mr 165,000 M-protein myomesin: a specific protein of cross-striated muscle cells. *J Cell Biol* 89: 185-193.

Eppenberger, H. M., Strehler, E. E., Doetschman, T. C., Rosenberg, U. B., Perriard, J. C., and Wallimann, T. (1982). Developmental history of the two M-line proteins MM-creatine kinase and myomesin during myogenesis. *Prog Clin Biol Res* . 85: 381-9.

Eppenberger, H. M., and Zuppinger, C. (1999). In vitro reestablishment of cell-cell contacts in adult rat cardiomyocytes. Functional role of transmembrane components in the formation of new intercalated disk-like cell contacts. *Faseb J.* 13 Suppl: S83-89.

Eppenberger, M. E., Hauser, I., Baechi, T., Schaub, M. C., Brunner, U. T., Dechesne, C. A., and Eppenberger, H. M. (1988). Immunocytochemical Analysis of the Regeneration of Myofibrils in Long-Term Cultures of Adult Cardiomyocytes of the Rat. *Dev. Biol.* 130: 1-15.

Eppenberger-Eberhardt, M., Aigner, S., Donath, M. Y., Kurer, V., Walther, P., Zuppinger, C., Schaub, M. C., and Eppenberger, H. M. (1997). IGF-I and bFGF differentially influence atrial natriuretic factor and alpha-smooth muscle actin expression in cultured atrial compared to ventricular adult rat cardiomyocytes. *J Mol Cell Cardiol* 29: 2027-2039.

Eppenberger-Eberhardt, M., Flamme, I., Kurer, V., and Eppenberger, H. M. (1990). Reexpression of α-Smooth Muscle Actin Isoform in Cultured Adult Rat Cardiomyocytes. *Dev. Biol.* 139: 269-278.

Eppenberger-Eberhardt, M., Messerli, M., Eppenberger, H. M., and Reinecke, M. (1993). New occurrence of atrial natriuretic factor and storage in secretorially active granules in adult rat ventricular cardiomyocytes in long-term culture. *J. Mol. Cell. Cardiol.* 25: 753-7.

Erickson, H. P. (1994). Reversible unfolding of fibronectin type III and immunoglobulin domains provides the structural basis for stretch and elasticity of titin and fibronectin. *Proc Natl Acad Sci U S A* 91: 10114-8.

Farah, C. S., and Reinach, F. C. (1995). The troponin complex and regulation of muscle contraction. *Faseb J.* 9: 755-767.

Fischman, D. A. (1967). An electron microscope study of myofibril formation in embryonic chick skeletal muscle. *J. Cell. Biol.* 32: 557-575.

Francis, R., and Waterston, R. H. (1991). Muscle cell attachment in Caenorhabditis elegans. *J. Cell. Biol.* 114: 465-479.

Franke, W. W., Stehr, S., Stumpp, S., Kuhn, C., Heid, H., Rackwitz, H. R., Schnolzer, M., Baumann, R., Holzhausen, H. J., and Moll, R. (1996). Specific immunohistochemical detection of cardiac/fetal alpha-actin in human cardiomyocytes and regenerating skeletal muscle cells. *Differentiation* 60: 245-250.

Freiburg, A., and Gautel, M. (1996). A molecular map of the interactions between titin and myosin-binding protein C: implications for sarcomeric assembly in familial hypertrophic cardiomyopathy. *Eur. J. Biochem.* 235: 317-323.

Freund, J. (1956). The mode of action of immunologic adjuvants. *Adv. Tuberc. Res.* 7: 168-170.

Furst, D. O., Nave, R., Osborn, M., and Weber, K. (1989). Repetitive titin epitopes with a 42 nm spacing coincide in relative position with known A band striations also identified by major myosin-associated proteins. An immunoelectron-microscopical study on myofibrils. *J. Cell. Sci.* 94: 119-125.

Furst, D. O., Osborn, M., Nave, R., and Weber, K. (1988). The organization of titin filaments in the half-sarcomere revealed by monoclonal antibodies in immunoelectron microscopy: a map of ten nonrepetitive epitopes starting at the Z line extends close to the M line. *J. Cell. Biol.* 106: 1563-1572.

Fürst, D. O., Osborn, M., and Weber, K. (1989). Myogenesis in the mouse embryo: differential onset of expression of myogenic proteins and the involvement of titin in myofibril assembly. *J. Cell. Biol.* 109: 517-527.

Furst, D. O., Vinkemeier, U., and Weber, K. (1992). Mammalian skeletal muscle C-protein: purification from bovine muscle, binding to titin and the characterization of a full-length human cDNA. *J Cell Sci* 102: 769-778.

Garner, I., Sassoon, D., Vandekerckhove, J., Alonso, S., and Buckingham, M. E. (1989). A developmental study of the abnormal expression of alpha-cardiac and alpha-skeletal actins in the striated muscle of a mutant mouse. *Dev. Biol.* 134: 236-245.

Garrels, J. I., and Gibson, W. (1976). Identification and characterization of multiple forms of actin. *Cell* 9: 793-805.

Gautel, M., and Goulding, D. (1996). A molecular map of titin/connectin elasticity reveals two different mechanisms acting in series. *FEBS Lett.* 385: 11-14.

Gautel, M., Goulding, D., Bullard, B., Weber, K., and Furst, D. O. (1996). The central Z-disk region of titin is assembled from a novel repeat in variable copy numbers. *J. Cell. Sci.* 109: 2747-2754.

Gautel, M., Leonard, K., and Labeit, S. (1993). Phosphorylation of KSP motifs in the C-terminal region of titin in differentiating myoblasts. *EMBO J.* 12: 3827-3834.

Gimona, M., Vandekerckhove, J., Goethals, M., Herzog, M., Lando, Z., and Small, J. V. (1994). Beta-actin specific monoclonal antibody. *Cell. Motil. Cytoskeleton* 27: 108-116.

Glyn, M. C., and Ward, B. J. (1998). A beta-actin isotype is present in rat cardiac endothelial cells but not in cardiac myocytes. *Microcirculation* 5: 259-264.

Goldfine, S. M., Einheber, S., and Fischman, D. A. (1991). Cell-free incorporation of newly synthesized myosin subunits into thick myofilaments. *J. Muscle Res. Cell. Motil.* 12: 161-170.

Goldstein, M. A., and Traeger, L. (1984). Ultrastractural changes in postnatal development of the cardiac myocyte. In *The developing heart*, M. J. Legato, 2 ed. (Boston: Martinus Nijhoff), pp. 1-20.

Goncharova, E. J., Kam, Z., and Geiger, B. (1992). The involvement of adherens junction components in myofibrillogenesis in cultured cardiac myocytes. *Development* 114: 173-183.

Goode, D. (1975). Mitosis of embryonic heart muscle cells in vitro. An immunfluorescence nad ultrastructural study. *Cytobiologie* 11: 203-229.

Gordon, D. J., Boyer, J. L., and Korn, E. D. (1977). Comparative biochemistry of non-muscle actins. *J. Biol. Chem.* 252: 8300-8309.

Goulding, D., Bullard, B., and Gautel, M. (1997). A survey of in situ sarcomere extension in mouse skeletal muscle. *J. Muscle Res. Cell. Motil.* 18: 465-472.

Granzier, H., Helmes, M., and Trombitas, K. (1996). Nonuniform elasticity of titin in cardiac myocytes: a study using immunoelectron microscopy and cellular mechanics. *Biophys. J.* 70: 430-442.

Granzier, H. L., and Irving, T. C. (1995). Passive tension in cardiac muscle: contribution of collagen, titin, microtubules, and intermediate filaments. *Biophys. J.* 68: 1027-1044.

Gregorio, C. C., and Fowler, V. M. (1995). Mechanisms of thin filament assembly in embryonic chick cardiac myocytes: tropomodulin requires tropomyosin for assembly. *J. Cell. Biol.* 129: 683-695.

Gregorio, C. C., Granzier, H., Sorimachi, H., and Labeit, S. (1999). Muscle assembly: a titanic achievement? *Curr. Opin. Cell. Biol* . 11: 18-25.

Gregorio, C. C., Trombitas, K., Centner, T., Kolmerer, B., Stier, G., Kunke, K., Suzuki, K., Obermayr, F., Herrmann, B., Granzier, H., Sorimachi, H., and Labeit, S. (1998). The NH2 terminus of titin spans the Z-disc: its interaction with a novel 19-kD ligand (T-cap) is required for sarcomeric integrity. *J. Cell Biol.* 143: 1013-1027.

Grove, B. K., Cerny, L., Perriard, J.-C., Eppenberger, H. M., and Thornell, L.-E. (1989). Fiber type-specific distribution of M-band proteins in chicken muscle. *J. Histochem. Cytochem.* 37: 447-454.

Grove, B. K., Cerny, L., Perriard, J. C., and Eppenberger, H. M. (1985). Myomesin and M-protein: expression of two M-band proteins in pectoral muscle and heart during development. *J. Cell Biol.* 101: 1413-1421.

Grove, B. K., Kurer, V., Lehner, C., Doetschman, T. C., Perriard, J. C., and Eppenberger, H. M. (1984). A new 185000-dalton skeletal muscle protein detected by monoclonal antibodies. *J. Cell Biol.* 98: 518-524.

Gunning, P., Ponte, P., Blau, H., and Kedes, L. (1983). alpha-skeletal and alpha-cardiac actin genes are coexpressed in adult human skeletal muscle and heart. *Mol. Cell. Biol.* 3: 1985-1995.

Gunning, P., Weinberger, R., Jeffrey, P., and Hardeman, E. (1998). Isoform sorting and the creation of intracellular compartments. *Annu. Rev. Cell. Dev. Biol.* 14: 339-372.

Hamburger, V., and Hamilton, H. L. (1992). A series of normal stages in the development of chick embryo. *Developmental Dynamics* 195: 231-272.

Handel, S. E., Greaser, M. L., Schultz, E., Wang, S. M., Bulinski, J. C., Lin, J. J., and Lessard, J. L. (1991). Chicken cardiac myofibrillogenesis studied with antibodies specific for titin and the muscle and nonmuscle isoforms of actin and tropomyosin. *Cell. Tissue Res.* 263: 419-430.

Handel, S. E., Wang, S. M., Greaser, M. L., Schultz, E., Bulinski, J. C., and Lessard, J. L. (1989). Skeletal muscle myofibrillogenesis as revealed with a monoclonal antibody to titin in combination with detection of the alpha- and gamma- isoforms of actin. *Dev. Biol.* 132: 35-44.

Hannan, A. J., Gunning, P., Jeffrey, P. L., and Weinberger, R. P. (1998). Structural compartments within neurons: developmentally regulated organization of microfilament isoform mRNA and protein. *Mol. Cell. Neurosci.* 11: 289-304.

Harder, B. A., Hefti, M. A., Eppenberger, H. M., and Schaub, M. C. (1998). Differential protein localization in sarcomeric and nonsarcomeric contractile structures of cultured cardiomyocytes. *J. Struct. Biol.* 122: 162-175.

Harder, B. A., Schaub, M. C., and Eppenberger, H. M. (1996). Influence of fibroblast growth factor (bFGF) and insulin-like growth factor (IGF-1) on cytoskeletal and contractile structures and on atrial natriuretic factor. *J. Mol. Cardiol.* 28: 19-31.

Harlow, E., and Lane, D. (1988). Antibodies: A Laboratory Manual, 2nd Edition (Cold Spring Harbor, NY: Cold Spring Harbor Laboratory).

Harris, D. E., and Warshaw, D. M. (1993). Smooth and skeletal muscle actin are mechanically indistinguishable in the in vitro motility assay. *Circ. Res.* 72: 219-224.

Hayakawa, K., Ono, S., Nagaoka, R., Saitoh, O., and Obinata, T. (1996). Differential assembly of cytoskeletal and sarcomeric actins in developing skeletal muscle cells in vitro. *Zoolog. Sci.* 13: 509-517.

Helfman, D. M., Berthier, C., Grossman, J., Leu, M., Ehler, E., Perriard, E., and Perriard, J. C. (1999). Nonmuscle tropomyosin-4 requires coexpression with other low molecular weight isoforms for binding to thin filaments in cardiomyocytes. *J. Cell Sci.* 112: 371-380.

Helmes, M., Trombitas, K., Centner, T., Kellermayer, M., Labeit, S., Linke, W. A., and Granzier, H. (1999). Mechanically driven contour-length adjustment in rat cardiac titin's unique N2B sequence: titin is an adjustable spring. *Circ. Res.* 84: 1339-1352.

Helmes, M., Trombitas, K., and Granzier, H. (1996). Titin develops restoring force in rat cardiac myocytes. *Circ Res.* 79: 619-626.

Herman, I. M. (1993). Actin isoforms. *Curr. Opin. Cell Biol.* 5: 48-55.

Hewett, T. E., Grupp, I. L., Grupp, G., and Robbins, J. (1994). Alpha-skeletal actin is associated with increased contractility in the mouse heart. *Circ. Res.* 74: 740-746.

Hill, M. A., and Gunning, P. (1993). Beta and gamma actin mRNAs are differentially located within myoblasts. *J. Cell. Biol.* 122: 825-832.

Hill, M. A., Schedlich, L., and Gunning, P. (1994). Serum-induced signal transduction determines the peripheral location of beta-actin mRNA within the cell. *J. Cell. Biol.* 126: 1221-1229.

Hiruma, T., and Hirakow, R. (1985). An ultrastructural topographical study on myofibrillogenesis in the heart of the chick embryo during pulsation onset period. *Anat. Embryol. (Berl)* 172: 325-329.

Holmes, K. C., Popp, D., Gebhard, W., and Kabsch, W. (1990). Atomic model of the actin filament. *Nature* 347: 44-49.

Horowits, R., Kempner, E. S., Bisher, M. E., and Podolsky, R. J. (1986). A physiological role for titin and nebulin in skeletal muscle. *Nature* 23: 160-164.

Horowits, R., and Podolsky, R. J. (1987). The positional stability of thick filaments in activated skeletal muscle depends on sarcomere length: evidence for the role of titin filaments. *J Cell Biol* 105: 2217-23.

Houmeida, A., Holt, J., Tskhovrebova, L., and Trinick, J. (1995). Studies of the interaction between titin and myosin. *J. Cell. Biol.* 131: 1471-1481.

Huang, C. Y. (1967). Electron microscopic study of the development of heart muscle of the frog Rana pipiens. *J. Ultrastruct. Res.* 20: 211-226.

Huxley, H. E. (1963). Electron microscope studies on the structure of natural and synthetic protein filaments from striated muscle. *J. Mol. Biol.* 7: 281-308.

Huxley, H. E., and Brown, W. (1967). The low-angle x-ray diagram of vertebrate striated muscle and its behaviour during contraction and rigor. *J. Mol. Biol.* 30: 383-434.

Huxley, H. E., and Hanson, J. (1954). Changes in the cross-striations of muscle during contraction and stretch and their structural interpretation. *Nature* 173: 973-976.

Improta, S., Krueger, J. K., Gautel, M., Atkinson, R. A., Lefevre, J. F., Moulton, S., Trewhella, J., and Pastore, A. (1998). The assembly of immunoglobulin-like modules in titin: implications for muscle elasticity. *J. Mol. Biol.* 284: 761-777.

Improta, S., Politou, A. S., and Pastore, A. (1996). Immunoglobulin-like modules from titin I-band: extensible components of muscle elasticity. *Structure* 4: 323-337.

Isaacs, W. B., Kim, I. S., Struve, A., and Fulton, A. B. (1989). Biosynthesis of titin in cultured skeletal muscle cells. *J. Cell. Biol.* 109: 2189-2195.

Ivester, C. T., Tuxworth, W. J., Cooper, G. t., and McDermott, P. J. (1995). Contraction accelerates myosin heavy chain synthesis rates in adult cardiocytes by an increase in the rate of translational initiation. *J. Biol. Chem.* 270: 21950-21957.

Janmey, P. A., and Chaponnier, C. (1995). Medical aspects of the actin cytoskeleton. *Curr. Opin. Cell Biol.* 7: 111-117.

Kabsch, W., Mannherz, H. G., Suck, D., Pai, E. F., and Holmes, K. C. (1990). Atomic structure of the actin: DNase I complex. *Nature* 347: 37-44.

Kabsch, W., and Vandekerckhove, J. (1992). Structure and function of actin. *Annu. Rev. Biophys. Biomol. Struct.* 21: 49-76.

Kaech, S., Fischer, M., Doll, T., and Matus, A. (1997). Isoform specificity in the relationship of actin to dendritic spines. *J Neurosci* 17: 9565-72.

Kaempfe, L. (1985). Evolution und stammegeschichte der organismen (Stutgart: Gustav Fischer), pp. 424.

Kapanci, Y., Burgan, S., Pietra, G. G., Conne, B., and Gabbiani, G. (1990). Modulation of actin isoform expression in alveolar myofibroblasts (contractile interstitial cells) during pulmonary hypertension. *Am. J. Pathol.* 136: 881-889.

Kelly, A. M., and Chacko, S. (1976). Myofibril organisation and mitosis in cultured cardiac muscle cells. *Dev. Biol.* 48: 421-430.

Kenny, P. A., Liston, E. M., and Higgins, D. G. (1999). Molecular evolution of immunoglobulin and fibronectin domains in titin and related muscle proteins. *Gene* 232: 11-23.

Kislauskis, E. H., Li, Z., Singer, R. H., and Taneja, K. L. (1993). Isoform-specific 3'-untranslated sequences sort alpha-cardiac and beta-cytoplasmic actin messenger RNAs to different cytoplasmic compartments [published erratum appears in J Cell Biol 1993 Dec;123(6 Pt 2):following 1907]. *J. Cell. Biol.* 123: 165-172.

Kislauskis, E. H., Zhu, X., and Singer, R. H. (1997). beta-Actin messenger RNA localization and protein synthesis augment cell motility [published erratum appears in J Cell Biol 1997 Jun 30;137(7):1683]. *J. Cell Biol.* 136: 1263-1270.

Kislauskis, E. H., Zhu, X., and Singer, R. H. (1994). Sequences Responsible for Intracellular Localization of beta-Actin messenger RNA Also Affect Cell Phenotype. *J. Cell Biol.* 127: 441-451.

Knight, P., and Trinick, J. (1984). Structure of the myosin projections on native thick filaments from vertebrate skeletal muscle. *J. Mol. Biol.* 177: 461-82.

Kolmerer, B., Olivieri, N., Witt, C. C., Herrmann, B. G., and Labeit, S. (1996). Genomic organization of M-line titin and its tissue-specific expression in two distinct isoforms. *J. Mol. Biol.* 256: 556-563.

Komiyama, M., Kouchi, K., Maruyama, K., and Shimada, Y. (1993). Dynamics of actin and assembly of connectin (titin) during myofibrillogenesis in embryonic chick cardiac muscle cells in vitro. *Dev. Dyn.* 196: 291-299.

Komiyama, M., Soldati, T., von Arx, P., and Perriard, J.-C. (1996). The intracompartmental sorting of myosin alkali light chain isoproteins reflects the sequence of developmental expression as determined by double epitope-tagging competition. *J. Cell Sci.* 109: 2089-2099.

Komuro, I., and Yazaki, Y. (1993). Control of cardiac gene expression by mechanical stress. *Annu. Rev. Physiol.* 55: 55-75.

Kouchi, K., Takahashi, H., and Shimada, Y. (1993). Incorporation of microinjected biotin-labelled actin into nascent myofibrils of cardiac myocytes: an immunoelectron microscopic study. *J. Muscle Res. Cell Motil.* 14: 292-301.

Kreis, T., and Vale, R. (1999). Guidebook to the cytoskeletal and motor proteins, 2nd Ed., (Oxford: Oxford university press).

Kumar, A., Crawford, K., Close, L., Madison, M., Lorenz, J., Doetschman, T., Pawlowski, S., Duffy, J., Neumann, J., Robbins, J., Boivin, G. P., O'Toole, B. A., and

Lessard, J. L. (1997). Rescue of cardiac alpha-actin-deficient mice by enteric smooth muscle gamma-actin. *Proc. Natl. Acad. Sci. U S A* 94: 4406-4411.

Labeit, S., and Kolmerer, B. (1995). Titins: giant proteins in charge of muscle ultrastructure and elasticity. *Science* 270: 293-296.

Laemmli, U. K. (1970). Cleavage of structural proteins during the assembly of the head of bacteriophage T4. *Nature* 227: 680-685.

Lavigueur, A., La Branche, H., Kornblihtt, A. R., and Chabot, B. (1993). A splicing enhancer in the human fibronectin alternate ED1 exon interacts with SR proteins and stimulates U2 snRNP binding. *Genes Dev.* 7: 2405-2417.

Lawrence, J. B., and Singer, R. H. (1986). Intracellular localization of messenger RNAs for cytoskeletal proteins. *Cell* 45: 407-415.

Li, F., Wang, X., Bunger, P. C., and Gerdes, A. M. (1997). Formation of binucleated cardiac myocytes in rat heart: I. Role of actin-myosin contractile ring. *J. Mol. Cell. Cardiol.* 29: 1541-1551.

Linke, W. A., Bartoo, M. L., Ivemeyer, M., and Pollack, G. H. (1996). Limits of titin extension in single cardiac myofibrils. *J. Muscle Res. Cell. Motil.* 17: 425-438.

Linke, W. A., and Granzier, H. (1998). A spring tale: new facts on titin elasticity. *Biophys. J.* 75: 2613-2614.

Linke, W. A., Ivemeyer, M., Labeit, S., Hinssen, H., Ruegg, J. C., and Gautel, M. (1997). Actin-titin interaction in cardiac myofibrils: probing a physiological role. *Biophys. J.* 73: 905-919.

Linke, W. A., Ivemeyer, M., Mundel, P., Stockmeier, M. R., and Kolmerer, B. (1998). Nature of PEVK-titin elasticity in skeletal muscle. *Proc. Natl. Acad. Sci. U S A* 95: 8052-8057.

Linke, W. A., Rudy, D. E., Centner, T., Gautel, M., Witt, C., Labeit, S., and Gregorio, C. C. (1999). I-band titin in cardiac muscle is a three-element molecular spring and is critical for maintaining thin filament structure. *J. Cell Biol.* 146: 631-644.

Linke, W. A., Stockmeier, M. R., Ivemeyer, M., Hosser, H., and Mundel, P. (1998). Characterizing titin's I-band Ig domain region as an entropic spring. *J. Cell Sci.* 111: 1567-1574.

Liu, F., Bauer, C. C., Ortiz, I., Cook, R. G., Schmid, M. F., and Epstein, H. F. (1998). beta-Filagenin, a newly identified protein coassembling with myosin and paramyosin in Caenorhabditis elegans. *J. Cell Biol.* 140: 347-353.

Lopez, A. J. (1998). Alternative splicing of pre-mRNA: developmental consequences and mechanisms of regulation. *Annu. Rev. Genet.* 32: 279-305.

Lowey, S., and Steiner, L. A. (1972). An immunochemical approach to the structure of myosin and the thick filament. *J. Mol. Biol.* 65: 111-126.

Lubit, B. W. (1984). Association of beta-cytoplasmic actin with high concentrations of acetylcholine receptor (AChR) in normal and anti-AChR-treated primary rat muscle cultures. *J. Histochem. Cytochem.* 32: 973-981.

Luby-Phelps, K. (1987). Hindered diffusion of inert tracer particles in the cytoplasm of mouse 3T3 cells. *PNAS* 84: 4910-4913.

Lund, A. H., Duch, M., and Pedersen, F. S. (1996). Increased cloning efficiency by temperature-cycle ligation. *Nucleic Acids Res* 24: 800-801.

Luther, P., and Squire, J. (1978). Three-dimensional structure of the vertebrate muscle M-region. *J. Mol. Biol.* 125: 313-324.

Luther, P. K. (1991). Three-dimensional reconstruction of a simple Z-band in fish muscle. *J. Cell Biol.* 113: 1043-1055.

Luther, P. K., Munro, P. M., and Squire, J. M. (1981). Three-dimensional structure of the vertebrate muscle A-band. III. M- region structure and myosin filament symmetry. *J. Mol. Biol.* 151: 703-730.

Luther, P. K., and Squire, J. M. (1980). Three-dimensional structure of the vertebrate muscle A-band. II. The myosin filament superlattice. *J Mol Biol* 141: 409-39.

Magid, A., and Law, D. J. (1985). Myofibrils bear most of the resting tension in frog skeletal muscle. *Science* 230: 1280-1282.

Manasek, F. J. (1968). Embryonic development of the heart. I. A light and electron microscopic study of myocardial development in the early chick embryo. *J. Morphol.* 125: 329-365.

Manasek, F. J. (1969). Embryonic development of the heart. II. Formation of the epicardium. *J. Embryol. Exp. Morphol.* 22: 333-348.

Manasek, F. J. (1968). Mitosis in developing cardiac muscle. *J. Cell. Biol.* 37: 191-196.

Maruyama, K. (1994). Connectin, an elastic protein of striated muscle. *Biophys. Chem.* 50: 73-85.

Maruyama, K., Endo, T., Kume, H., Kawamura, Y., Kanzawa, N., Kimura, S., and Kawashima, S. (1994). A partial connectin cDNA encoding a novel type of RSP motifs isolated from chicken embryonic skeletal muscle. *J Biochem (Tokyo)* 115: 147-9.

Maruyama, K., Matsubara, S., Natori, R., Nonomura, Y., Kimura, S., Ohashi, K., Murakami, F., Handa, S., and Eguchi, G. (1977). Connectin, an elastic protein of muscle. *J. Biochem.* 82: 317-337.

Masaki, T., and Takaiti, O. (1974). M-protein. *J. Biochem. Tokyo* 75: 367-380.

Matsubara, I., Goldman, Y. E., and Simmons, R. M. (1984). Changes in the lateral filament spacing of skinned muscle fibres when cross-bridges attach. *J Mol Biol* 173: 15-33.

Mayans, O., van der Ven, P. F., Wilm, M., Mues, A., Young, P., Furst, D. O., Wilmanns, M., and Gautel, M. (1998). Structural basis for activation of the titin kinase domain during myofibrillogenesis. *Nature* 395: 863-9.

McHugh, K. M., Crawford, K., and Lessard, J. L. (1991). A comprehensive analysis of the developmental and tissue-specific expression of the isoactin multigene family in the rat. *Dev. Biol.* 148: 442-458.

McHugh, K. M., and Lessard, J. L. (1988). The development expression of the rat alpha-vascular and gamma-enteric smooth muscle isoactins: isolation and characterization of a rat gamma- enteric actin cDNA. *Mol. Cell. Biol.* 8: 5224-5231.

McHugh, K. M., and Lessard, J. L. (1988). The nucleotide sequence of a rat vascular smooth muscle alpha-actin cDNA. *Nucleic Acids Res.* 16: 41-67.

McKenna, N., Meigs, J. B., and Wang, Y. L. (1985). Identical distribution of fluorescently labeled brain and muscle actins in living cardiac fibroblasts and myocytes. *J. Cell Biol.* 100: 292-296.

Messerli, J. M., van der Voort, H. T. M., Rungger-Brändle, E., and Perriard, J.-C. (1993). Three-dimensional visualization of multi-channel volume data: the amSFP algorithm. *Cytometry* 14: 725-735.

Messerli, M., Eppenberger, M. E., Rutishauser, B., Schwarb, P., von Arx, P., Koch-Schneidemann, S., Eppenberger, H. M., and Perriard, J.-C. (1993). Remodeling of Cardiomocyte Cytocarchitecture Visualized by 3D Confocal Microscopy. *Histochemistry* 100: 193-202.

Micheva, K. D., Vallee, A., Beaulieu, C., Herman, I. M., and Leclerc, N. (1998). beta-Actin is confined to structures having high capacity of remodelling in developing and adult rat cerebellum. *Eur. J. Neurosci.* 10: 3785-3798.

Millevoi, S., Trombitas, K., Kolmerer, B., Kostin, S., Schaper, J., Pelin, K., Granzier, H., and Labeit, S. (1998). Characterization of nebulette and nebulin and emerging concepts of their roles for vertebrate Z-discs. *J. Mol. Biol.* 282: 111-23.

Millman, B. M. (1998). The filament lattice of striated muscle. *Physiol Rev.* 78: 359-391.

Millman, B. M., and Nickel, B. G. (1980). Electrostatic forces in muscle and cylindrical gel systems. *Biophys. J.* 32: 49-63.

Milner, D. J., Weitzer, G., Tran, D., Bradley, A., and Capetanaki, Y. (1996). Disruption of muscle architecture and myocardial degeneration in mice lacking desmin. *J. Cell. Biol.* 134: 1255-1270.

Moncman, C. L., and Wang, K. (1999). Functional dissection of nebulette demonstrates actin binding of nebulin-like repeats and Z-line targeting of SH3 and linker domains. *Cell Motil. Cytoskeleton* 44: 1-22.

Moncman, C. L., and Wang, K. (1995). Nebulette: a 107 kD nebulin-like protein in cardiac muscle. *Cell Motil. Cytoskeleton* 32: 205-225.

Moos, M., and Gallwitz, D. (1983). Structure of two human beta-actin-related processed genes one of which is located next to a simple repetitive sequence. *Embo J.* 2: 757-61.

Mounier, N., Gouy, M., Mouchiroud, D., and Prudhomme, J. C. (1992). Insect muscle actins differ distinctly from invertebrate and vertebrate cytoplasmic actins. *J Mol Evol* 34: 406-415.

Mounier, N., and Sparrow, J. C. (1997). Structural comparisons of muscle and nonmuscle actins give insights into the evolution of their functional differences. *Journal of Molecular Evolution* 44: 89-97.

Nadal-Ginard, B., Smith, C. W., Patton, J. G., and Breitbart, R. E. (1991). Alternative splicing is an efficient mechanism for the generation of protein diversity: contractile protein genes as a model system. *Adv. Enzyme Regul.* 31: 261-286.

Nave, R., Furst, D. O., and Weber, K. (1989). Visualization of the polarity of isolated titin molecules: a single globular head on a long thin rod as the M band anchoring domain? *J. Cell. Biol.* 109: 2177-2187.

Ng, S. Y., Gunning, P., Eddy, R., Ponte, P., Leavitt, J., Shows, T., and Kedes, L. (1985). Evolution of the functional human beta-actin gene and its multi- pseudogene family: conservation of noncoding regions and chromosomal dispersion of pseudogenes. *Mol. Cell. Biol.* 5: 2720-2732.

Nikcevic, G., Heidkamp, M. C., Perhonen, M., and Russell, B. (1999). Mechanical activity in heart regulates translation of alpha-myosin heavy chain mRNA but not its localization. *Am. J. Physiol.* 276: H2013-H2019.

North, A. J., Gimona, M., Lando, Z., and Small, J. V. (1994). Actin isoform compartments in chicken gizzard smooth muscle cells. *J. Cell Sci.* 107: 445-455.

Obermann, W. M., Plessmann, U., Weber, K., and Furst, D. O. (1995). Purification and biochemical characterization of myomesin, a myosin- binding and titin-binding protein, from bovine skeletal muscle. *Eur. J. Biochem.* 233: 110-115.

Obermann, W. M. J., Gautel, M., Steiner, F., Vanderven, P. F. M., Weber, K., and Furst, D. O. (1996). The Structure Of the Sarcomeric M Band: Localization Of Defined

Domains Of Myomesin, M Protein, and the 250 Kd Carboxy Terminal Region Of Titin By Immunoelectron Microscopy. *J. Cell Biol.* 134: 1441-1453.

Obermann, W. M. J., Gautel, M., Weber, K., and Furst, D. O. (1997). Molecular Structure Of the Sarcomeric M Band: Mapping Of Titin and Myosin Binding Domains In Myomesin and the Identification Of a Potential Regulatory Phosphorylation Site In Myomesin. *Embo Journal* 16: 211-220.

Obermann, W. M. J., van der Ven, P. F. M., Steiner, F., Weber, K., and Fürst, D. O. (1998). Mapping of a myosin-binding domain and a regulatory phosphorylation site in M-protein, a structural protein of the sarcomeric M band. *Mol. Biol. Cell* 9: 829-840.

Ohtsuka, H., Yajima, H., Maruyama, K., and Kimura, S. (1997). The N-terminal Z repeat 5 of connectin/titin binds to the C-terminal region of alpha-actinin. *Biochem. Biophys. Res. Commun.* 235: 1-3.

Okagaki, T., Weber, F. E., Fischman, D. A., Vaughan, K. T., Mikawa, T., and Reinach, F. C. (1993). The major myosin-binding domain of skeletal muscle MyPB-C (C-protein) resides in the COOH-terminal, immunoglobulin C2 motif. *J. Cell Biol.* 123: 619-626.

Otey, C. A., Kalnoski, M. H., and Bulinski, J. C. (1987). Identification and quantification of actin isoforms in vertebrate cells and tissues. *J. Cell. Biochem.* 34: 113-124.

Otey, C. A., Kalnoski, M. H., Lessard, J. L., and Bulinski, J. C. (1986). Immunolocalization of the gamma isoform of nonmuscle actin in cultured cells. *J Cell Biol* 102: 1726-1737.

Otey, C. A., Kalnosky, M. H., and Bulinski, J. C. (1988). Immunolocalization of muscle and nonmuscle isoforms of actin in myogenic cells and adult skeletal muscle. *Cell Motil Cytoskel* 9: 337-348.

Pardo, J. V., Pittenger, M. F., and Craig, S. W. (1983). Subcellular sorting of isoactins: selective association of gamma actin with skeletal muscle mitochondria. *Cell* 32: 1093-103.

Pask, H. T., Jones, K. L., Luther, P. K., and Squire, J. M. (1994). M-band structure, M-bridge interactions and contraction speed in vertebrate cardiac muscles. *J Muscle Res Cell Motil* 15: 633-45 Issn: 0142-4319.

Peng, I., and Fischman, D. A. (1991). Post-translational incorporation of actin into myofibrils in vitro: evidence for isoform specificity. *Cell Motil Cytoskeleton* 20: 158-68.

Periasamy, M., Strehler, E. E., Garfinkel, L. I., Gubits, R. M., Ruiz-Opazo, N., and Nadal-Ginard, B. (1984). Fast skeletal muscle myosin light chains 1 and 3 are produced from a single gene by a combined process of differential RNA transcription and splicing. *J. Biol. Chem.* 259: 13595-13604.

Perriard, J.-C., Achtnich, U., Cerny, L., Eppenberger, H. M., Grove, B. K., Hossle, H. P., and Schäfer, B. (1986). Expression of M-band proteins during myogenesis. *Mol. Biol. Musc. Dev.*: 693-707.

Pfuhl, M., and Pastore, A. (1995). Tertiary structure of an immunoglobulin-like domain from the giant muscle protein titin: a new member of the I set. *Structure* 3: 391-401.

Pittenger, M. F., Kazzaz, J. A., and Helfman, D. M. (1994). Functional properties of non-muscle tropomyosin isoforms. *Curr. Opin. Cell Biol.* 6: 96-104.

Politou, A. S., Thomas, D. J., and Pastore, A. (1995). The folding and stability of titin immunoglobulin-like modules, with implications for the mechanism of elasticity. *Biophys. J.* 69: 2601-10.

Pollard, T. D. (1990). Actin. *Curr. Opin. Cell. Biol.* 2: 33-40.

Ponte, P., Gunning, P., Blau, H., and Kedes, L. (1983). Human actin genes are single copy for alpha-skeletal and alpha-cardiac actin but multicopy for beta- and gamma-cytoskeletal genes: 3' untranslated regions are isotype specific but are conserved in evolution. *Mol Cell Biol* 3: 1783-91.

Price, M. G. (1987). Skelemins: cytoskeletal proteins located at the periphery of M-discs in mammalian striated muscle. *J. Cell Biol.* 104: 1325-1336.

Price, M. G., and Gomer, R. H. (1993). Skelemin, a cytoskeletal M-disc periphery protein, contains motifs of adhesion/recognition and intermediate filament proteins. *J. Biol. Chem.* 268: 21800-21810.

Przybylski, R. J., and Blumberg, J. M. (1966). Ultrastructural aspects of myogenesis in the chick. *Lab. Invest.* 15: 836-863.

Rall, J. A. (1981). Mechanics and energetics of contraction in striated muscle of the sea scallop, Placopecten magellanicus. *J Physiol (Lond)* 321: 287-95.

Reddy, K. B., Gascard, P., Price, M. G., Negrescu, E. V., and Fox, J. E. B. (1998). Identification of an interaction between the M-band protein skelemin and beta-integrin subunits. Colocalization of a skelemin-like protein with beta1- and beta3-integrins in non-muscle cells. *J. Biol. Chem.* 273: 35039-35047.

Reggiani, C., Potma, E. J., Bottinelli, R., Canepari, M., Pellegrino, M. A., and Stienen, G. J. (1997). Chemo-mechanical energy transduction in relation to myosin isoform composition in skeletal muscle fibres of the rat. *J. Physiol. (Lond.)* 502: 449-60.

Remane, A., Storch, V., Welsch, U. (1979). Systematische Zoologie. Stamme des Tierreichs, 2nd Edition (Stutgart: Fisher).

Rhee, D., Sanger, J. M., and Sanger, J. W. (1994). The premyofibril: evidence for its role in myofibrillogenesis. *Cell Motil Cytoskeleton* 28: 1-24.

Rief, M., Gautel, M., Schemmel, A., and Gaub, H. E. (1998). The mechanical stability of immunoglobulin and fibronectin III domains in the muscle protein titin measured by atomic force microscopy. *Biophys J* 75: 3008-14.

Ronnov-Jessen, L., Van Deurs, B., Nielsen, M., and Petersen, O. W. (1992). Identification, paracrine generation, and possible function of human breast carcinoma myofibroblasts in culture. *In Vitro Cell Dev Biol* 28A: 273-83.

Rothen-Rutishauser, B. M., Ehler, E., Perriard, E., Messerli, J. M., and Perriard, J. C. (1998). Different behaviour of the non-sarcomeric cytoskeleton in neonatal and adult rat cardiomyocytes. *J Mol Cell Cardiol* 30: 19-31.

Royuela, M., Fraile, B., Cervera, M., and Paniagua, R. (1997). Immunocytochemical electron microscopic study and western blot analysis of myosin, paramyosin and miniparamyosin in the striated muscle of the fruit fly Drosophila melanogaster and in obliquely striated and smooth muscles of the earthworm Eisenia foetida. *J Muscle Res Cell Motil* 18: 169-77.

Rumyantsev, P. P. (1977). Interrelations of the proliferation and differentiation processes during cardiact myogenesis and regeneration. *Int. Rev. Cytol.* 51: 186-273.

Ruzicka, D. L., and Schwartz, R. J. (1988). Sequential activation of a-actin genes during avian cardiogenesis : vascular smoots muscle a-actin gene transcripts mark the onset of cardiomyocyte differentiation. *The Journal of Cell Biology* 107: 2575-2586.

Ryan, K. J., and Cooper, T. A. (1996). Muscle-specific splicing enhancers regulate inclusion of the cardiac troponin T alternative exon in embryonic skeletal muscle. *Mol Cell Biol* 16: 4014-23.

Sadano, H., Taniguchi, S., Kakunaga, T., and Baba, T. (1988). cDNA cloning and sequence of a new type of actin in mouse B16 melanoma. *J. Biol. Chem.* 263: 15868-15871.

Sawtell, N. M., Hartman, A. L., and Lessard, J. L. (1988). Unique isoactins in the brush border of rat intestinal epithelial cells. *Cell Motil. Cytoskeleton* 11: 318-325.

Sawtell, N. M., and Lessard, J. L. (1989). Cellular distribution of smooth muscle actins during mammalian embryogenesis: expression of the a-vascular but not the g-enteric isoform in differentiating striated myocytes. *J Cell Biology* 109: 2929-2937.

Schachat, F. H., Diamond, M. S., and Brandt, P. W. (1987). Effect of different troponin T-tropomyosin combinations on thin filament activation. *J. Mol. Biol.* 198: 551-4.

Schaub, M. C., Hefti, M. A., Harder, B. A., and Eppenberger, H. M. (1997). Various hypertrophic stimuli induce distinct phenotypes in cardiomyocytes. *J Mol Med* 75: 901-20.

Schaub, M. C., Hefti, M. A., Zuellig, R. A., and Morano, I. (1998). Modulation of contractility in human cardiac hypertrophy by myosin essential light chain isoforms. *Cardiovasc Res* 37: 381-404.

Schein, C. H. (1990). Solubility as a function of protein structure and solvent components. *Biotechnology (N Y)* 8: 308-17.

Schiaffino, S., and Reggiani, C. (1996). Molecular diversity of myofibrillar proteins: gene regulation and functional significance. *Physiol. Rev.* 76: 371-423.

Schiaffino, S., Samuel, J. L., Sassoon, D., Lompre, A. M., Garner, I., Marotte, F., Buckingham, M., Rappaport, L., and Schwartz, K. (1989). Nonsynchronous accumulation of alpha-skeletal actin and beta-myosin heavy chain mRNAs during early stages of pressure-overload--induced cardiac hypertrophy demonstrated by in situ hybridization. *Circ Res* 64: 937-48.

Schmid, M. F., and Epstein, H. F. (1998). Muscle thick filaments are rigid coupled tubules, not flexible ropes. *Cell Motil Cytoskeleton* 41: 195-201.

Schneider, W. J., Slaughter, C. J., Goldstein, J. L., Anderson, R. G., Capra, J. D., and Brown, M. S. (1983). Use of antipeptide antibodies to demonstrate external orientation of the NH2-terminus of the low density lipoprotein receptor in the plasma membrane of fibroblasts. *J Cell Biol* 97: 1635-1640.

Schoenberg, M. (1980). Geometrical factors influencing muscle force development. II. Radial forces. *Biophys J* 30: 69-77.

Schoenenberger, C. A., Brault, V., Reedy, M. C., and Saunder, U. (1995). Ectopic expression of actin isoforms in the indirect flight muscle of drosophila. *Mol.Biol. Cell* 6s: 19a.

Schultheiss, T., Lin, Z. X., Lu, M. H., Murray, J., Fischman, D. A., Weber, K., Masaki, T., Imamura, M., and Holtzer, H. (1990). Differential distribution of subsets of myofibrillar proteins in cardiac nonstriated and striated myofibrils. *J Cell Biol* 110: 1159-1172.

Sen, A., Dunnmon, P., Henderson, S. A., Gerard, R. D., and Chien, K. R. (1988). Terminally differentiated neonatal rat myocardial cells proliferate and maintain specific differentiated functions following expression of SV40 large T antigen. *J. Biol. Chem.* 263: 19132-19136.

Sheterline, P., Clayton, J., and Sparrow, J. (1995). Actin. *Protein Profile. 1995;* 2: 1-103.

Sheterline, P., and Sparrow, J. C. (1994). Actin. *Protein Profile* 1: 1-121.

Shuster, C. B., and Herman, I. M. (1995). Indirect association of ezrin with F-actin: isoform specificity and calcium sensitivity. *J Cell Biol* 128: 837-848.

Shuster, C. B., Lin, A. Y., Nayak, R., and Herman, I. M. (1996). Beta-CAP73: A novel beta actin-specific binding protein. *Cell Motility and the Cytoskeleton* 35: 175-187.

Siu, B. L., Niimura, H., Osborne, J. A., Fatkin, D., MacRae, C., Solomon, S., Benson, D. W., Seidman, J. G., and Seidman, C. E. (1999). Familial dilated cardiomyopathy locus maps to chromosome 2q31. *Circulation* 99: 1022-1026.

Sjostrom, M., and Squire, J. M. (1977). Fine structure of the A-band in cryo-sections. The structure of the A-band of human skeletal muscle fibres from ultra-thin cryo-sections negatively stained. *J Mol Biol* 109: 49-68.

Skalli, O., Gabbiani, G., Babai, F., Seemayer, T. A., Pizzolato, G., and Schurch, W. (1988). Intermediate filament proteins and actin isoforms as markers for soft tissue tumor differentiation and origin. II. Rhabdomyosarcomas. *Am J Pathol* 130: 515-531.

Skalli, O., Gabbiani, G., Babai, F., Seemayer, T. A., Pizzolato, G., and Schurch, W. (1988). Intermediate filament proteins and actin isoforms as markers for soft tissue tumor differentiation and origin. II. Rhabdomyosarcomas. *Am. J. Pathol.* 130: 515-531.

Skalli, O., Ropraz, P., Trzeciak, A., Benzonana, G., Gillessen, D., and Gabbiani, G. (1986). A monoclonal antibody against alpha-smooth muscle actin: a new probe for smooth muscle differentiation. *J Cell Biol.* 103: 2787-2796.

Small, J. V., Fürst, D. O., and Thornell, L. E. (1992). The cytoskeletal lattice of muscle cells. *Eur. J. Biochem.* 208: 559-572.

Smith, D. B., and Johnson, K. S. (1988). Single-step purification of polypeptides expressed in Escherichia coli as fusions with glutathione S-transferase. *Gene* 67: 31-40.

Smolich, J. J. (1995). Ultrastructural and functional features of the developing mammalian heart: a brief overview. *Reprod. Fertil. Dev.* 7: 451-461.

Soldati, T., and Perriard, J. C. (1991). Intracompartmental Sorting of Essential Myosin Light Chains: Molecular Dissection and In Vivo Monitoring by Epitope Tagging. *Cell* 66: 277-289.

Sorimachi, H., Freiburg, A., Kolmerer, B., Ishiura, S., Stier, G., Gregorio, C. C., Labeit, D., Linke, W. A., Suzuki, K., and Labeit, S. (1997). Tissue-specific expression and alpha-actinin binding properties of the Z-disc titin: implications for the nature of vertebrate Z-discs. *J. Mol. Biol.* 270: 688-695.

Squire, J., Cantino, M., Chew, M., Denny, R., Harford, J., Hudson, L., and Luther, P. (1998). Myosin rod-packing schemes in vertebrate muscle thick filaments. *J. Struct. Biol.* 122: 128-138.

Squire, J. M. (1997). Architecture and function in the muscle sarcomere. *Curr. Opin. Struct. Bio.l* 7: 247-257.

Squire, J. M. (1975). Muscle filament structure and muscle contraction. *Annu. Rev. Biophys. Bioeng.* 4: 137-163.

Squire, J. M. (1981). The structural basis of muscular contraction (New York: Plenum Press).

Steiner, F., Weber, K., and Furst, D. (1999). M-band proteins myomesin and skelemin are incoded by the same gene:analysis of its organisation and expression. *Genomics* 56: 78-89.

Stolz, M., and Wallimann, T. (1998). Myofibrillar interaction of cytosolic creatine kinase (CK) isoenzymes: allocation of N-terminal binding epitope in MM-CK and BB-CK. *J. Cell Sci.* 111: 1207-1216.

Strehler, E. E., Carlsson, E., Eppenberger, H. M., and Thornell, L. E. (1983). Ultrastructural localization of M-band proteins in chicken breast muscle as revealed by combined immunocytochemistry and ultramicrotomy. *J Mol Biol* 166: 141-158.

Strehler, E. E., Pelloni, G., Heizmann, C. W., and Eppenberger, H. M. (1980). Biochemical and ultrastructural aspects of Mr 165,000 M-protein in cross-striated chicken muscle. *J Cell Biol* 86: 775-783.

Sussman, M. A., Welch, S., Cambon, N., Klevitsky, R., Hewett, T. E., Price, R., Witt, S. A., and Kimball, T. R. (1998). Myofibril degeneration caused by tropomodulin overexpression leads to dilated cardiomyopathy in juvenile mice. *J. Clin. Invest.* 101: 51-61.

Sutherland, C. J., Esser, K. A., Elsom, V. L., Gordon, M. L., and Hardeman, E. C. (1993). Identification of a program of contractile protein gene expression initiated upon skeletal muscle differentiation. *Dev. Dyn.* 196: 25-36.

Suzuki, H., Komiyama, M., Konno, A., and Shimada, Y. (1998). Exchangeability of actin in cardiac myocytes and fibroblasts as determined by fluorescence photobleaching recovery. *Tissue Cell* 30: 274-280.

Taniguchi, S., Kawano, T., Kakunaga, T., and Baba, T. (1986). Differences in expression of a variant actin between low and high metastatic B16 melanoma. *J. Biol. Chem.* 261: 6100-6106.

Thornell, L. E., Eriksson, A., Johansson, B., Kjorell, U., Franke, W. W., Virtanen, I., and Lehto, V. P. (1985). Intermediate filament and associated proteins in heart Purkinje fibers: a membrane-myofibril anchored cytoskeletal system. *Ann N Y Acad Sci* 455: 213-240.

Tokuyasu, K. T. (1983). Visualization of longitudinally-oriented intermediate filaments in frozen sections of chicken cardiac muscle by a new staining method. *J Cell Biol* 97: 562-565.

Tokuyasu, K. T., and Maher, P. A. (1987). Immunocytochemical studies of cardiac myofibrillogenesis in early chick embryos. I. Presence of immunofluorescent titin spots in premyofibril stages. *J. Cell. Biol.* 105: 2781-2793.

Tokuyasu, K. T., and Maher, P. A. (1987). Immunocytochemical studies of cardiac myofibrillogenesis in early chick embryos. II. Generation of alpha-actinin dots within titin spots at the time of the first myofibril formation. *J Cell Biol* 105: 2795-2801.

Towbin, J. A. (1998). The role of cytoskeletal proteins in cardiomyopathies. *Curr Opin Cell Biol* 10: 131-139.

Trinick, J. (1994). Titin and nebulin: protein rulers in muscle? *Trends Biochem Sci* 19: 405-409.

Trinick, J. (1996). Titin as a scaffold and spring. Cytoskeleton. *Curr Biol* 6: 258-260.

Trinick, J., and Tskhovrebova, L. (1999). Titin: a molecular control freak. *Trends Cell Biol.* 9: 377-380.

Trombitas, K., Freiburg, A., Centner, T., Labeit, S., and Granzier, H. (1999). Molecular dissection of N2B cardiac titin's extensibility. *Biophys J* 77: 3189-3196.

Trombitas, K., Greaser, M., Labeit, S., Jin, J. P., Kellermayer, M., Helmes, M., and Granzier, H. (1998). Titin extensibility in situ: entropic elasticity of permanently folded and permanently unfolded molecular segments. *J Cell Biol* 140: 853-859.

Tskhovrebova, L., Trinick, J., Sleep, J. A., and Simmons, R. M. (1997). Elasticity and unfolding of single molecules of the giant muscle protein titin. *Nature* 387: 308-312.

Turnacioglu, K. K., Mittal, B., Dabiri, G. A., Sanger, J. M., and Sanger, J. W. (1997). An N-terminal fragment of titin coupled to green fluorescent protein localizes to the Z-bands in living muscle cells: overexpression leads to myofibril disassembly. *Mol Biol Cell* 8: 705-717.

Vaitukaitis, J. L. (1981). Production of antisera with small doses of immunogen: Multiple intradermal injections. *Methods Enzymol.* 73: 46-52.

van der Loop, F., van der Ven, P., Fürst, D. O., Gautel, M., van, E. G., and Ramaekers, F. C. (1996). Integration of titin into the sarcomeres of cultured differentiating human skeletal muscle cells. *Eur J Cell Biol* 69: 301-307.

van Der Ven, P. F., Bartsch, J. W., Gautel, M., Jockusch, H., and Furst, D. O. (2000). A functional knock-out of titin results in defective myofibril assembly [In Process Citation]. *J. Cell. Sci.* 113: 1405-1414.

van der Ven, P. F. M., Ehler, E., Perriard, J.-C., and Fürst, D. O. (1999). Thick filament assembly occurs after the formation of a cytoskeletal scaffold. *J. Muscle Res. Cell Motil.* 20: 569-579.

van Deursen, J., Heerschap, A., Oerlemans, F., Ruitenbeek, W., Jap, P., ter Laak, H., and Wieringa, B. (1993). Skeletal muscles of mice deficient in muscle creatine kinase lack burst activity. *Cell* 74: 621-631.

Vandekerckhove, J., Bugaisky, G., and Buckingham, M. (1986). Simultaneous expression of skeletal muscle and heart actin proteins in various striated muscle tissues and cells. A quantitative determination of the two actin isoforms. *J. Biol. Chem.* 261: 1838-1843.

Vandekerckhove, J., and Weber, K. (1981). Actin typing on total cellular extracts. A highly sensitive protein-chemical procedure able to distinguish different actins. *Eur. J. Biochem.* 113: 595-603.

Vandekerckhove, J., and Weber, K. (1978). At least six different actins are expresed in a higher mammal: an analysis based on the amino acid sequence of the amino-terminal tryptic peptide. *J Mol Biol* 126: 783-802.

Vandekerckhove, J., and Weber, K. (1984). Chordate muscle actins differ distinctly from invertebrate muscle actins. The evolution of the different vertebrate muscle actins. *J Mol Biol* 179: 391-413.

Vinkemeier, U., Obermann, W., Weber, K., and Fürst, D. O. (1993). The globular head domain of titin extends into the center of the sarcomeric M band. *J. Cell Science* 106: 319-330.

von Arx, P., Bantle, S., Soldati, T., and Perriard, J.-C. (1995). Dominant Negative Effect of Cytoplasmic Actin Isoproteins on Cardiomyocyte Cytoarchitecture and Function. *J. Cell Biol.* 131: 1759-1773.

Wallimann, T., and Eppenberger, H. M. (1985). Localization and function of M-line-bound creatine kinase. M-band model and creatine phosphate shuttle. *Cell Muscle Motil.* 6: 239-285.

Wallimann, T., Wyss, M., Brdiczka, D., Nicolay, K., and Eppenberger, H. M. (1992). Intracellular compartmentation, structure and function of creatine kinase isoenzymes in tissues with high and fluctuating energy demands: the "phosphocreatine circuit" for cellular energy homeostasis. *Biochem J* 281: 21-40.

Wang, K., McCarter, R., Wright, J., Beverly, J., and Ramirez-Mitchell, R. (1991). Regulation of skeletal muscle stiffness and elasticity by titin isoforms: a test of the segmental extension model of resting tension. *Proc Natl Acad Sci U S A* 88: 7101-7105.

Wang, K., McCarter, R., Wright, J., Beverly, J., and Ramirez-Mitchell, R. (1993). Viscoelasticity of the sarcomere matrix of skeletal muscles. The titin- myosin composite filament is a dual-stage molecular spring. *Biophys J* 64: 1161-1177.

Wang, K., McClure, J., and Tu, A. (1979). Titin: major myofibrillar components of striated muscle. *Proc Natl Acad Sci U S A* 76: 3698-3702.

Wang, K., and Ramirez-Mitchell, R. (1983). A network of transverse and longitudinal intermediate filaments is associated with sarcomeres of adult vertebrate skeletal muscle. *J Cell Biol* 96: 562-570.

Wang, K., and Wright, J. (1988). Architecture of the sarcomere matrix of skeletal muscle: immunoelectron microscopic evidence that suggests a set of parallel inextensible nebulin filaments anchored at the Z line. *J. Cell. Biol.* 107: 2199-2212.

Weber, K. T., Sun, Y., Tyagi, S. C., and Cleutjens, J. P. (1994). Collagen network of the myocardium: function, structural remodeling and regulatory mechanisms. *J Mol Cell Cardiol* 26: 279-92.

Weydert, A., Daubas, P., Lazaridis, I., Barton, P., Garner, I., Leader, D. P., Bonhomme, F., Catalan, J., Simon, D., and Guenet, J. L. (1985). Genes for skeletal muscle myosin heavy chains are clustered and are not located on the same mouse chromosome as a cardiac myosin heavy chain gene. *Proc. Natl. Acad. Sci. U S A* 82: 7183-7187.

Woodcock, M. J., Mitchell, J. J., Low, R. B., Kieny, M., Sengel, P., Rubbia, L., Skalli, O., Jackson, B., and Gabbiani, G. (1988). Alpha-smooth muscle actin is transiently expressed in embryonic rat cardiac and skeletal muscles. *Differentiation* 39: 161-166.

Xu, R., Teng, J., and Cooper, T. A. (1993). The cardiac troponin T alternative exon contains a novel purine-rich positive splicing element. *Mol Cell Biol* 13: 3660-3674.

Xu, S., Brenner, B., and Yu, L. C. (1993). State-dependent radial elasticity of attached cross-bridges in single skinned fibres of rabbit psoas muscle [corrected and republished article originally printed in J Physiol (Lond) 1993 Feb;461:283-99]. *J Physiol (Lond)* 465: 749-765.

Yao, X., Chaponnier, C., Gabbiani, G., and Forte, J. G. (1995). Polarized distribution of actin isoforms in gastric parietal cells. *Mol Biol Cell* 6: 541-557.

Yoshioka, T., Nagami, K., Tamaki, T., and Nakano, S. (1986). The effects of detergent on the contractility and ultrastructure of frog skeletal muscle. *Jpn. J. Physiol.* 36: 379-390.

Young, P., Ferguson, C., Banuelos, S., and Gautel, M. (1998). Molecular structure of the sarcomeric Z-disk: two types of titin interactions lead to an asymmetrical sorting of alpha-actinin. *Embo J.* 17: 1614-1624.

Curriculum Vitae

Personal data

Name: Irina Agarkova
Date of birth: October 2, 1963
Place of birth: Yalta, USSR
Citizenship: Russia
Civil status: married, one son (1988)

Education

1980-1986: Moscow Institute of Physics and Technology, Moscow, USSR
1986: MS Diploma in Physics, Moscow Institute of Physics and Technology, Diploma Thesis: "Mechanics of Artificial Heart".
1986-1988: Graduate School, Laboratory of Bioelectrochemistry, Institute of Electrochemistry, Moscow.
1993-1994: Part time student at Weizmann Institute, Rehovot, Israel
1994-1996: Student at Biology Department, Swiss Federal Institute of Technology Zurich
March 1996: Passed exams in Cell Biology, Microbiology, Molecular Genetics, Immunology required to get admitted to the Graduate School in Biology with Physics MS Diploma
1996-2000: PhD student at the Swiss Institute of Cell Biology. Supervisor: Prof. Dr. J.-C.Perriard

Publications in refereed journals:

Agarkova, I., Auerbach, D., Ehler, E., and Perriard, J. C. (2000). A novel marker for vertebrate embryonic heart, the EH-myomesin isoform. *J. Biol. Chem.* 275: 10256-10264.

Agarkova, I., Serov, S., Prasovov, V., and Chernomordic, L. (1987). Application of electron-field mediated DNA trasfer for genetic transformation of eucariotic cells. *Biologicheskie membrani* 4: 1289-1295.

Conference Proceedings

Agarkova I., Rothen-Ruthishauser B., Chaponnier C., Perriard J.-C. Expression of the different actin isoforms in cultivated neonatal and adult rat cardiomyocytes. 2nd International Workshop on "Cardiac Cells in Culture: Molecular Mechanisms of Hypertrophy", Ascona, Switzerland, 5-9 March (1997).

Agarkova I., Andreoli C., Ehler E., Periard J.-C. Analysis of tissue-specific myomesin isoforms expression in chicken embryo using specific polyclonal antisera. 13th European Cytoskeletal Forum, Strasbourg, France, 22-26 August (1998).

Perriard J.-C., Ehler E., Agarkova I., Auerbach D., Giro P., Leu M, Nemir M. Myofibrillogenesis in cardiomyocytes in situ and the role of M-band.
39th American Society for Cell Biology Annual Meeting, December 11-15, 1999; Washington, *USA Supplement to Molecular Biology of the Cell* 10: 168a (1999)

Agarkova I, Auerbach D, Ehler E and Periard J.-C. A novel marker for vertebrate embryonic heart: the EH-myomesin isoform, "Cardiomyocytes in culture: Diffferentiation and Development of Pathological Phenotypes", 3rd International Workshop, Ascona, Switzerland,1-3 March (2000).

Acknowledgements

First of all I would like to thank **Prof. Jean-Claude Perriard** for his continuous support and encouragement of the work that forms this Thesis, his useful suggestions and, finally, for giving me a research freedom providing thereby an ideal atmosphere for the creative research.

I would also like to thank **Prof. Hans M. Eppenberger** for his supervision of this work and useful comments.

I am grateful to **Prof. Markus Schaub** for his comments on the manuscript and for co-reviewing this thesis.

I thank all members of our group but especially **Dani Auerbach** and **Elisabeth Ehler** for stimulating discussions and for correcting numerous mistakes in my texts. Separate thanks are due to **Eveline Perriard** for laborious preparation of the primary cultures of embryonic chicken myocytes and also to **Cristoph Andreoli** for his help in expressing of recombinant myomesin fragments.